

Enantioselective α -Amination of 1,3-Dicarbonyl Compounds Using Squaramide Derivatives as Hydrogen Bonding Catalysts

Hideyuki Konishi, Tin Yiu Lam, Jeremiah P. Malerich, and Viresh H. Rawal*

Department of Chemistry, University of Chicago, 5735 South Ellis Avenue, Chicago, IL 60637

Email: vrawal@uchicago.edu

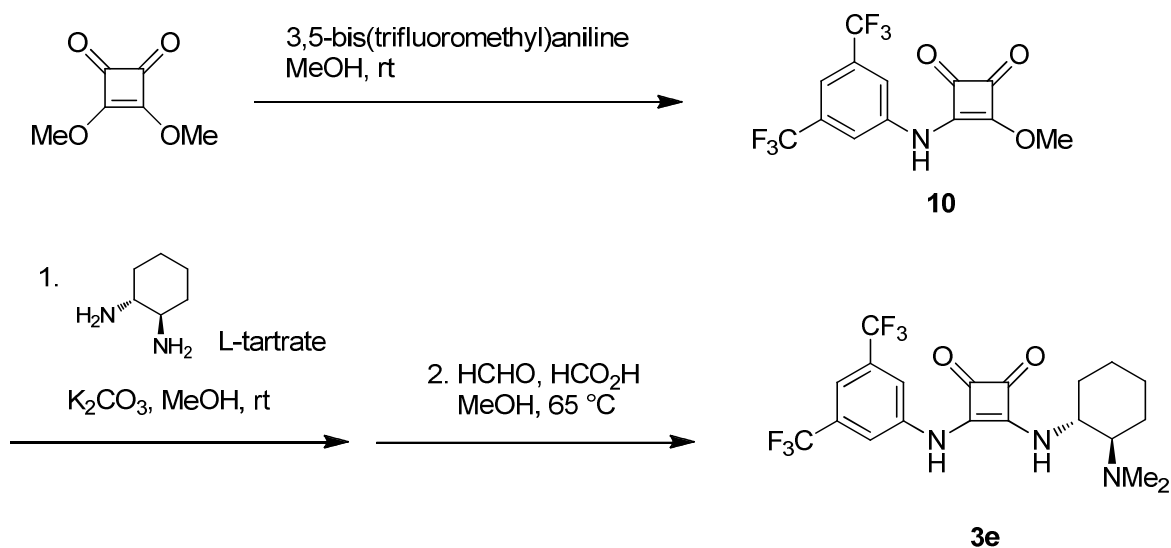
Supporting Information Table of Contents

S2	General methods and materials
S2	Preparation of squaramide catalysts
S4	General experimental procedure of α -hydrazination reactions
S4	Analytical data of α -hydrazination products
S10	Synthesis of azodicarboxylate 7
S11	Determination of the absolute stereochemistry of hydrazination products 6b and 6e (a) Discussion
S15	Determination of the absolute stereochemistry of hydrazination products 6b and 6e (b) Experimental procedures
S16	X-ray crystal structure of 22
S17	References
S19	NMR spectra
S39	HPLC traces
S57	X-ray crystal structure data for 22

General. All reactions were performed in oven dried or flame dried glassware under N₂ atmosphere. Reactions were monitored by TLC on Whatman silica gel 60 Å F254 plates visualized by anisaldehyde and ceric ammonium molybdate staining solutions. Flash column chromatography was performed on Dynamic Adsorbents 32-63 µm Flash silica gel. NMR spectra were measured on Bruker DRX and DMX spectrometers at 500 MHz for ¹H spectra and 125 MHz for ¹³C spectra and calibrated from residual solvent signal (chloroform at 7.26 ppm and DMSO at 2.50 ppm for ¹H spectra; chloroform at 77.0 ppm and DMSO at 39.51 ppm for ¹³C spectra). Infrared spectra were measured on a Nicolet 6700 FT-IR spectrometer on NaCl plates. Mass spectral analysis was performed by the CUNY Mass Spectrometry Facility at Hunter College (New York, NY) directed by Dr. Clifford Soll. Enantiomeric excesses (ee) were determined by HPLC analysis using an Agilent 1100 Series instrument with Daicel Chiralpak IA or Chiralpak OD-H columns, as indicated. Melting point was measured using a Laboratory Devices MEL-TEMP Apparatus or a Thomas Hoover Uni-Melt Capillary Melting Point Apparatus. Optical rotation was measured on a Jasco DIP-1000 Digital Polarimeter at the indicated concentration with units g/100 mL.

Materials. All commercially available reagents were used as received unless otherwise stated. Methylene chloride (CH₂Cl₂), tetrahydrofuran (THF), and toluene were purified by passage over activated alumina. MeOH (99.8%, extra dry) was purchased from Acros Organics. 3,4-Dimethoxy-3-cyclobutene-1,2-dione (dimethyl squarate) is a generous gift from Professor Leo A. Paquette (Ohio State University). β-Ketoesters **1a**, **1b**, **1c**, **1g**, and 1,3-diketone **1h** were purchased from Aldrich and distilled prior to use. 1,3-Dicarbonyl compounds **1d**,¹ **1e**,² **1f**,³ **1i**,⁴ **1j-1k**,⁵ **1l**,⁶ **1m**,⁷ **1n**,⁸ and **1o**⁹ were synthesized according to precedent literature. Azodicarboxylates **2** and **5** were purchased from Aldrich. Pyridine was AcroSeal™ anhydrous grade. *N*-Bromosuccinimide was recrystallized from H₂O. Et₃N was distilled from CaH₂.

Preparation of squaramide catalysts. Squaramide catalysts **3a-3l** were synthesized according to previous reports^{10,11} or by a representative experimental procedure shown below.

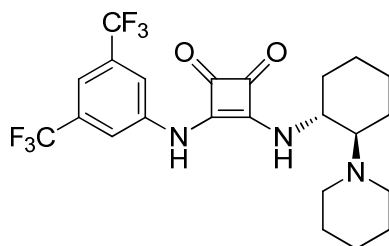


Squaramide 3e. To a solution of 3,4-dimethoxy-3-cyclobutene-1,2-dione (2.00 g, 14.1 mmol) in MeOH (20 mL) was added 3,5-bis(trifluoromethyl)aniline (2.40 mL, 15.5 mmol, 1.1 equiv). The mixture was

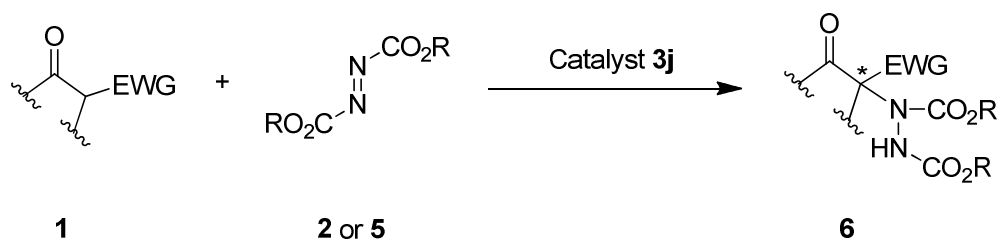
stirred at rt for 2d (yellow precipitate was generated). The reaction mixture was filtered with the aid of MeOH. Obtained yellow solid was dried *in vacuo* to give **10** (4.59 g, 13.5 mmol, 96%).

To a suspension of (*R,R*)-1,2-diaminocyclohexanes L-tartrate (857 mg, 3.24 mmol, 1.1 equiv) in MeOH (10 mL) was added K₂CO₃ (896 mg, 6.49 mmol, 2.2 equiv). The reaction mixture was stirred at rt for 1h and then **10** (1.00 g, 2.95 mmol) was added. The resulting mixture was stirred at rt for 2h, diluted with CHCl₃ (100 mL) and then filtered through a pad of Celite with the aid of CHCl₃. The filtrate and washings were combined and concentrated *in vacuo* to give the crude amine.

To a solution of the crude amine in MeOH (10 mL) was added 37% aqueous HCHO (5 mL, 67 mmol, 23 equiv) and HCO₂H (5 mL, 133 mmol, 45 equiv) at rt. The reaction mixture was stirred under reflux for 12 h, then basified by 6 M aq NaOH to pH12 and extracted with CH₂Cl₂. The combined organic layers were dried over MgSO₄ and then concentrated. Obtained residue was purified by recrystallization from *i*-PrOH and H₂O to give squaramide catalyst **3e** (663 mg, 1.48 mmol, 50%) as a white solid: Mp 196-198 °C (Decomp.); ¹H NMR (500 MHz, DMSO-*d*₆) δ 10.36 (br s, 1H), 8.07 (s, 2H), 7.85 (br s, 1H), 7.65 (s, 1H), 3.78-3.93 (m, 1H), 2.36-2.46 (m, 1H), 2.19 (s, 6H), 2.04-2.14 (m, 1H), 1.80-1.90 (m, 1H), 1.71-1.79 (m, 1H), 1.63-1.70 (m, 1H), and 1.13-1.41 (m, 4H); ¹³C NMR (125 MHz, DMSO-*d*₆) δ 184.4, 179.9, 169.4, 162.2, 141.2, 131.7, 131.4, 131.1, 130.9, 126.4, 124.2, 122.0, 119.9, 117.9, 114.5, 66.1, 54.7, 39.9, 34.4, 24.3, and 21.2; IR (film) 3207, 3149, 2944, 2866, 2788, 1790, 1671, 1654, 1579, 1531, 1488, 1473, 1454, 1379, 1276, 1174, and 1121 cm⁻¹; HRMS (ESI) [M+H]⁺ calcd for C₂₀H₂₁F₆N₃O₂: 450.1611; found 450.1605; [α]_D²⁸ -50.76 (*c* 1.00, DMSO).



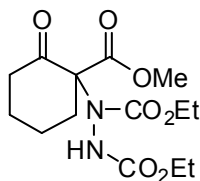
Squaramide 3j: Prepared according to published procedure¹¹ in 65% yield. Yellow solid. Mp 136-138 °C (Decomp.); ¹H NMR (500 MHz, DMSO-*d*₆) δ 10.22 (br s, 1H), 8.06 (s, 2H), 7.65 (s, 1H), 7.61 (br s, 1H), 3.82-4.00 (m, 1H), 2.55-2.68 (m, 2H), 2.18-2.37 (m, 3H), 1.98-2.12 (m, 1H), 1.79-1.91 (m, 1H), 1.63-1.79 (m, 2H), and 1.17-1.43 (m, 10H); ¹³C NMR (125 MHz, DMSO-*d*₆) δ 184.6, 180.0, 170.1, 161.6, 141.2, 131.7, 131.4, 131.2, 130.9, 126.4, 124.2, 122.1, 119.9, 117.8, 114.5, 68.2, 54.4, 49.4, 33.8, 26.3, 24.7, 24.4, 24.3, and 23.3; IR (film) 3245, 3084, 2934, 2859, 2805, 1794, 1673, 1593, 1558, 1473, 1452, 1379, 1278, 1181, and 1134 cm⁻¹; HRMS (ESI) [M+H]⁺ calcd for C₂₃H₂₅F₆N₃O₂: 490.1924; found 490.1930; [α]_D²⁸ -18.62 (*c* 0.43, DMSO).



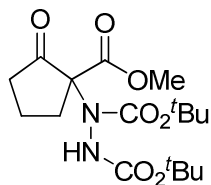
Typical experimental procedure for α -hydrazination reaction of 1,3-dicarbonyl compound using squaramide catalyst at room temperature. To a solution of squaramide catalyst **3** (0.1-2 mol%) in toluene (0.500 mL) was added azodicarboxylate **2** or **5** (0.500 mmol, 1.0 equiv) and 1,3-dicarbonyl compound **1** (0.750 mmol, 1.5 equiv or 0.550 mmol, 1.1 equiv). The mixture was stirred at rt until TLC analysis showed that **2** or **5** was completely consumed. The reaction mixture was directly purified by silica gel chromatography to afford the desired product **4** or **6**. Enantiomeric excess was determined by HPLC analysis using IA or OD-H column.

Representative experimental procedure for α -hydrazination reaction of 1,3-dicarbonyl compound using squaramide catalyst at low temperature (Table 2, entry 14). To a solution of squaramide catalyst **3j** (2.45 mg, 0.005 mmol, 1 mol%) in toluene (0.200 mL) was added azodicarboxylate **5** (127 mg, 0.500 mmol, 1.0 equiv) and the reaction mixture was cooled to the indicated temperature. A solution of β -ketoester **11** (115 mg, 0.550 mmol, 1.1 equiv) in toluene (0.200 mL) was slowly added to the reaction mixture, followed by a rinse with toluene (0.100 mL). The mixture was stirred at the indicated temperature until TLC analysis showed that **5** was completely consumed. The reaction mixture was directly purified by column chromatography on silica gel (hexanes/EtOAc 15/1 to 4/1) to afford the desired product **6l** (217 mg, 0.501 mmol, quant. yield). Enantiomeric excess was determined by HPLC analysis using IA column and found to be 90% ee.

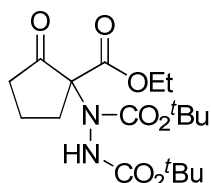
Note on spectroscopic data. Due to restricted rotation around the carbamate C-N bonds, the hydrazination products exist as mixtures of rotamers at room temperature. As a result, complex ^1H and ^{13}C spectra with broad and/or multiple signals are obtained. Therefore, instead of listing the chemical shifts in the characterization data, the actual spectra reproduced below are indicated.



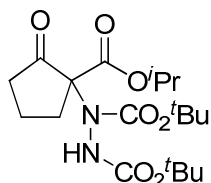
Diethyl 1-(1-(methoxycarbonyl)-2-oxocyclohexyl)hydrazine-1,2-dicarboxylate (4**):** Purification by column chromatography on silica gel (hexanes/EtOAc 15/1 to 8/1); colorless oil; ^1H NMR (500 MHz, CDCl_3) see below; ^{13}C NMR (125 MHz, CDCl_3) see below; IR (neat) 3296, 2952, 1728, 1444, 1375, 1326, 1278, 1219, 1120, 1093, 1061, 762, 567 cm^{-1} ; HRMS (ESI) $[\text{M} + \text{Na}]^+$ calcd for $\text{C}_{14}\text{H}_{23}\text{N}_2\text{O}_7$: 331.1500; found 331.1304; $[\alpha]_D^{25} +12.92$ (c 1.00, CHCl_3 , 92% ee); HPLC (CHIRALPAC IA, 0.46 $\text{cm}\phi \times 25$ cmL , hexanes/2-propanol = 95/5, flow rate 1.0 mL/min, UV detection at 220 nm) $t_R = 22.4$ min (minor), $t_R = 25.9$ min (major), 95% ee.



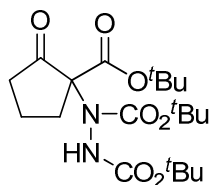
Di-tert-butyl 1-(1-(methoxycarbonyl)-2-oxocyclopentyl)hydrazine-1,2-dicarboxylate (6b): Purification by column chromatography on silica gel (hexanes to hexanes/EtOAc 4/1); colorless oil; ^1H NMR (500 MHz, CDCl_3) see below; ^{13}C NMR (125 MHz, CDCl_3) see below; IR (neat) 3328, 2978, 1734, 1456, 1367, 1244, 1154, 998, 756 cm^{-1} ; HRMS (ESI) $[\text{M} + \text{Na}]^+$ calcd for $\text{C}_{17}\text{H}_{28}\text{N}_2\text{O}_7$: 395.1789; found 395.1790; $[\alpha]_{\text{D}}^{29} +5.74$ (c 1.44, CHCl_3 , 96% ee); HPLC (CHIRALPAC IA, 0.46 $\text{cm}\varnothing \times 25$ cmL , hexanes/ethanol = 95/5, flow rate 1.0 mL/min , UV detection at 210 nm) $t_{\text{R}} = 7.1$ min (minor), $t_{\text{R}} = 7.9$ min (major).



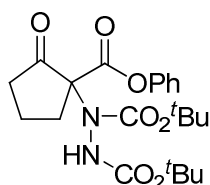
Di-tert-butyl 1-(1-(ethoxycarbonyl)-2-oxocyclopentyl)hydrazine-1,2-dicarboxylate (6c)¹²: Purification by column chromatography on silica gel (hexanes to hexanes/EtOAc 9/1); colorless oil. Analytical data matched previously reported values.¹² $[\alpha]_{\text{D}}^{30} +3.52$ (c 1.20, CHCl_3 , 96% ee); Lit.¹² $[\alpha]_{\text{D}}^{32} -3.47$ (c 1.09, CHCl_3 , 97% ee); HPLC (CHIRALPAC IA, 0.46 $\text{cm}\varnothing \times 25$ cmL , hexanes/ethanol = 95/5, flow rate 1.0 mL/min , UV detection at 210 nm) $t_{\text{R}} = 6.0$ min (minor), $t_{\text{R}} = 6.5$ min (major).



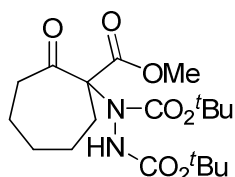
Di-tert-butyl 1-(1-(isopropoxycarbonyl)-2-oxocyclopentyl)hydrazine-1,2-dicarboxylate (6d): Purification by column chromatography on silica gel (hexanes to hexanes/EtOAc 9/1); colorless oil that solidified to white solid on standing at 4 $^{\circ}\text{C}$; Mp 68-70 $^{\circ}\text{C}$; ^1H NMR (500 MHz, CDCl_3) see below; ^{13}C NMR (125 MHz, CDCl_3) see below; IR (neat) 3331, 2979, 1725, 1457, 1367, 1241, 1155, 1104, 1033, 979, 918, 852, 758, 534 cm^{-1} ; HRMS (ESI) $[\text{M} + \text{Na}]^+$ calcd for $\text{C}_{19}\text{H}_{32}\text{N}_2\text{O}_7$: 423.2102; found 423.2104; $[\alpha]_{\text{D}}^{28} +1.63^{\circ}$ (c 1.10, CHCl_3 , 96% ee); HPLC (CHIRALPAC IA, 0.46 $\text{cm}\varnothing \times 25$ cmL , hexanes/2-propanol = 95/5, flow rate 1.0 mL/min , UV detection at 210 nm) $t_{\text{R}} = 7.9$ min (minor), $t_{\text{R}} = 11.1$ min (major).



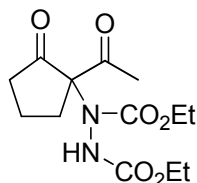
Di-tert-butyl 1-(1-(tert-butoxycarbonyl)-2-oxocyclopentyl)hydrazine-1,2-dicarboxylate (6e)¹³ : Purification by column chromatography on silica gel (hexanes to hexanes/EtOAc 9/1); colorless oil. Analytical data matched previously reported values.¹³ $[\alpha]_D^{29} +2.40$ (*c* 0.91, CHCl₃, 94% ee); Lit.¹³ $[\alpha]_D^{rt} -2.7$ (*c* 1.0, CHCl₃, 89% ee); HPLC (CHIRALPAC IA, 0.46 cm \times 25 cmL, hexanes/2-propanol = 98/2, flow rate 1.0 mL/min, UV detection at 210 nm) $t_R = 14.9$ min (minor), $t_R = 19.4$ min (major).



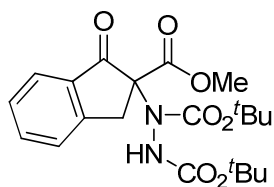
Di-tert-butyl 1-(1-(phenoxycarbonyl)-2-oxocyclopentyl)hydrazine-1,2-dicarboxylate (6f): Purification by column chromatography on silica gel (hexanes to hexanes/EtOAc 4/1); white flakes; Mp 35 - 37 °C; ¹H NMR (500 MHz, CDCl₃) see below; ¹³C NMR (125 MHz, CDCl₃) see below; IR (neat) 3342, 2978, 2933, 1747, 1711, 1592, 1492, 1457, 1368, 1245, and 1160 cm⁻¹; HRMS (ESI) [M + Na]⁺ calcd for C₂₂H₃₀N₂O₇: 457.1945; found 457.1954; $[\alpha]_D^{27} +1.83$ (*c* 1.00, CHCl₃, 95% ee); HPLC (CHIRALPAC IA, 0.46 cm \times 25 cmL, hexanes/2-propanol = 97/3, flow rate 1.0 mL/min, UV detection at 210 nm) $t_R = 18.2$ min (minor), $t_R = 27.1$ min (major).



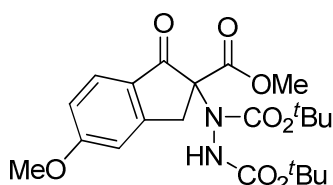
Di-tert-butyl 1-(1-(methoxycarbonyl)-2-oxocycloheptyl)hydrazine-1,2-dicarboxylate (6g): Purification by column chromatography on silica gel (hexanes to hexanes/EtOAc 9/1); white flakes; Mp 45 - 46 °C; ¹H NMR (500 MHz, CDCl₃) see below; ¹³C NMR (125 MHz, CDCl₃) see below; IR (neat) 3306, 2978, 2934, 1723, 1477, 1456, 1368, 1238, and 1152 cm⁻¹; HRMS (ESI) [M + Na]⁺ calcd for C₁₉H₃₂N₂O₇: 423.2102; found 423.2106; $[\alpha]_D^{30} +11.67$ (*c* 1.02, CHCl₃, 94% ee); HPLC (CHIRALPAC OD-H, 0.46 cm \times 25 cmL, hexanes/2-propanol = 97/3, flow rate 1.0 mL/min, UV detection at 210 nm) $t_R = 5.9$ min (major), $t_R = 7.9$ min (minor).



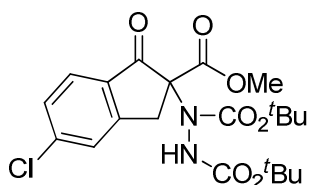
Diethyl 1-(1-acetyl-2-oxocyclopentyl)hydrazine-1,2-dicarboxylate (6h): Purification by column chromatography on silica gel (hexanes/EtOAc 4/1 to 2/1); colorless oil; ¹H NMR (500 MHz, CDCl₃) see below; ¹³C NMR (125 MHz, CDCl₃) see below; IR (neat) 3298, 2982, 1750, 1717, 1510, 1404, 1377, 1335, and 1235 cm⁻¹; HRMS (ESI) [M + Na]⁺ calcd for C₁₃H₂₀N₂O₆: 323.1214; found 323.1214; $[\alpha]_D^{30} -119.29$ (*c* 0.54, CHCl₃, 91% ee); HPLC (CHIRALPAC OD-H, 0.46 cm \times 25 cmL, hexanes/ethanol = 95/5, flow rate 1.0 mL/min, UV detection at 210 nm) $t_R = 9.2$ min (major), $t_R = 10.8$ min (minor).



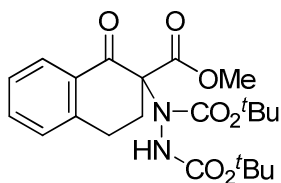
Di-tert-butyl 1-(2-(methoxycarbonyl)-1-oxo-2,3-dihydro-1H-inden-2-yl)hydrazine-1,2-dicarboxylate (6i): Purification by column chromatography on silica gel (hexanes/EtOAc 15/1 to 4/1); colorless oil; ^1H NMR (500 MHz, CDCl_3) see below; ^{13}C NMR (125 MHz, CDCl_3) see below; IR (neat) 3328, 2978, 1728, 1608, 1477, 1367, 1247, 1151, 1082, 1007, 853, 752 cm^{-1} ; HRMS (ESI) $[\text{M} + \text{Na}]^+$ calcd for $\text{C}_{21}\text{H}_{28}\text{N}_2\text{O}_7$: 443.1789; found 443.1793; $[\alpha]_D^{25} +93.64$ (c 1.00, CHCl_3 , 88% ee); HPLC (CHIRALPAC IA, 0.46 $\text{cm}\phi \times 25$ cmL, hexanes/2-propanol = 90/10, flow rate 1.0 mL/min, UV detection at 220 nm) $t_R = 12.3$ min (minor), $t_R = 15.8$ min (major).



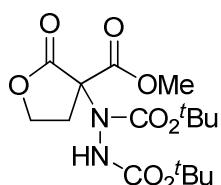
Di-tert-butyl 1-(5-methoxy-2-(methoxycarbonyl)-1-oxo-2,3-dihydro-1H-inden-2-yl)hydrazine-1,2-dicarboxylate (6j): Purification by column chromatography on silica gel (hexanes/EtOAc 20/1); pale yellow oil; ^1H NMR (500 MHz, CDCl_3) see below; ^{13}C NMR (125 MHz, CDCl_3) see below; IR (neat) 2978, 1717, 1600, 1490, 1367, 1257, 1151, 1082, 1007, 756 cm^{-1} ; HRMS (ESI) $[\text{M} + \text{Na}]^+$ calcd for $\text{C}_{22}\text{H}_{30}\text{N}_2\text{O}_8$: 473.1894; found 473.1904; $[\alpha]_D^{25} +116.28$ (c 1.00, CHCl_3 , 90% ee); HPLC (CHIRALPAC IA, 0.46 $\text{cm}\phi \times 25$ cmL, hexanes/2-propanol = 90/10, flow rate 0.5 mL/min, UV detection at 220 nm) $t_R = 35.5$ min (minor), $t_R = 40.8$ min (major).



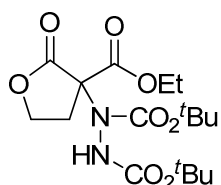
Di-tert-butyl 1-(5-chloro-2-(methoxycarbonyl)-1-oxo-2,3-dihydro-1H-inden-2-yl)hydrazine-1,2-dicarboxylate (6k): Purification by column chromatography on silica gel (hexanes/EtOAc 40/1 to 4/1); pale yellow oil; ^1H NMR (500 MHz, CDCl_3) see below; ^{13}C NMR (125 MHz, CDCl_3) see below; IR (neat) 3329, 2979, 1732, 1600, 1456, 1368, 1248, 1205, 1151, 1070, 1008, 901, 851, 756 cm^{-1} ; HRMS (ESI) $[\text{M} + \text{Na}]^+$ calcd for $\text{C}_{21}\text{H}_{27}\text{ClN}_2\text{O}_7$: 477.1399; found 477.1403; $[\alpha]_D^{25} +88.96$ (c 1.00, CHCl_3 , 88% ee); HPLC (CHIRALPAC IA, 0.46 $\text{cm}\phi \times 25$ cmL, hexanes/2-propanol = 97/3, flow rate 0.8 mL/min, UV detection at 220 nm) $t_R = 29.9$ min (major), $t_R = 41.9$ min (minor).



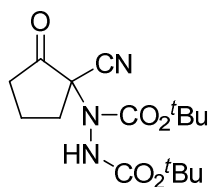
Di-tert-butyl 1-(2-(methoxycarbonyl)-1-oxo-1,2,3,4-tetrahydronaphthalen-2-yl)hydrazine-1,2-dicarboxylate (6l): Purification by column chromatography on silica gel (hexanes/EtOAc 15/1 to 4/1); white needles; Mp 120-121 °C; ^1H NMR (500 MHz, CDCl_3) see below; ^{13}C NMR (125 MHz, CDCl_3) see below; IR (neat) 2978, 1721, 1602, 1481, 1455, 1368, 1298, 1238, 1155, 1054, 853, 756, 573 cm^{-1} ; HRMS (ESI) $[\text{M} + \text{Na}]^+$ calcd for $\text{C}_{22}\text{H}_{30}\text{N}_2\text{O}_7$: 457.1945; found 457.1950; $[\alpha]^{23}_{\text{D}} +24.04$ (c 1.00, CHCl_3 , 90% ee); HPLC (CHIRALPAC IA, 0.46 $\text{cm}\varnothing \times 25$ cmL , hexanes/2-propanol = 80/20, flow rate 1.0 mL/min , UV detection at 220 nm) $t_R = 8.8$ min (major), $t_R = 12.8$ min (minor).



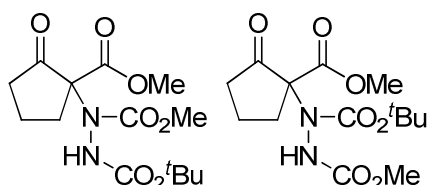
Di-tert-butyl 1-(3-(methoxycarbonyl)-2-oxotetrahydrofuran-3-yl)hydrazine-1,2-dicarboxylate (6m): Purification by column chromatography on silica gel (hexanes/EtOAc 15/1 to 9/1); white solid; Mp 151-152 °C; ^1H NMR (500 MHz, CDCl_3) see below; ^{13}C NMR (125 MHz, CDCl_3) see below; IR (neat) 3385, 2977, 1786, 1741, 1495, 1456, 1367, 1246, 1164, 1020, 853, 757 cm^{-1} ; HRMS (ESI) $[\text{M} + \text{Na}]^+$ calcd for $\text{C}_{16}\text{H}_{26}\text{N}_2\text{O}_8$: 397.1581; found 397.1583; $[\alpha]^{24}_{\text{D}} +48.00$ (c 1.00, CHCl_3 , 98% ee); HPLC (CHIRALPAC OD-H, 0.46 $\text{cm}\varnothing \times 25$ cmL , hexanes/2-propanol = 97/3, flow rate 0.5 mL/min , UV detection at 220 nm) $t_R = 16.7$ min (minor), $t_R = 19.1$ min (major).



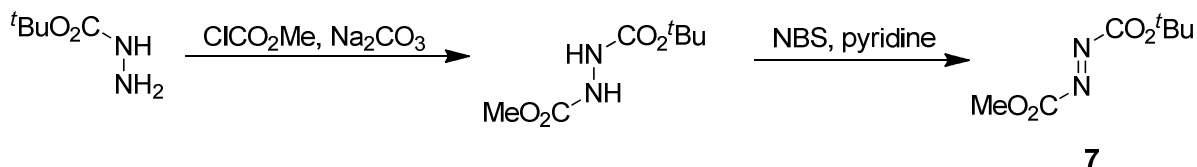
Di-tert-butyl 1-(3-(ethoxycarbonyl)-2-oxotetrahydrofuran-3-yl)hydrazine-1,2-dicarboxylate (6n): Purification by column chromatography on silica gel (hexanes/EtOAc 9/1 to 4/1); colorless oil; ^1H NMR (500 MHz, CDCl_3) see below; ^{13}C NMR (125 MHz, CDCl_3) see below; IR (neat) 3332, 2979, 1789, 1739, 1480, 1368, 1260, 1155, 1091, 1027, 802 cm^{-1} ; HRMS (ESI) $[\text{M} + \text{Na}]^+$ calcd for $\text{C}_{17}\text{H}_{28}\text{N}_2\text{O}_8$: 411.1738; found 411.1741; $[\alpha]^{25}_{\text{D}} +37.10$ (c 0.63, CHCl_3 , 95% ee); HPLC (CHIRALPAC IA, 0.46 $\text{cm}\varnothing \times 25$ cmL , hexanes/2-propanol = 97/3, flow rate 1.0 mL/min , UV detection at 220 nm) $t_R = 13.4$ min (minor), $t_R = 15.7$ min (major).



Di-tert-butyl 1-(1-cyano-2-oxocyclopentyl)hydrazine-1,2-dicarboxylate (60): Purification by column chromatography on silica gel (hexanes/EtOAc 15/1); white needles; Mp 139-140 °C; ^1H NMR (500 MHz, CDCl_3) see below; ^{13}C NMR (125 MHz, CDCl_3) see below; IR (neat) 3310, 2979, 1772, 1711, 1506, 1369, 1257, 1153, 955, 848, 759 cm^{-1} ; HRMS (ESI) $[\text{M} + \text{Na}]^+$ calcd for $\text{C}_{16}\text{H}_{25}\text{N}_3\text{O}_5$: 362.1686; found 362.1692; $[\alpha]_D^{24} +8.96$ (c 1.00, CHCl_3 , 90% ee); HPLC (CHIRALPAC IA, 0.46 $\text{cm}\varnothing \times 25$ cmL , hexanes/2-propanol = 90/10, flow rate 1.0 mL/min , UV detection at 220 nm) $t_R = 7.7$ min (major), $t_R = 10.9$ min (minor).



2-tert-Butyl 1-methyl 1-(1-(methoxycarbonyl)-2-oxocyclopentyl)hydrazine-1,2-dicarboxylate (8) and 1-tert-Butyl 2-methyl 1-(1-(methoxycarbonyl)-2-oxocyclopentyl)hydrazine-1,2-dicarboxylate (9): Purification by column chromatography on silica gel (hexanes/EtOAc 9/1 to 4/1); colorless oil; a 66:34 mixture of two regioisomers (determined by HPLC analysis, see below); ^1H NMR (500 MHz, CDCl_3) see below; ^{13}C NMR (125 MHz, CDCl_3) see below; IR (neat) 3328, 2978, 1734, 1456, 1367, 1244, 1154, 998, 756 cm^{-1} ; HRMS (ESI) $[\text{M} + \text{Na}]^+$ calcd for $\text{C}_{14}\text{H}_{22}\text{N}_2\text{O}_7$: 353.1319; found 353.1326; HPLC (CHIRALPAC IA, 0.46 $\text{cm}\varnothing \times 25$ cmL , hexanes/ethanol = 95/5, flow rate 1.0 mL/min , UV detection at 210 nm) major regioisomer: $t_R = 10.3$ min (minor), $t_R = 13.3$ min (major); minor regioisomer: $t_R = 11.3$ min (minor), $t_R = 18.8$ min (major).

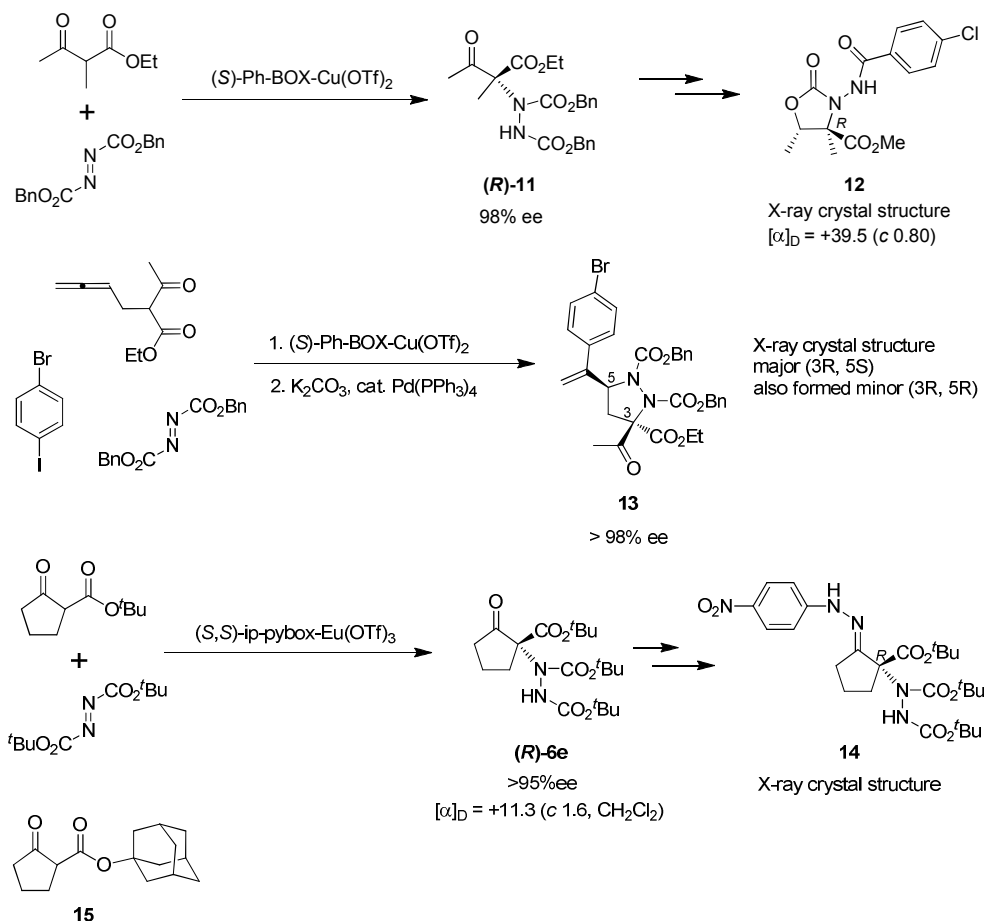


Synthesis of *tert*-butyl methyl azodicarboxylate (7).¹⁴ A solution of *tert*-butyl carbazate (1.0 g, 7.6 mmol, 1.0 equiv) in 15 mL of CH₂Cl₂ was cooled at -78 °C while methyl chloroformate (0.70 mL, 0.86 g, 9.1 mmol, 1.2 equiv) was added dropwise over 5 min. Sodium carbonate (0.802 g, 7.6 mmol, 1.0 equiv) was then added in one portion. The reaction mixture was allowed to warm to rt and stirred for 24 h, then filtered through a pad of Celite with the aid of CH₂Cl₂ and concentrated to give 1.297 g (90% yield) of *tert*-butyl methyl hydrazinedicarboxylate¹⁵ as a white solid: Mp 102-104 °C (Lit.¹⁵ 101-101.5 °C); ¹H NMR (500 MHz, CDCl₃) δ 6.37 (br s, 1H), 6.26 (br s, 1H), 3.76 (s, 3H), and 1.48 (s, 9H); ¹³C NMR (125 MHz, CDCl₃) δ 157.4, 155.9, 81.4, 52.7, and 27.9; IR (neat) 3307, 2979, 1715, 1508, 1368, 1245, 1161, and 1062 cm⁻¹; HRMS (ESI) [M + Na]⁺ calcd for C₇H₁₄N₂O₄: 213.0846; found 213.0847. To a solution of *tert*-butyl methyl hydrazinedicarboxylate (0.476 g, 2.50 mmol, 1.0 equiv) and pyridine (0.20 mL, 0.20 g, 2.5 mmol, 1.0 equiv) in 6 mL of CH₂Cl₂ was added *N*-bromosuccinimide (0.445 g, 2.50 mmol, 1.0 equiv). The reaction mixture was stirred at rt for 20 min and then diluted with 30 mL of CH₂Cl₂. This was then washed with two 40-mL portions of H₂O, 40 mL of 1M NaOH solution, 40 mL of sat NaCl solution, dried over MgSO₄, filtered, and then concentrated to 0.394 g (84% yield) of *tert*-butyl methyl azodicarboxylate (7) as an orange oil: ¹H NMR (500 MHz, CDCl₃) δ 4.07 (s, 3H), and 1.63 (s, 9H); ¹³C NMR (125 MHz, CDCl₃) δ 160.9, 158.9, 87.1, 55.3, and 27.6; IR (neat) 2986, 1778, 1458, 1438, 1398, 1373, 1249, and 1150 cm⁻¹; HRMS (ESI) [2M + Na]⁺ calcd for C₇H₁₂N₂O₄: 399.1486; found 399.1468.

Determination of the absolute stereochemistry of hydrazination products **6b** and **6e**.

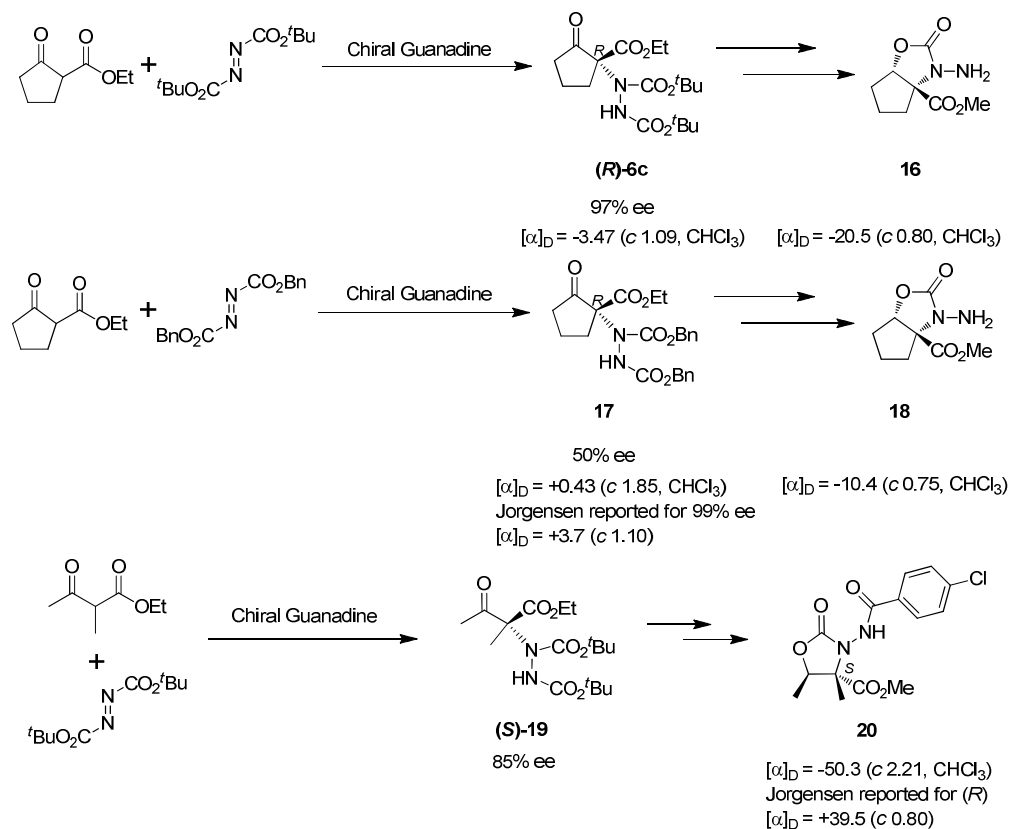
(a) Discussion

We are interested in the determination of the absolute stereochemistry of our hydrazination products to aid our study on the mechanism of asymmetric induction by the squaramide catalysts. A survey of the literature showed that a number of X-ray crystal structures have been solved to assign absolute configurations of these types of compounds. These reports are the following: (a) Jørgensen et al.¹⁶ reported (*R*) configuration for compound **11** by solving the X-ray crystal structure of derivative **12**. In the same work, cyclic β -keto esters were also used as substrates but the absolute stereochemistry of those products was not discussed; (b) Ma et al.¹⁷ analyzed the X-ray crystal structure of pyrazolidine derivative **13**, of which the stereochemistry at C-3 was controlled by the same Lewis acid catalyst as in Jørgensen's work, to get to the same conclusion of (*R*) configuration at the aminated carbon (3*R*); (c) Vallribera et al.¹⁸ examined these reactions with related catalysts and cyclic β -keto esters as substrates. Absolute stereochemistry of (*R*) for compound **6e** was assigned based on X-ray crystal structure of hydrazone **14**. In the same paper, the authors also studied reaction of β -keto ester **15** and the X-ray crystal structure of the hydrazination product was reported to show (*R*) configuration at the amino center.



A number of papers have since assigned the absolute stereochemistry of these amination products from their respective studies by correlation of optical rotation. Of these reports two showed the detail of their analysis including optical rotation data. The work of Terada et al.¹² used both acyclic and cyclic β -

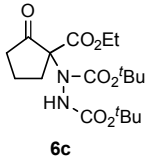
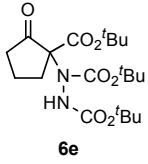
keto esters as substrates and the absolute stereochemistry of both types of products was assigned. For product **6c** from a cyclic substrate, derivative **16** was synthesized for the assignment of stereochemistry. To obtain the optical rotation value for compound **16** of known absolute stereochemistry, compound **18** was independently synthesized from amination product **17**, which was assigned (*R*) configuration by comparison of optical rotation data reported by Jørgensen et al.. This assignment is based on the assumption that acyclic and cyclic β -keto esters received the same sense of asymmetric induction in Jørgensen's work. This assignment for compound **17** allowed the amino center of derivative **16** to be assigned (*R*) configuration by correlation and similarly for compound **6c**. Intriguingly, product **19** from an acyclic β -keto ester substrate was converted to derivative **20** and assigned (*S*) configuration based on correlation with compound **12** in Jørgensen's report. As a result, Terada et al. reported that acyclic and cyclic β -keto esters provided products with opposite enantioselection under chiral guanadine catalysis, whereas this conclusion was based on the assumption that acyclic and cyclic β -keto esters produced products with the same enantioselection under chiral Lewis acid catalysis. Maruoka et al.¹⁹ later reported both compounds **6c** and **6e** and their optical rotation data. Compound **6c** generated from chiral phosphonium salt PTC conditions was assigned (*S*) configuration by correlation to Terada's results.



The relevant optical rotation data from literature and our work is summarized in Table 1. This comparison suggests (*S*) configuration for compound **6c** and (*R*) configuration for compound **6e** in the squaramide catalyzed reactions. We are skeptical that the steric difference of the ester groups should result in opposite enantioselection. Furthermore, there are uncertainties in both of the reported assignments. For the assignment of compound **6c** there was the assumption of analogy for fundamentally different substrate types (acyclic and cyclic). The assignment of compound **6e** relied on the X-ray

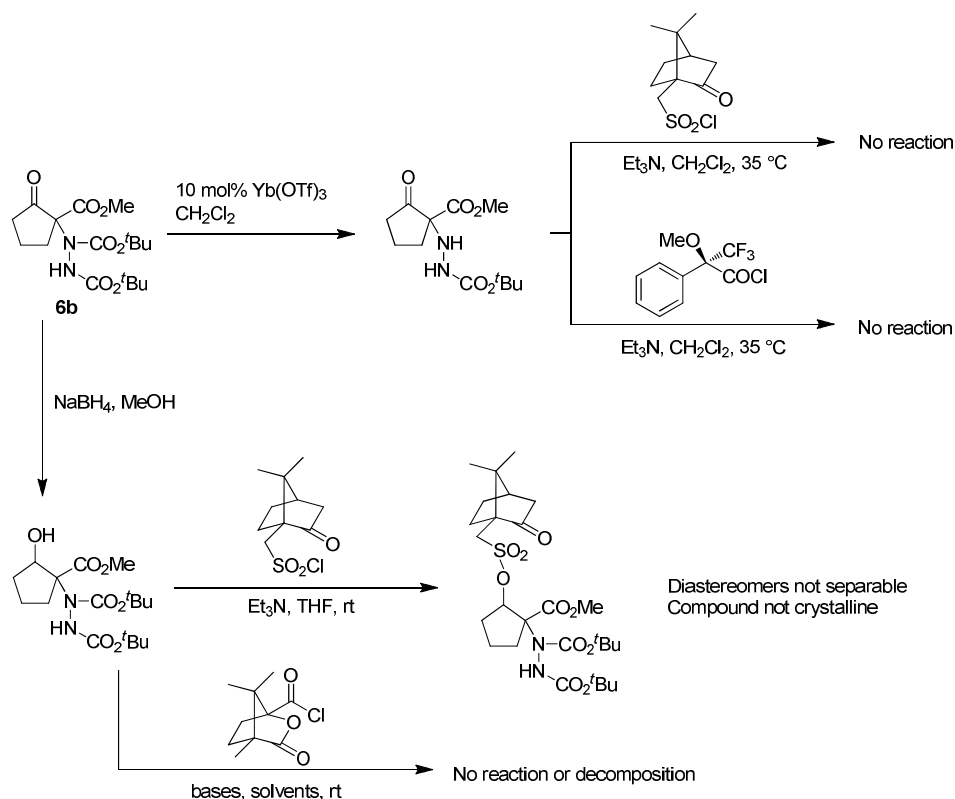
structure analysis of compound **14** which contains C, H, N, and O atoms but no heavy atoms at all. In view of these questions, we decided to assign the absolute stereochemistry of our products unambiguously.

Table 1. Comparison of Optical Rotation Data

$[\alpha]$ and assignment Compound	Terada	Vallribera	Maruoka	Rawal
 <p>6c</p>	97% ee, (<i>R</i>) $[\alpha]_D = -3.47$ (<i>c</i> 1.09, CHCl ₃)	NA	73% ee, (<i>S</i>) by correlation $[\alpha]_D = +2.25$ (<i>c</i> 1.22, CHCl ₃)	96% ee $[\alpha]_D^{30} +3.52$ (<i>c</i> 1.20, CHCl ₃)
 <p>6e</p>	NA	> 95% ee, (<i>R</i>) $[\alpha]_D = +11.3$ (<i>c</i> 1.6, CH ₂ Cl ₂)	95% ee $[\alpha]_D = +2.42$ (<i>c</i> 0.88, CHCl ₃)	94% ee $[\alpha]_D^{29} +2.40$ (<i>c</i> 0.91, CHCl ₃) $[\alpha]_D^{31} +1.62$ (<i>c</i> 1.60, CH ₂ Cl ₂)

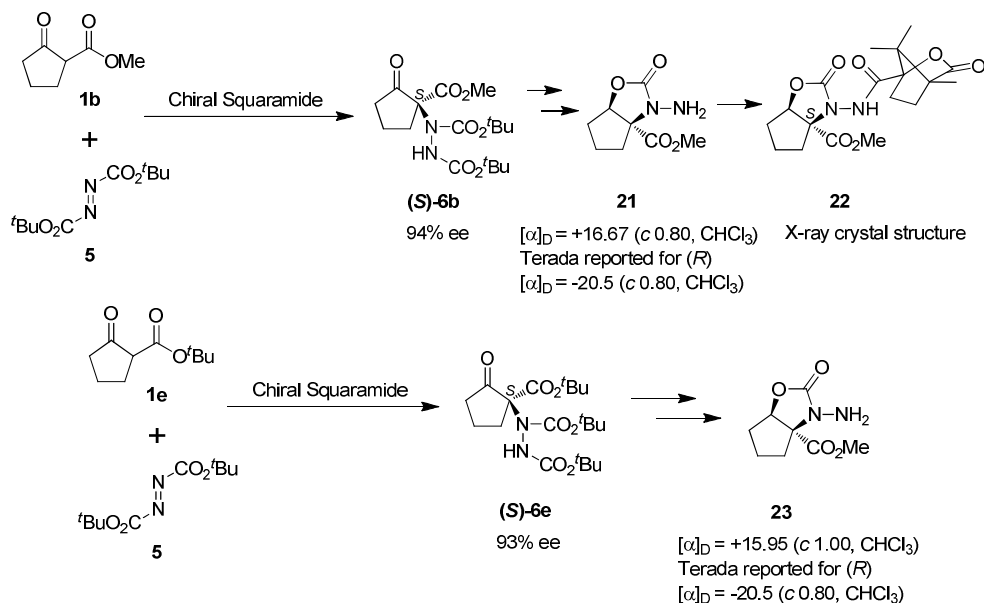
We have synthesized hydrazination products **6b** from the methyl ester and **6e** from the *tert*-butyl ester in high ee's. In preliminary work, samples of **6b** with 94% ee were obtained in reactions of β -keto ester **1b** with 1.1 equivalence of azodicarboxylate **5** in the presence of 0.5-1.0 mol% of catalyst **3e** in toluene at room temperature. These were used in the studies of absolute stereochemistry assignment. Initially, we attempted derivatization of **6b** by well-known chiral agents including 10-camphorsulfonyl chloride, Mosher's acid chloride, and camphanic chloride (Scheme 1). These agents are known to form crystalline (sulfonyl)esters or (sulfonyl)amides to aid the assignment of absolute configuration by X-ray crystal structure analysis. However, the synthesis and crystallization of these desired products have proven difficult.

Scheme 1. Initial Studies for the Assignment of Absolute Stereochemistry



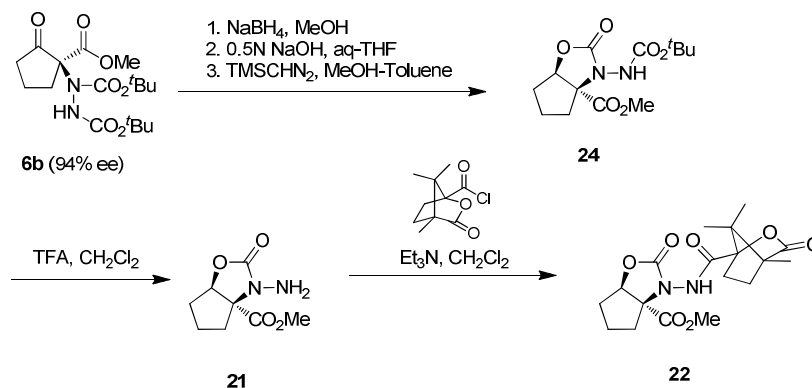
Eventually, we converted **6b** to amine **21**, then to amide **22** with (1*S*)-camphanic chloride. The X-ray crystal structure of amide **22** revealed (*S*) configuration at the quaternary amino center of **6b**. The optical rotation of amine **21** is correlated to Terada's report and thus confirms their assignment of (*R*) configuration for their product (–)-**6c** (which then affirms (*S*) configuration for (+)-**6c** from our squaramide catalyzed reactions, see Table 1). This also concludes that Jørgensen's hydrazination products derived from cyclic substrates indeed have (*R*) stereochemistry (from correlation of compounds **21** and **18**, then extension to compound **17**).

For compound (+)-**6e**, a similar sequence of transformation also led to amine **23**. (*S*) configuration for (+)-**6e** was then confirmed by correlation of derivative **23** to compound **21**. As a result, we can conclude that in our and Maruoka's work, both the ethyl and *tert*-butyl ester substrates provided products with (*S*) configuration at the newly formed stereocenter (Table 1). We also suggest that based on the optical rotation reported for compound **6e** by Vallribera et al.: [α]_D = +11.3 (*c* 1.6, CH₂Cl₂),¹⁸ their product should have (*S*) instead of the reported (*R*) configuration.



(b) Experimental procedures

Synthesis of amide 22 from 6b (unoptimized).

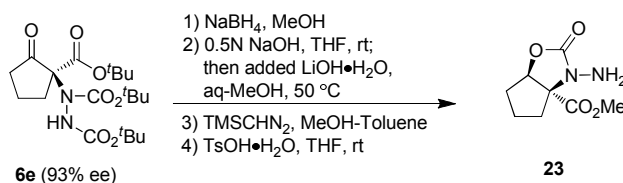


6b (0.390 g, 1.05 mmol, 94% ee) was converted to 0.217 g (69% yield) of known compound **24** via published procedure.¹² To a solution of **24** (0.190 g, 0.63 mmol) in 5 mL of CH₂Cl₂ was added trifluoroacetic acid (1.0 mL, 1.5 g, 13 mmol). The reaction mixture was heated at 40 °C for 5 min and then stirred at rt for 30 min. The volatile was removed and the residue was diluted with 5 mL of H₂O. This solution was neutralized with 10 mL of sat NaHCO₃ solution and then extracted with five 15-mL portions of EtOAc. The combined organic layers were washed with 15 mL of sat NaCl solution, dried over Na₂SO₄, filtered, and concentrated to 0.058 g of a yellow oil. This was purified by column chromatography on silica gel (hexanes/EtOAc 1/1 to 2/3) to afford 0.033 g (26% yield) of amine **21** as a very pale yellow oil. Analytical data matched previously reported values.¹² $[\alpha]_D^{24} +16.67$ (c 0.80, CHCl₃); Lit.¹² $[\alpha]_D^{32} -20.5$ (c 0.80, CHCl₃).

A solution of **21** (0.033g, 0.16 mmol, 1 equiv) in 1.6 mL of CH₂Cl₂ was cooled at 0 °C and treated with (1S)-(-)-camphanic chloride (0.071 g, 0.33 mmol, 2 equiv) followed by Et₃N (0.046 mL, 0.033 g, 0.33 mmol, 2 equiv). The resulting solution was stirred at rt for 5 h, quenched with 5 mL of sat NH₄Cl

solution and then extracted with five 10-mL portions of EtOAc. The combined organic phases were washed with 10 mL of sat NaCl solution, dried over Na₂SO₄, filtered, and concentrated to 0.088 g of a yellow paste. This was purified by column chromatography on silica gel (hexanes/EtOAc 4/1 to 2/1) to provide 0.036 g (57% yield) of amide **22** as a white solid: Mp 142-143 °C; ¹H NMR (500 MHz, CDCl₃) δ 8.25 (s, 1H), 4.95 (d, 1H, J = 5.6 Hz), 3.83 (s, 3H), 2.46-2.58 (m, 1H), 2.05-2.30 (m, 3H), 1.87-2.00 (m, 5H), 1.63-1.75 (m, 1H), 1.12 (s, 3H), 1.11 (s, 3H), and 1.08 (s, 3H); ¹³C NMR (125 MHz, CDCl₃) δ 177.7, 171.8, 166.9, 153.7, 91.7, 83.4, 73.5, 55.0, 54.6, 53.3, 34.4, 30.3, 28.7, 23.5, 16.3, 16.3, and 9.6; IR (film) 3296, 2967, 2881, 1784, 1740, 1707, 1497, 1446, 1397, 1317, 1284, 1243, 1125, and 1110 cm⁻¹; HRMS (ESI) [M+H]⁺ calcd for C₁₈H₂₄N₂O₇: 381.1656; found 381.1663; [α]_D²⁴ -66.54 (c 0.80, CHCl₃).

Synthesis of **23** from **6e** (unoptimized).



Amine **23** (0.010 g, 9% overall yield) was prepared from **6e** (0.238 g, 0.57 mmol, 93% ee) in a similar manner as the reported procedure.¹² Stronger basic conditions and elevated temperature was required in step 2 for the hydrolysis of the *tert*-butyl ester. Analytical data matched previously reported values.¹² [α]_D²⁵ +15.95 (c 1.00, CHCl₃); Lit.¹² [α]_D³² -20.5 (c 0.80, CHCl₃).

X-ray crystal structure of **22.** Crystallization from MeOH and H₂O yielded crystals of suitable quality for X-ray diffraction analysis.

Data Collection

An irregular broken fragment (0.40 x 0.40 x 0.40 mm) was selected under a stereo-microscope while immersed in Fluorolube oil to avoid possible reaction with air. The crystal was removed from the oil using a tapered glass fiber that also served to hold the crystal for data collection. The crystal was mounted and centered on a Bruker SMART APEX system at 100 K. Rotation and still images showed the diffractions to be sharp. Frames separated in reciprocal space were obtained and provided an orientation matrix and initial cell parameters. Final cell parameters were obtained from the full data set.

A “full sphere” data set was obtained which samples approximately all of reciprocal space to a resolution of 0.75 Å using 0.3° steps in ω using 10 second integration times for each frame. Data collection was made at 100 K. Integration of intensities and refinement of cell parameters were done using SAINT.²⁰ Absorption corrections were applied using SADABS²⁰ based on redundant diffractions.

Structure solution and refinement

The space group was determined as P2₁ based on systematic absences and intensity statistics. Direct methods were used to locate most C atoms from the E-map. Repeated difference Fourier maps

allowed recognition of all expected C, O and N atoms. Following anisotropic refinement of all non-H atoms, ideal H-atom positions were calculated. Final refinement was anisotropic for all non-H atoms, and isotropic-riding for H atoms. No anomalous bond lengths or thermal parameters were noted. All ORTEP diagrams have been drawn with 50% probability ellipsoids.

Equations of interest:

$$R_{\text{int}} = \Sigma |F_o^2 - \langle F_c^2 \rangle| / \Sigma |F_o^2|$$

$$R1 = \Sigma ||F_o| - |F_c|| / \Sigma |F_o|$$

$$wR2 = [\Sigma [w (F_o^2 - F_c^2)^2] / \Sigma [w (F_o^2)^2]]^{1/2}$$

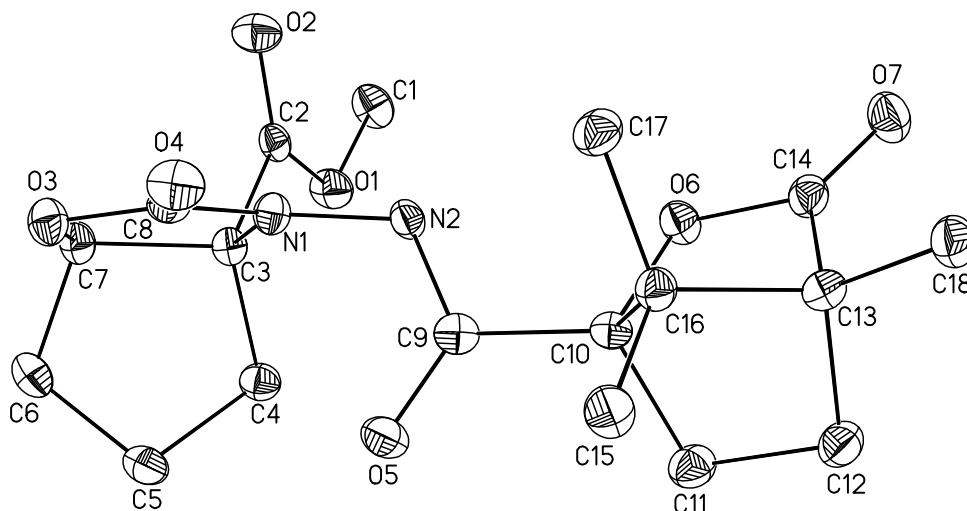
$$\text{Goof} = S = [\Sigma [w (F_o^2 - F_c^2)^2] / (n-p)]^{1/2}$$

$$\text{where: } w = q / \sigma^2 (F_o^2) + (aP)^2 + bP;$$

$$n = \text{number of independent reflections;}$$

$$q, a, b, P \text{ as defined in [1]}$$

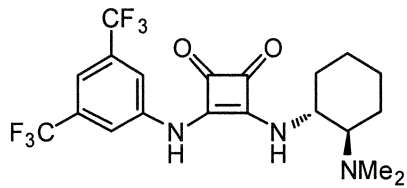
$$p = \text{number of parameters refined.}$$



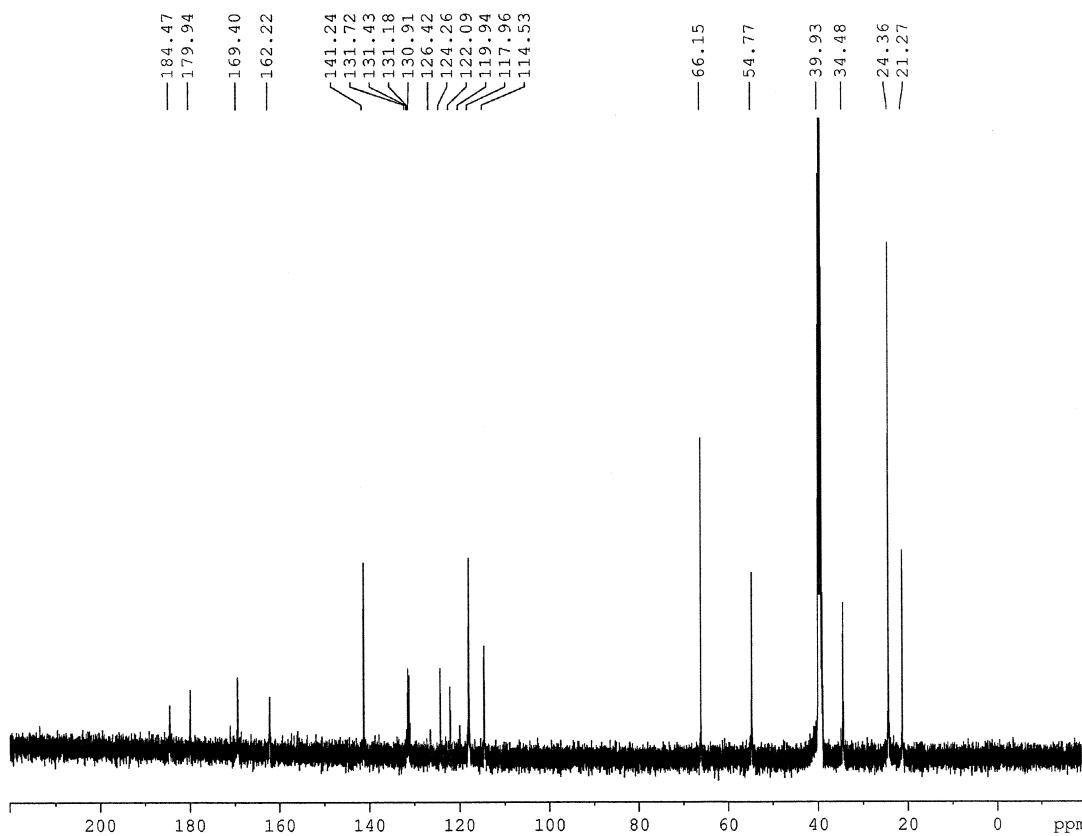
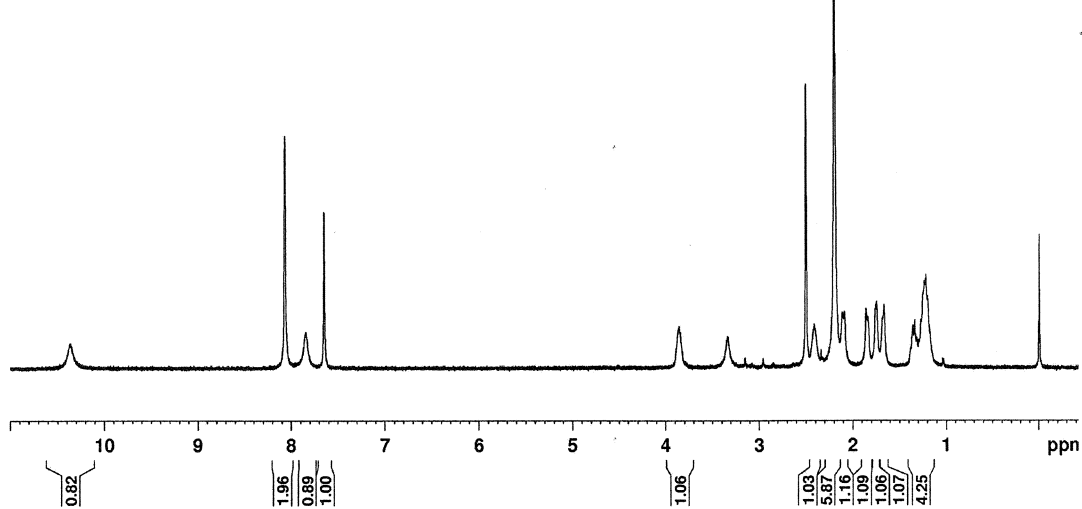
References

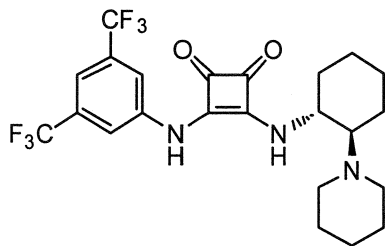
- (1) Christoffers, J.; Rößler, U.; Werner, T. *Eur. J. Org. Chem.* **2000**, 701-705.
- (2) Henderson, D.; Richardson, K. A.; Taylor, R. J. K. *Synthesis* **1983**, 996-997.
- (3) Presset, M.; Coquerel, Y.; Rodriguez, J. *J. Org. Chem.* **2009**, *74*, 415-418.
- (4) Emelen, K. V.; Wit, T. D.; Hoornaert, G. J.; Compennolle, F. *Tetrahedron* **2002**, *58*, 4225-4236.
- (5) Kobayashi, S.; Gustafsson, T.; Shimizu, Y.; Kiyohara, H.; Matsubara, R. *Org. Lett.* **2006**, *8*, 4923-4925.
- (6) Chakrabarty, M.; Sarkar, S.; Harigaya, Y. *Synthesis* **2003**, 2292-2294.
- (7) Quesada, M. L.; Schlessinger, R. H. *J. Org. Chem.* **1978**, *43*, 346-347.
- (8) Bukowska, M.; Prejzner, J. *Pol. J. Chem.* **1986**, *60*, 957-959.

- (9) Liu, H.-J.; Ly, T. W.; Tai, C.-L.; Wu, J.-D.; Liang, J.-K.; Guo, J.-C.; Tseng, N.-W.; Shia, K.-S. *Tetrahedron* **2003**, *59*, 1209-1226.
- (10) Malerich, J. P.; Hagihara, K.; Rawal, V. H. *J. Am. Chem. Soc.* **2008**, *130*, 14416-14417.
- (11) Zhu, Y.; Malerich, J. P.; Rawal, V. H. *Angew. Chem. Int. Ed.* **2010**, *49*, 153-156.
- (12) Terada, M.; Nakano, M.; Ube, H. *J. Am. Chem. Soc.* **2006**, *126*, 16044-16045.
- (13) Saaby, S.; Bella, M.; Jørgensen, K. A. *J. Am. Chem. Soc.* **2004**, *126*, 8120-8121.
- (14) This procedure is a modification of the method reported in: Mackay, D.; McIntyre, D. D. *Can. J. Chem.* **1984**, *62*, 335-360.
- (15) Zecchini, G. P.; Torrini, I.; Paradisi, M. P.; Lucente, G.; Mastropietro, G.; Spisani, S. *Amino Acids* **1998**, *14*, 301-309.
- (16) Marigo, M.; Juhl, K.; Jørgensen, K. A. *Angew. Chem. Int. Ed.* **2003**, *42*, 1367-1369.
- (17) Ma, S.; Jiao, N.; Zheng, Z.; Ma, Z.; Lu, Z.; Ye, L.; Deng, Y.; Chen, G. *Org. Lett.* **2004**, *6*, 2193-2196.
- (18) Comelles, J.; Pericas, À.; Moreno-Mañas, M.; Vallribera, A.; Drudis-Solé, G.; Lledos, A.; Parella, T.; Roglans, A.; García-Granda, S.; Rocas-Fernández, L. *J. Org. Chem.* **2007**, *72*, 2077-2087.
- (19) He, R.; Wang, X.; Hashimoto, T.; Maruoka, K. *Angew. Chem. Int. Ed.* **2008**, *47*, 9466-9468.
- (20) All software and sources of scattering factors are contained in the SHELXTL (version 5.1) program library (G. Sheldrick, Bruker Analytical X-ray Systems, Madison, WI).

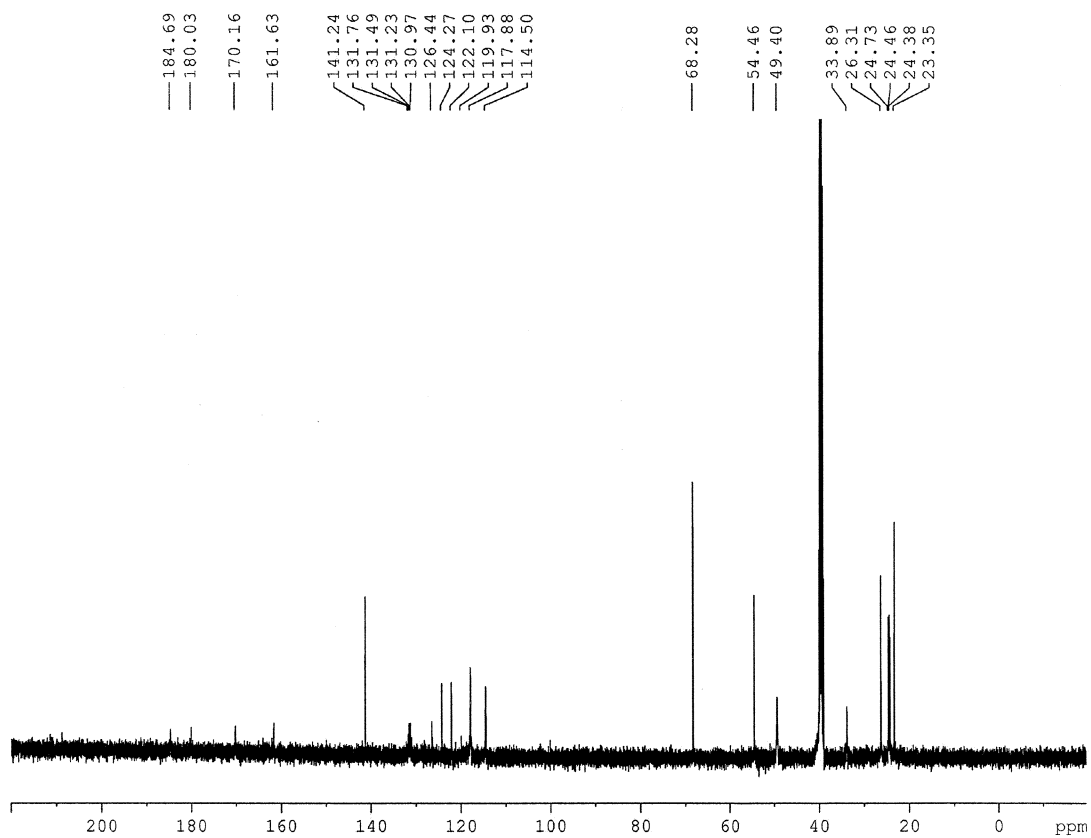
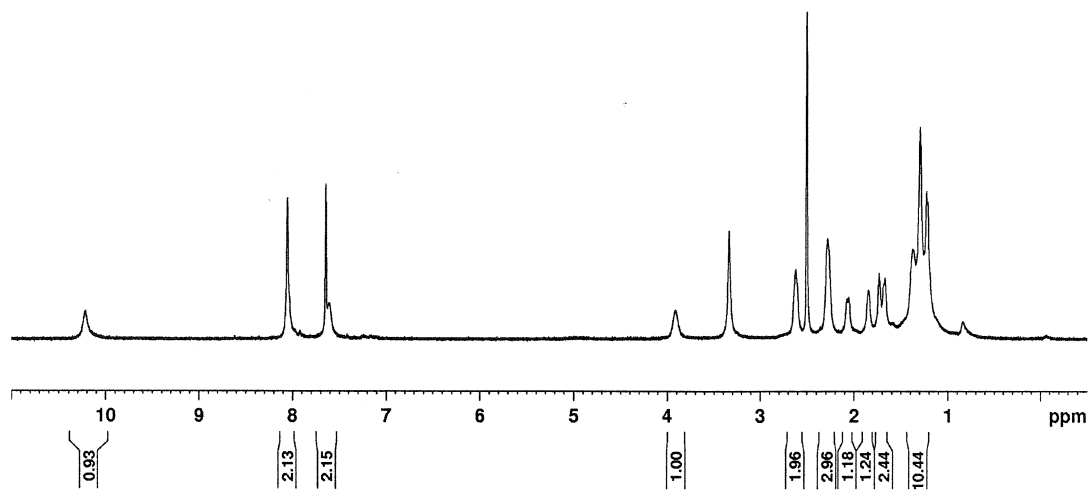


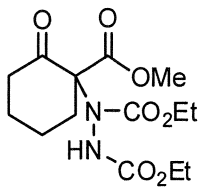
3e (inDMSO-d₆)



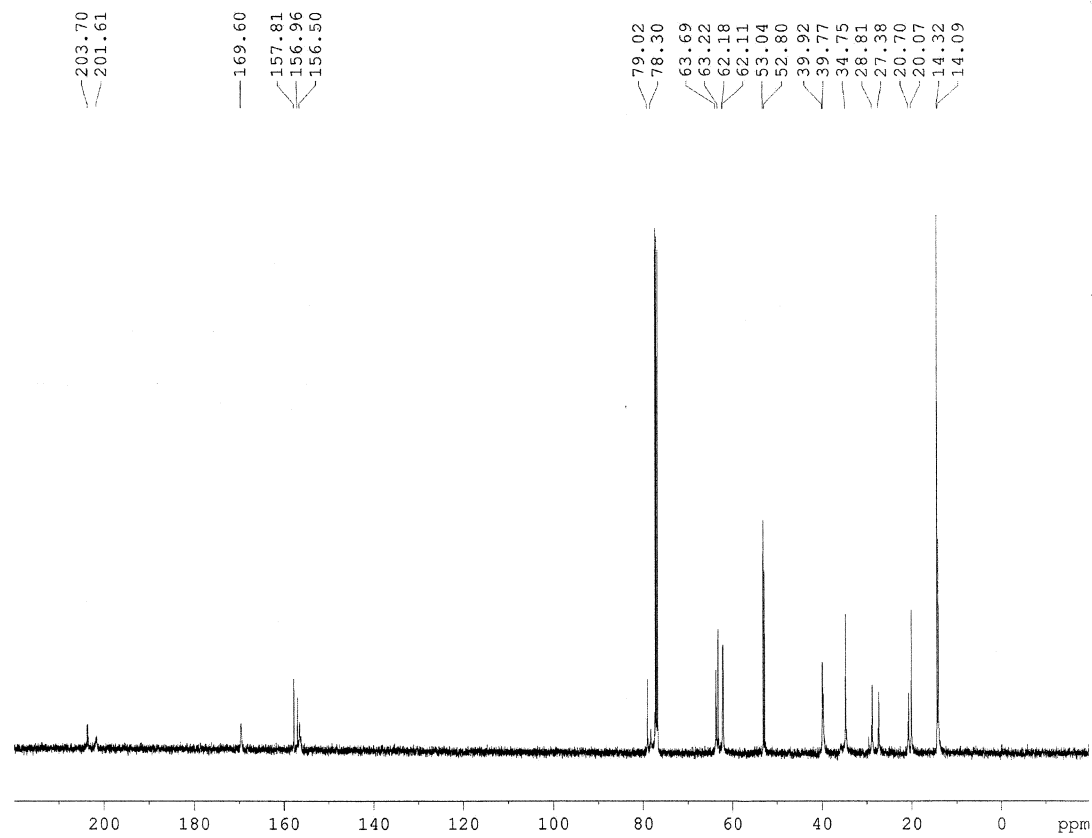
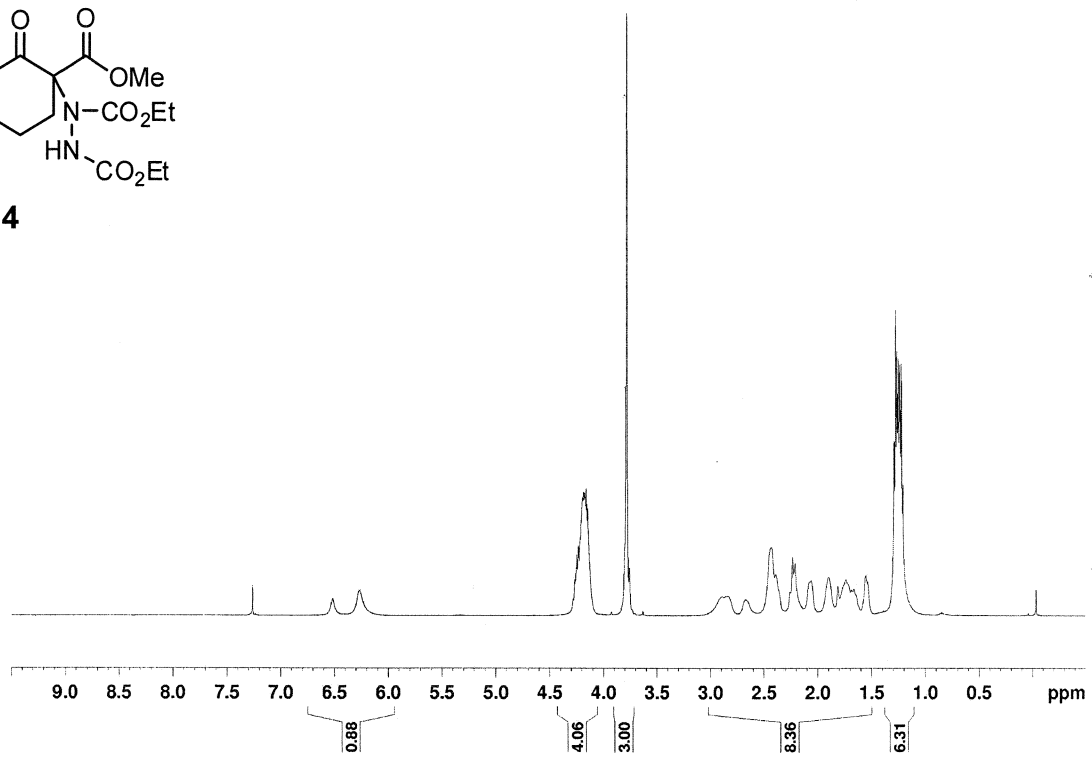


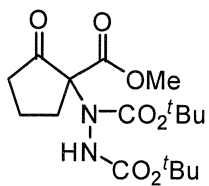
3j (inDMSO-d₆)



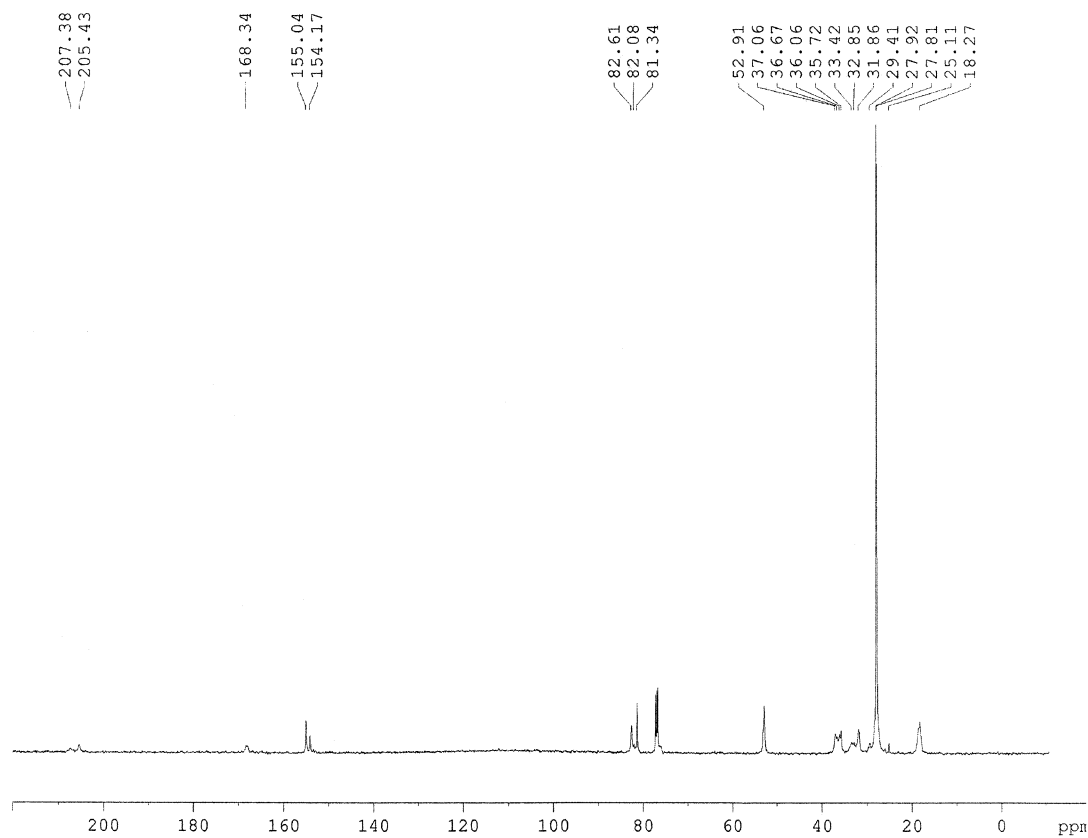
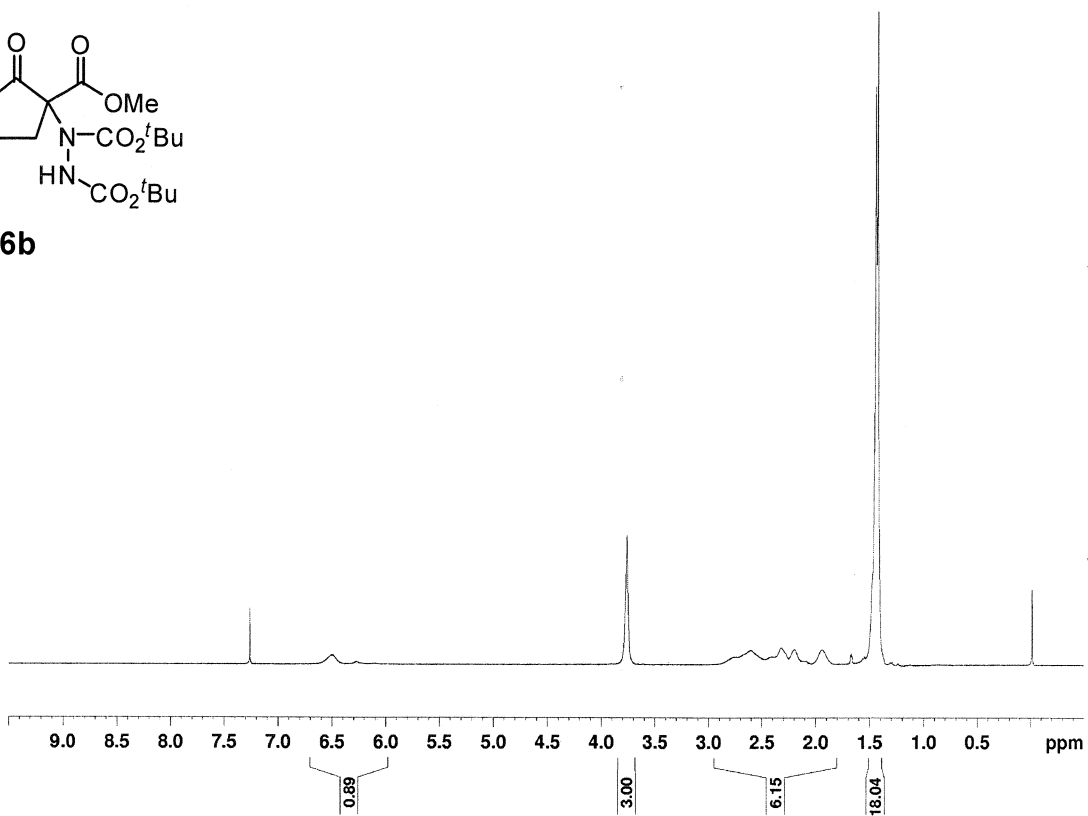


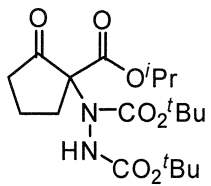
4



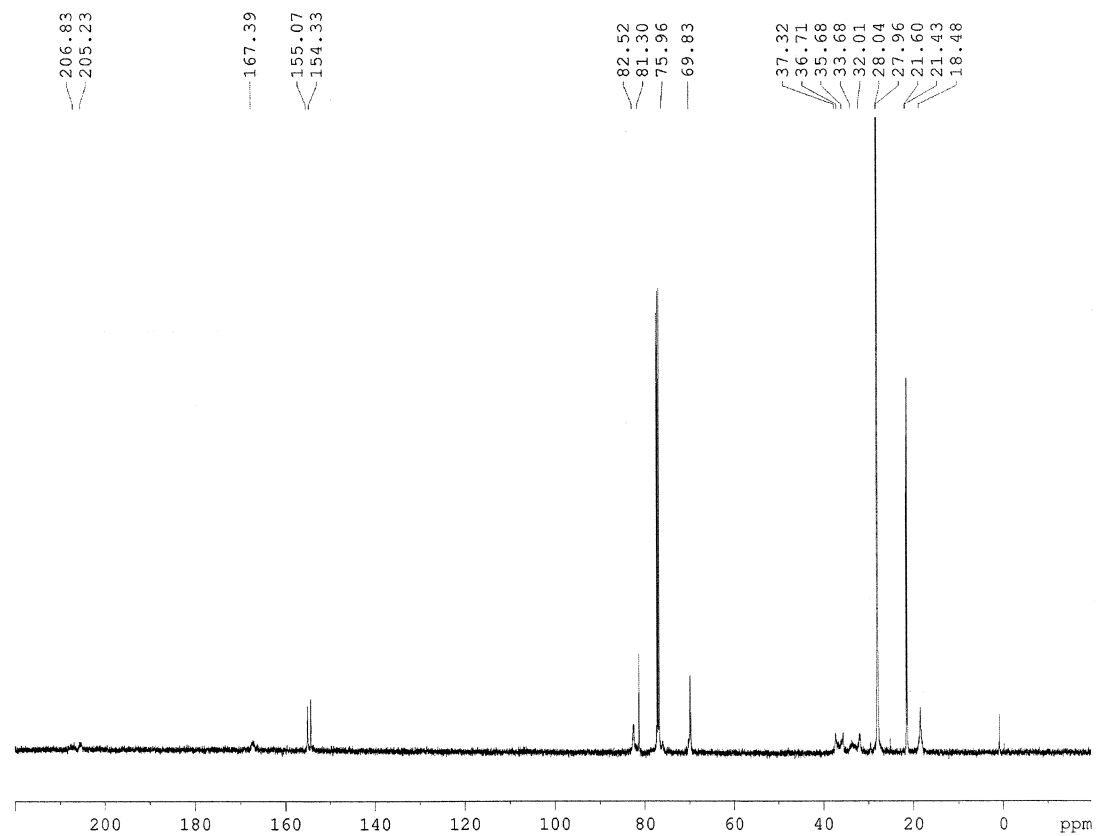
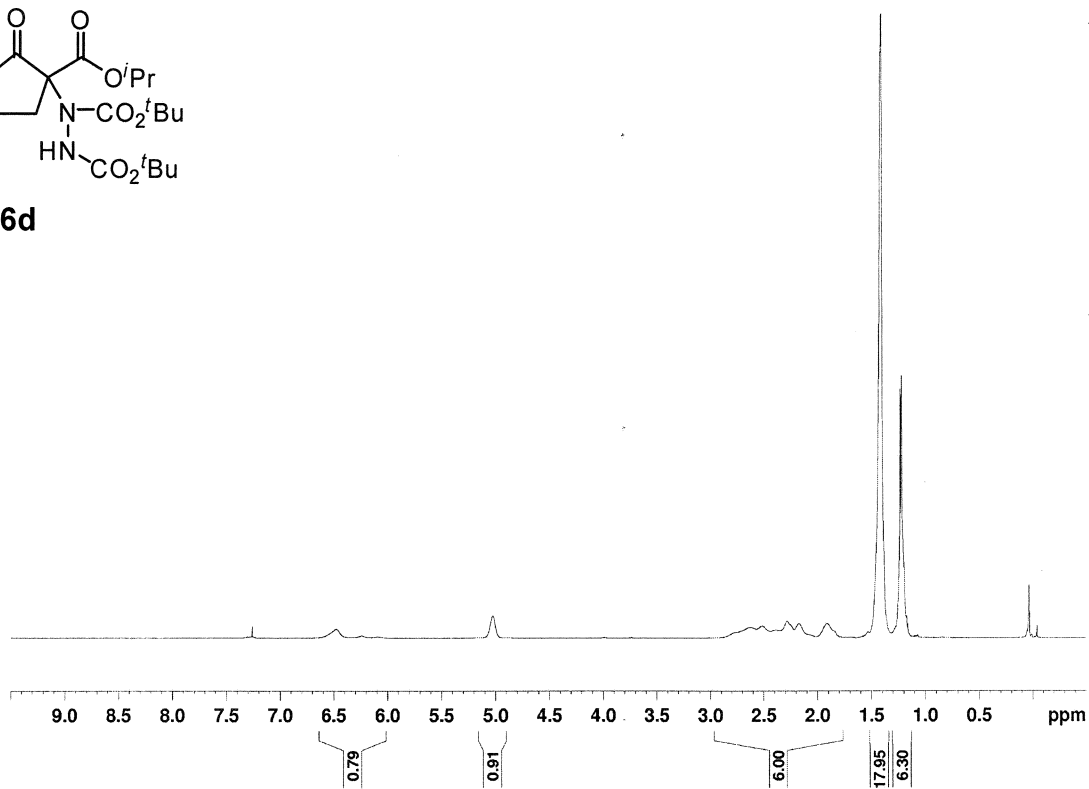


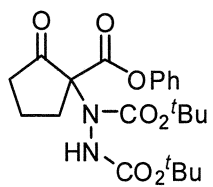
6b



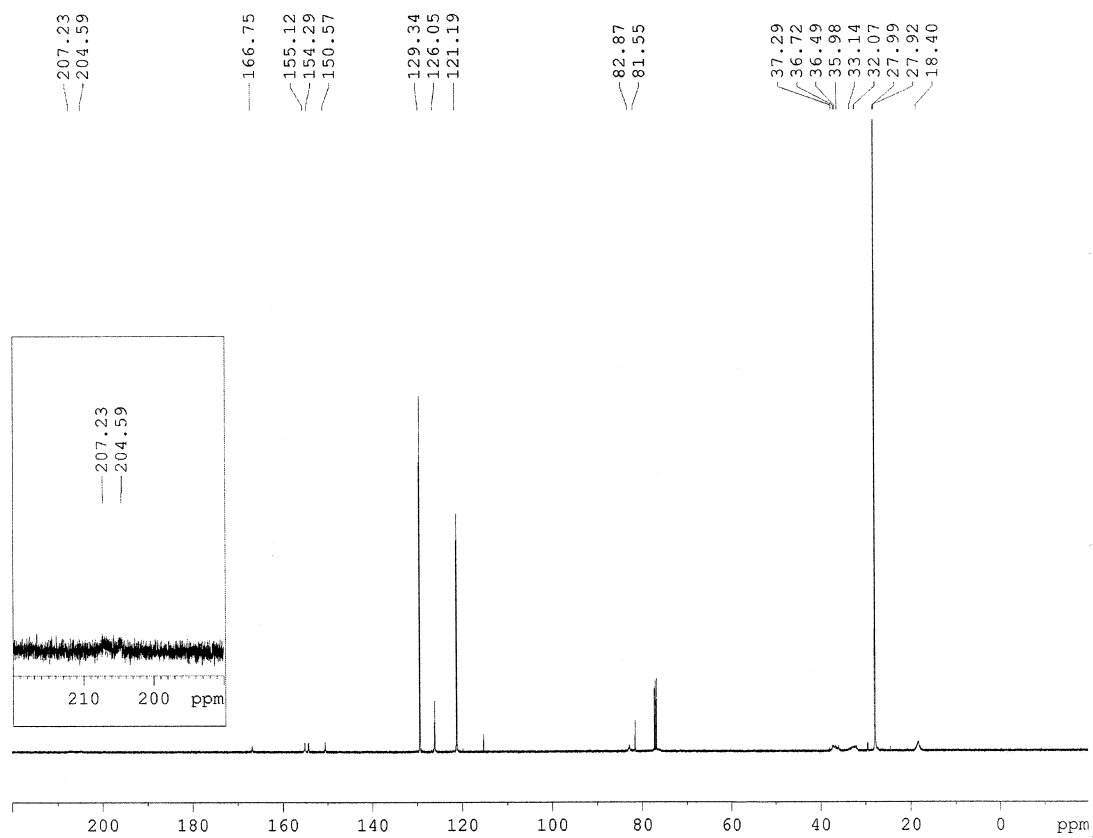
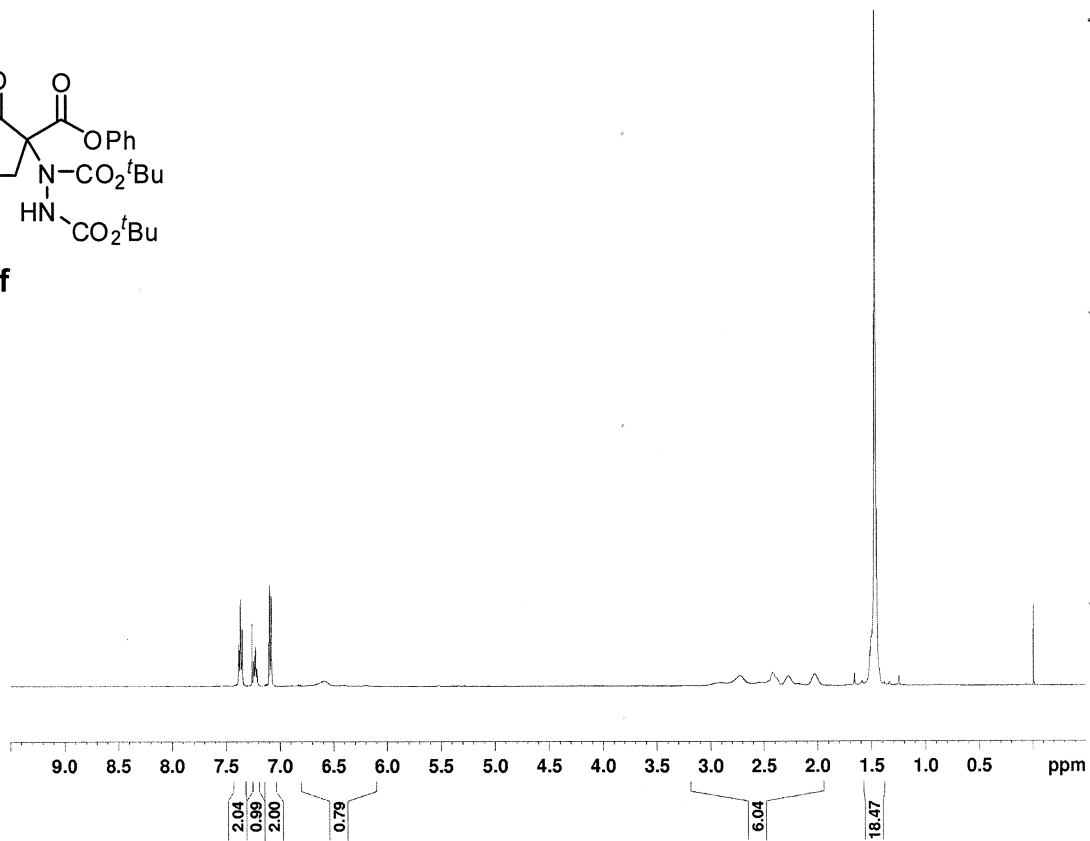


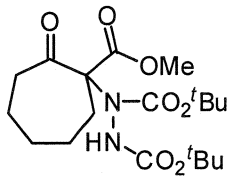
6d



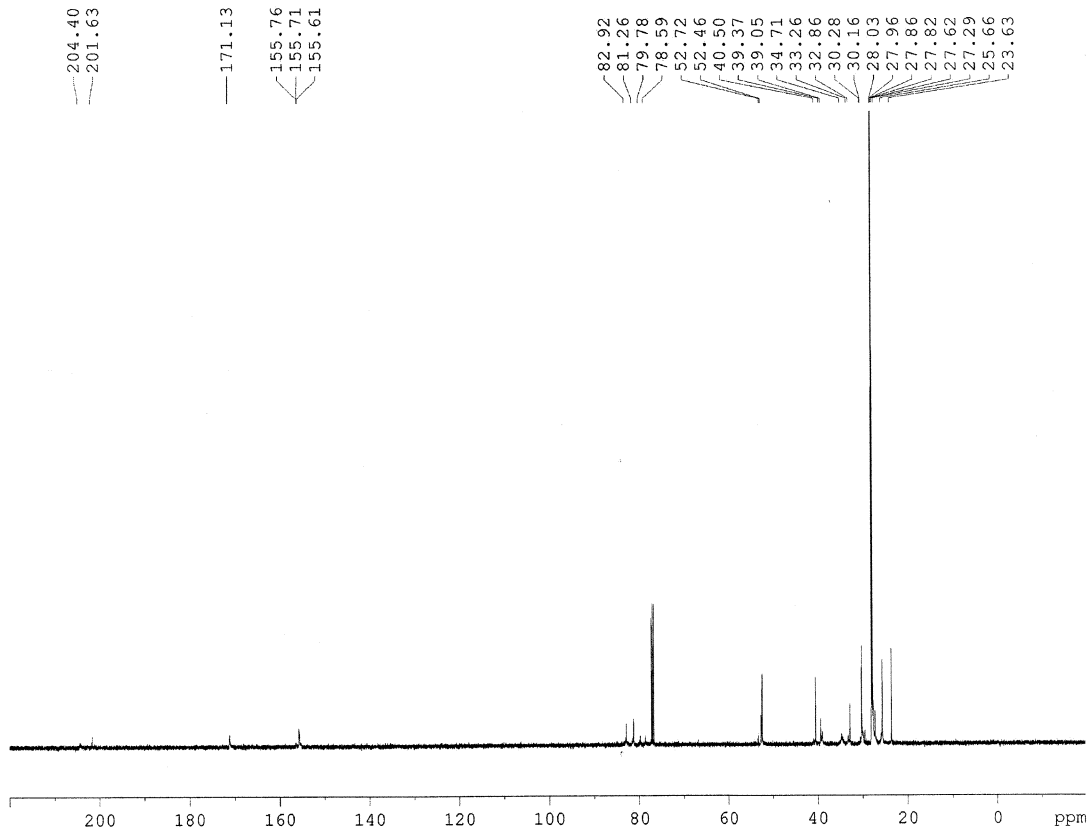
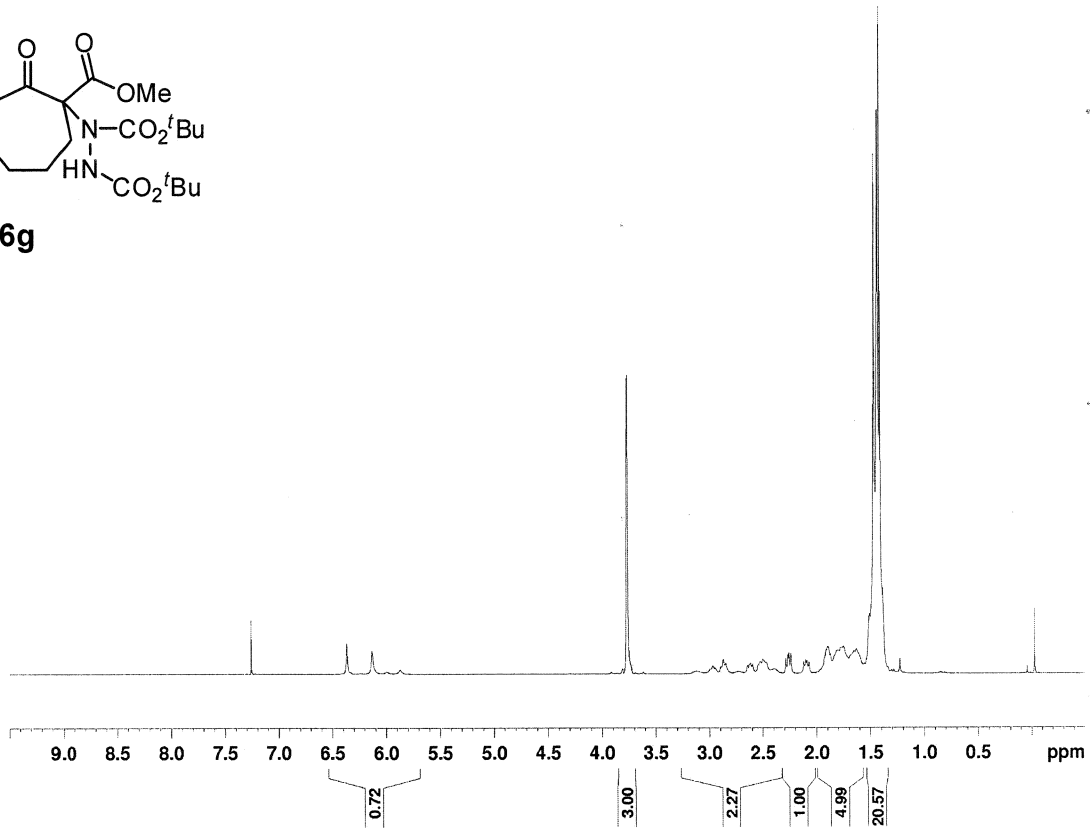


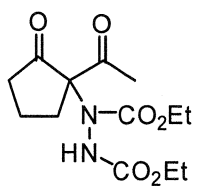
6f



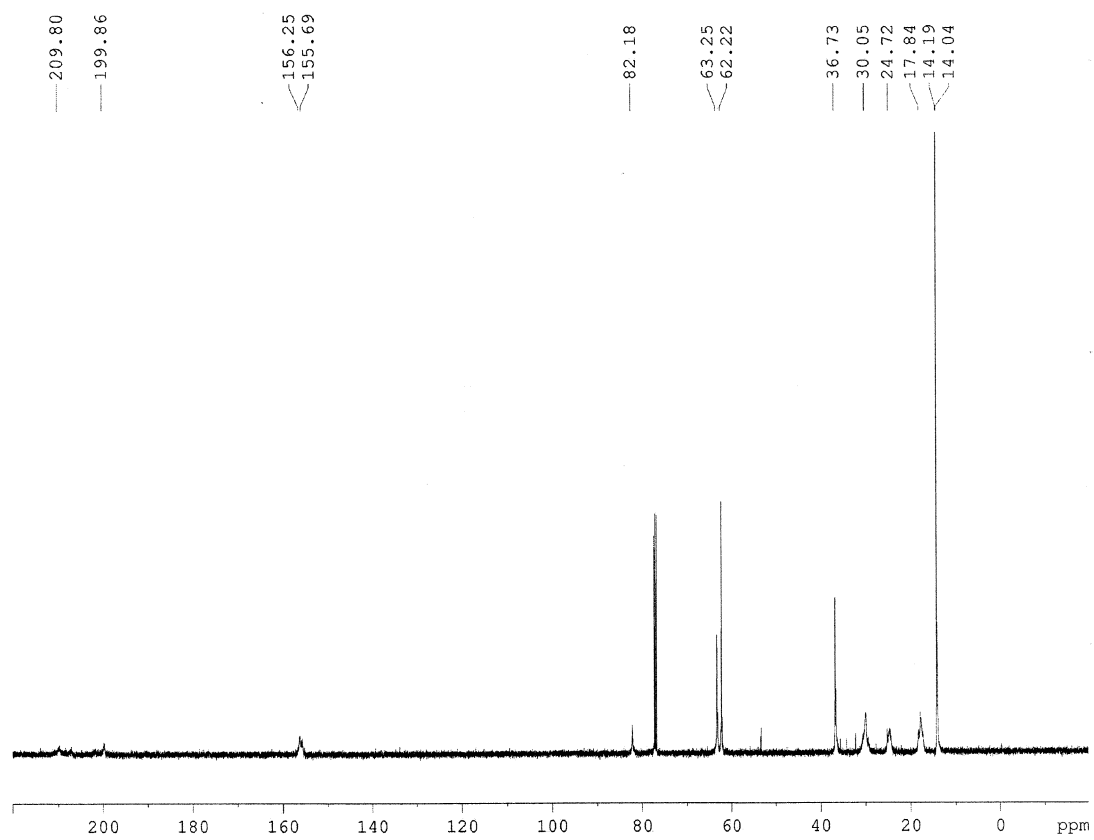
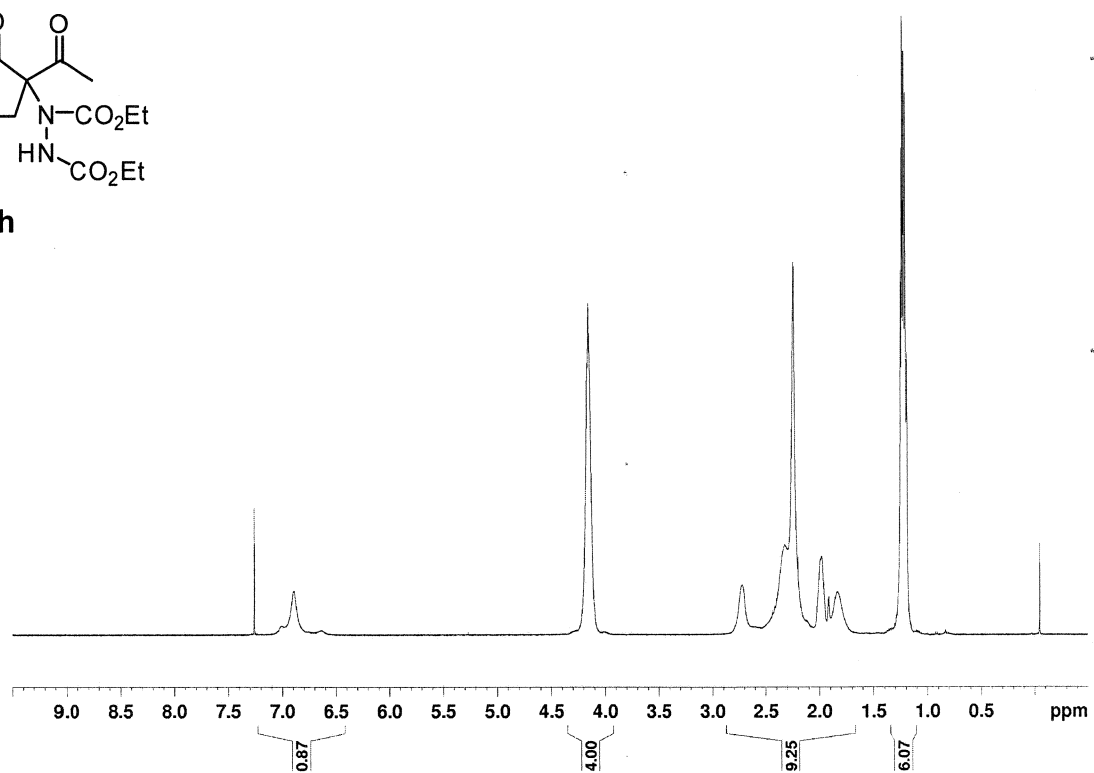


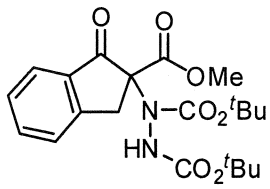
6g



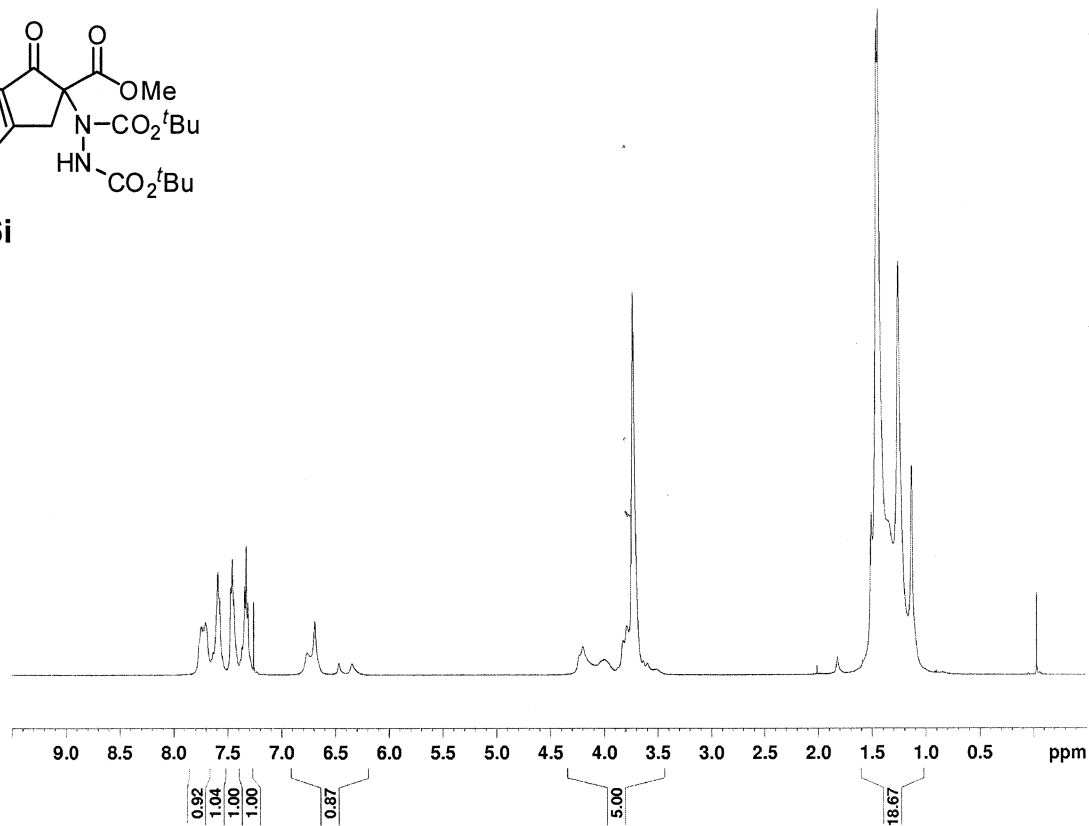


6h

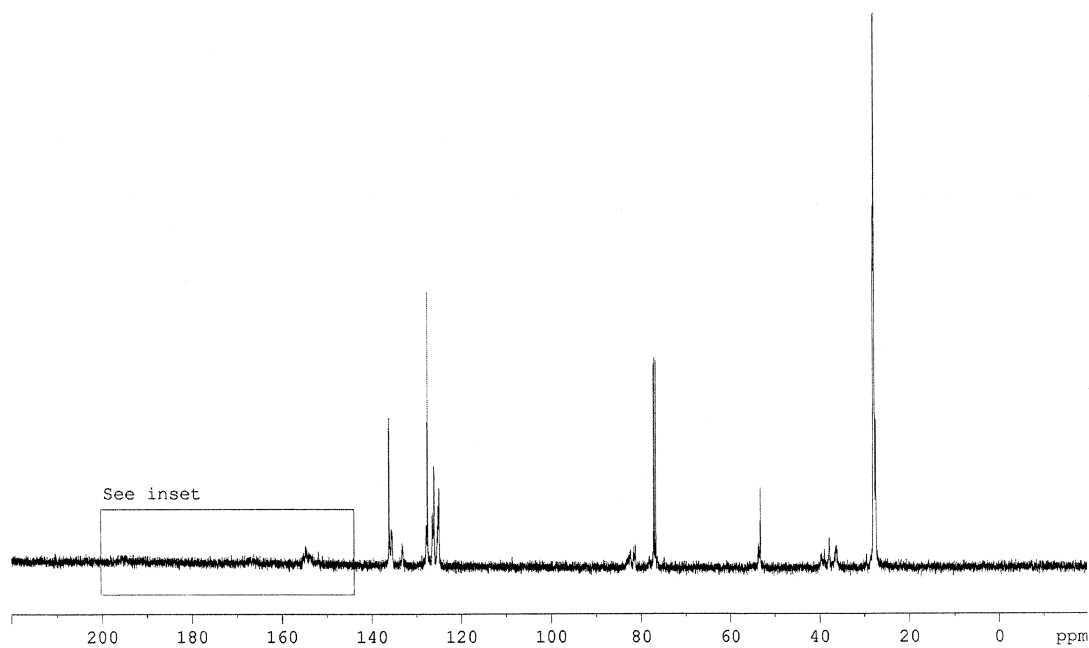




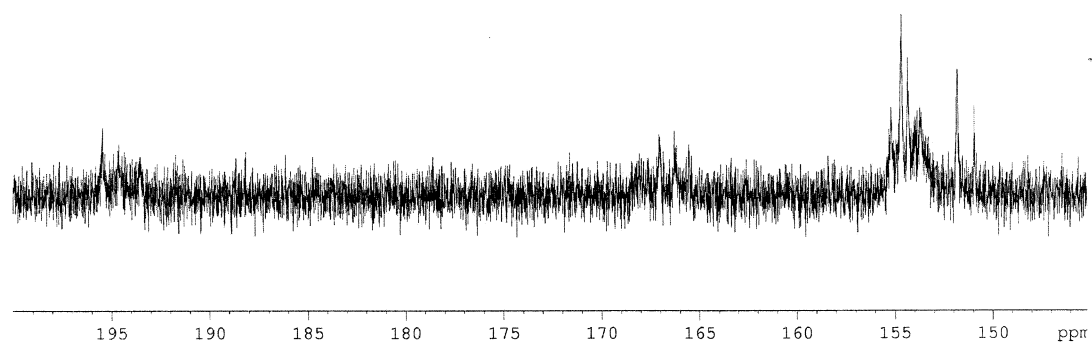
6i

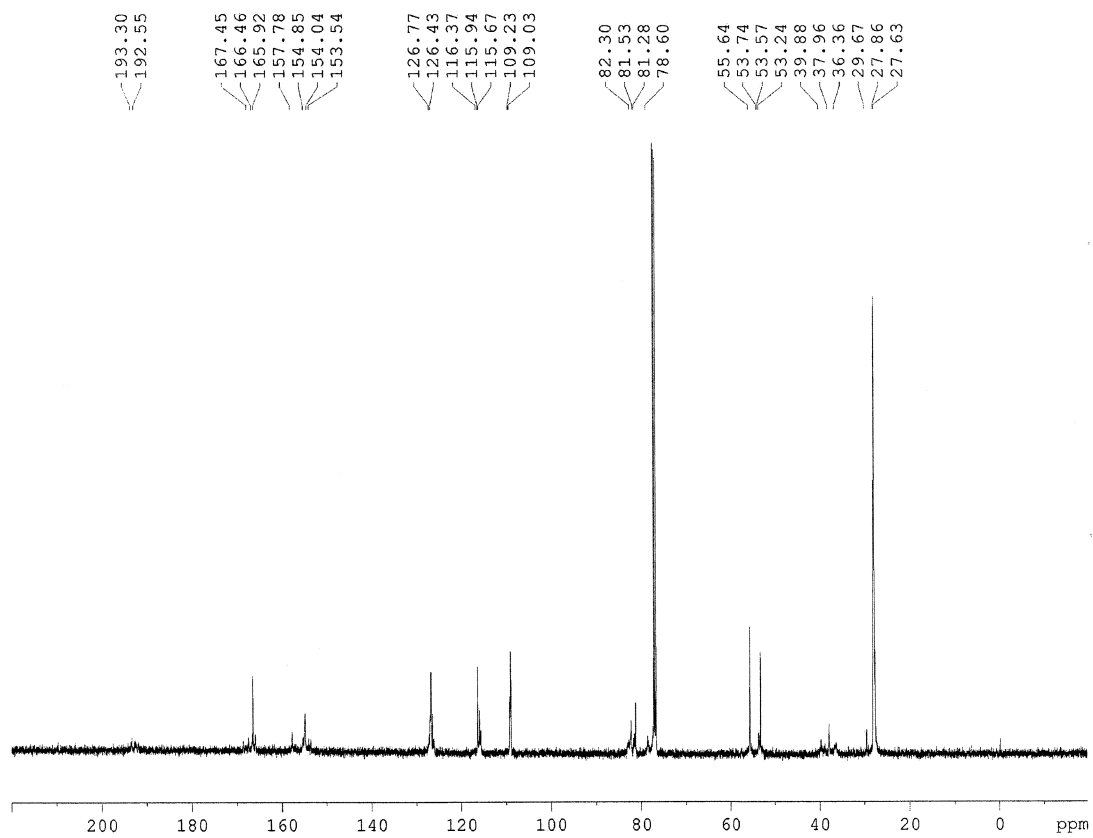
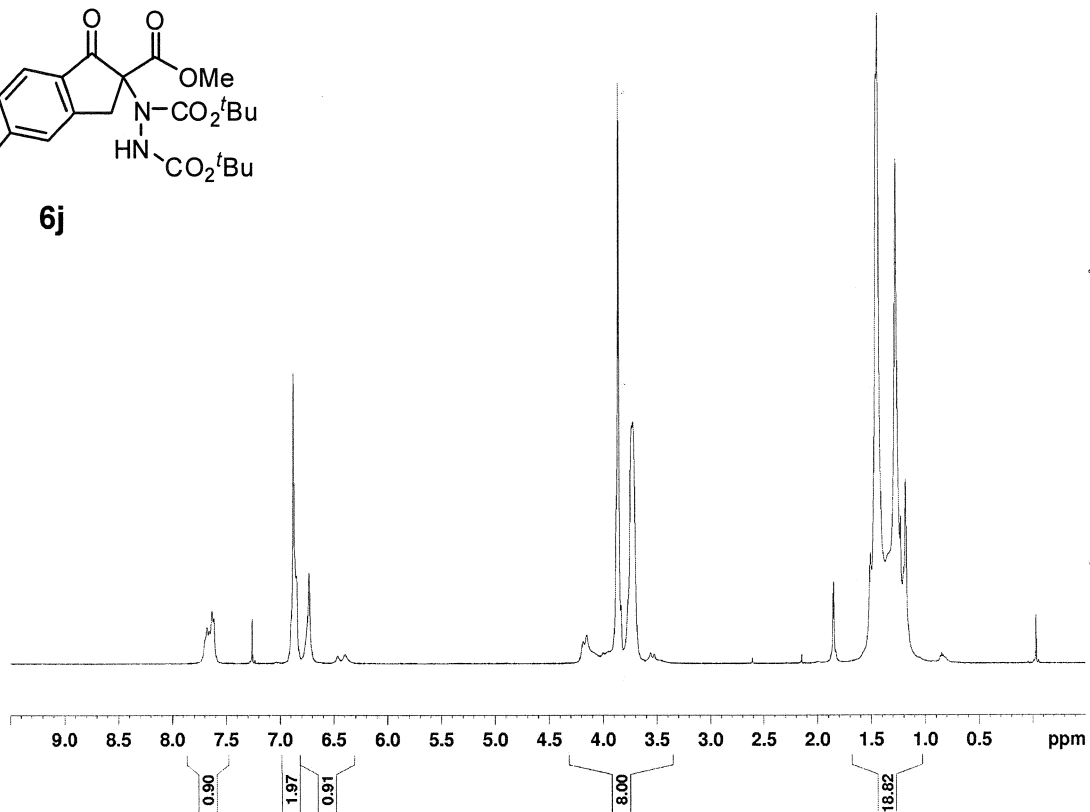
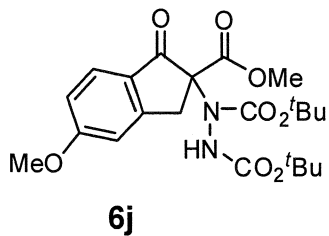


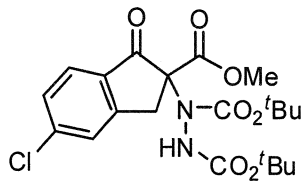
- 136.10
- 135.64
- 133.22
- 127.79
- 127.53
- 126.47
- 126.10
- 125.22
- 124.95
- 82.43
- 81.82
- 81.63
- 81.37
- 78.20
- 76.46
- 53.79
- 53.62
- 53.28
- 39.68
- 39.00
- 37.90
- 36.41
- 28.07
- 28.01
- 27.87
- 27.51



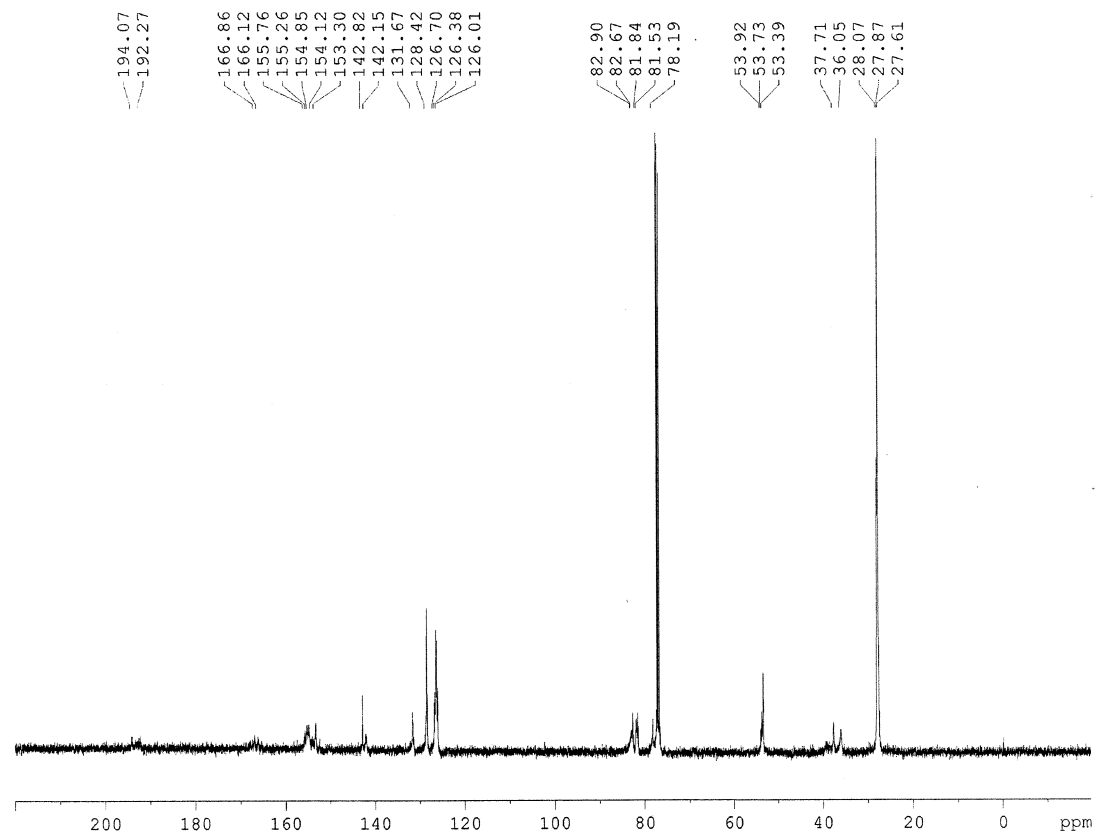
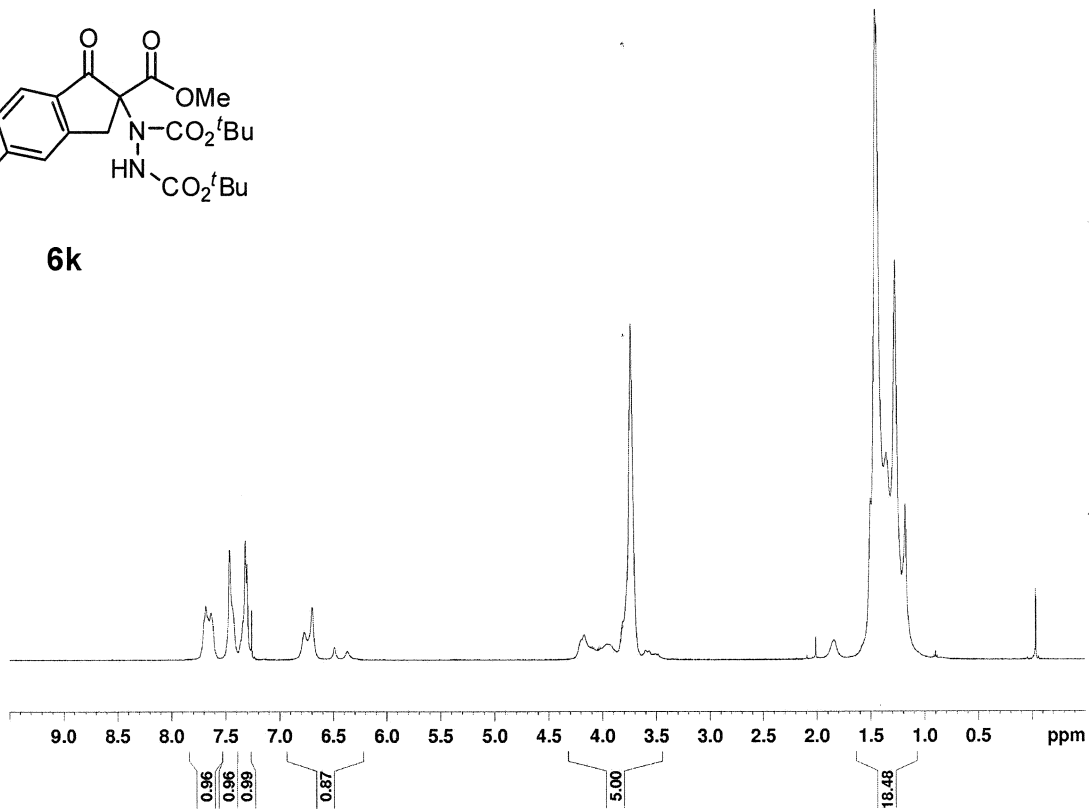
Inset for Compound **6i**

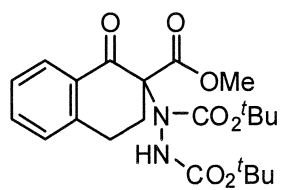




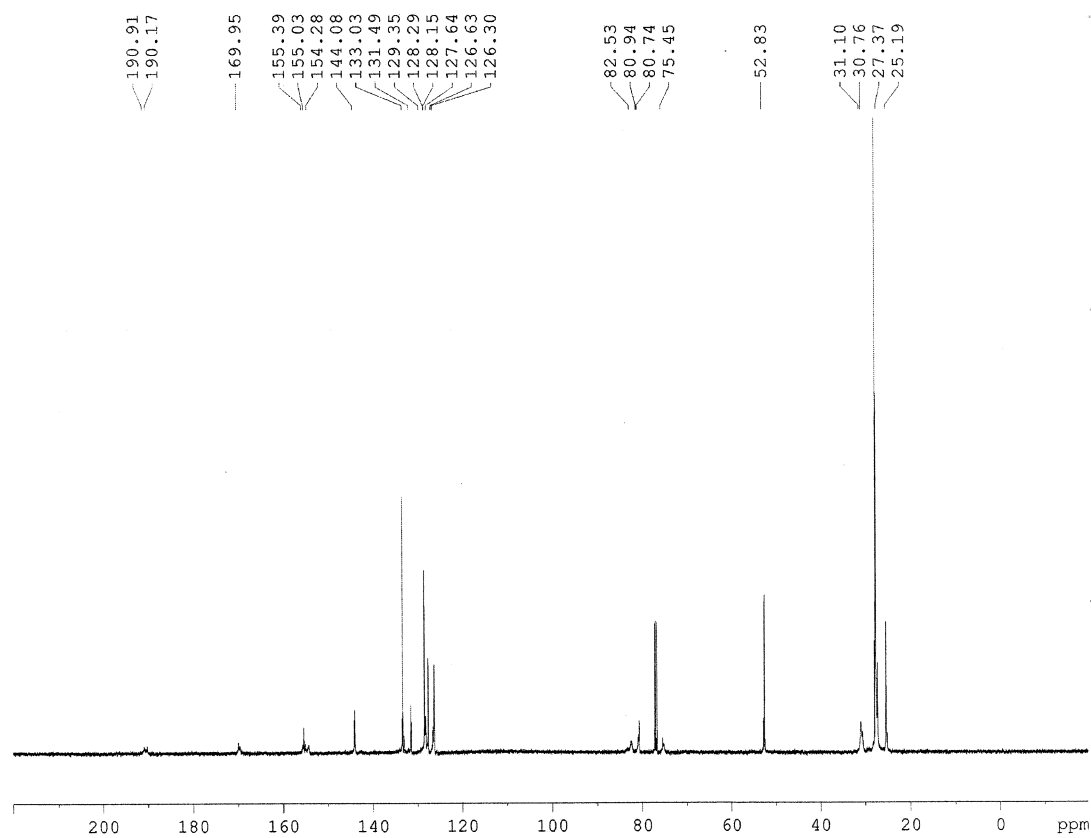
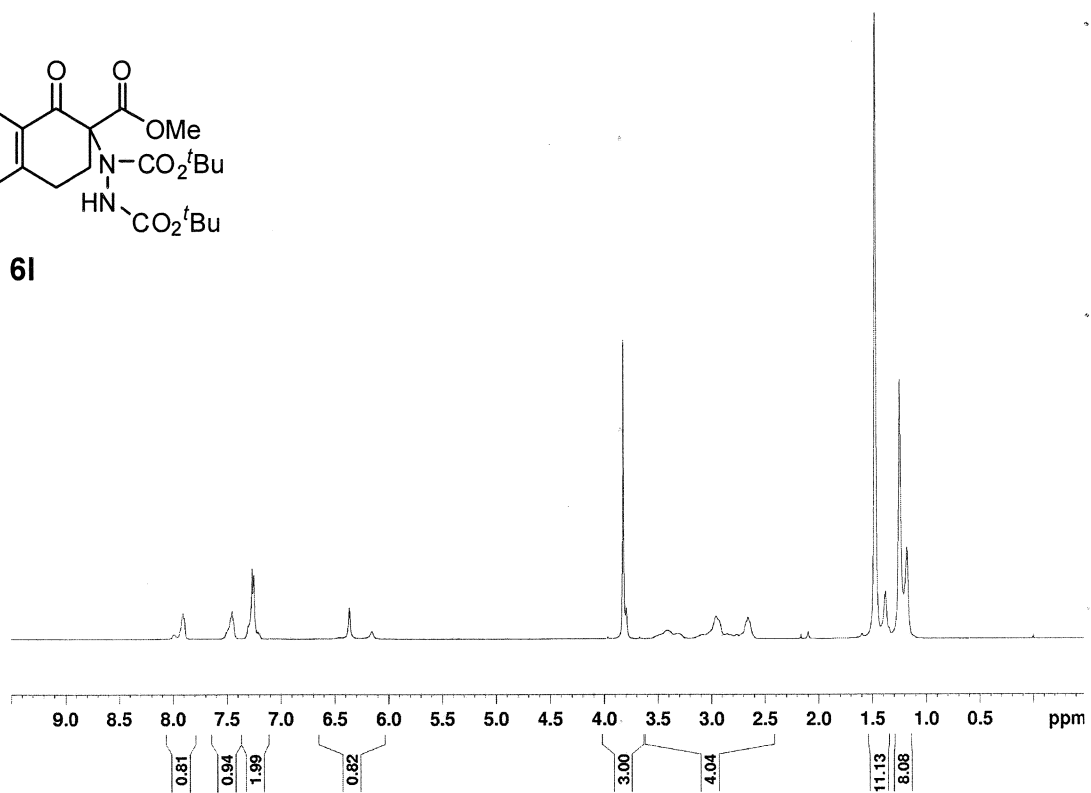


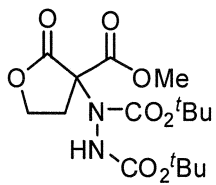
6k



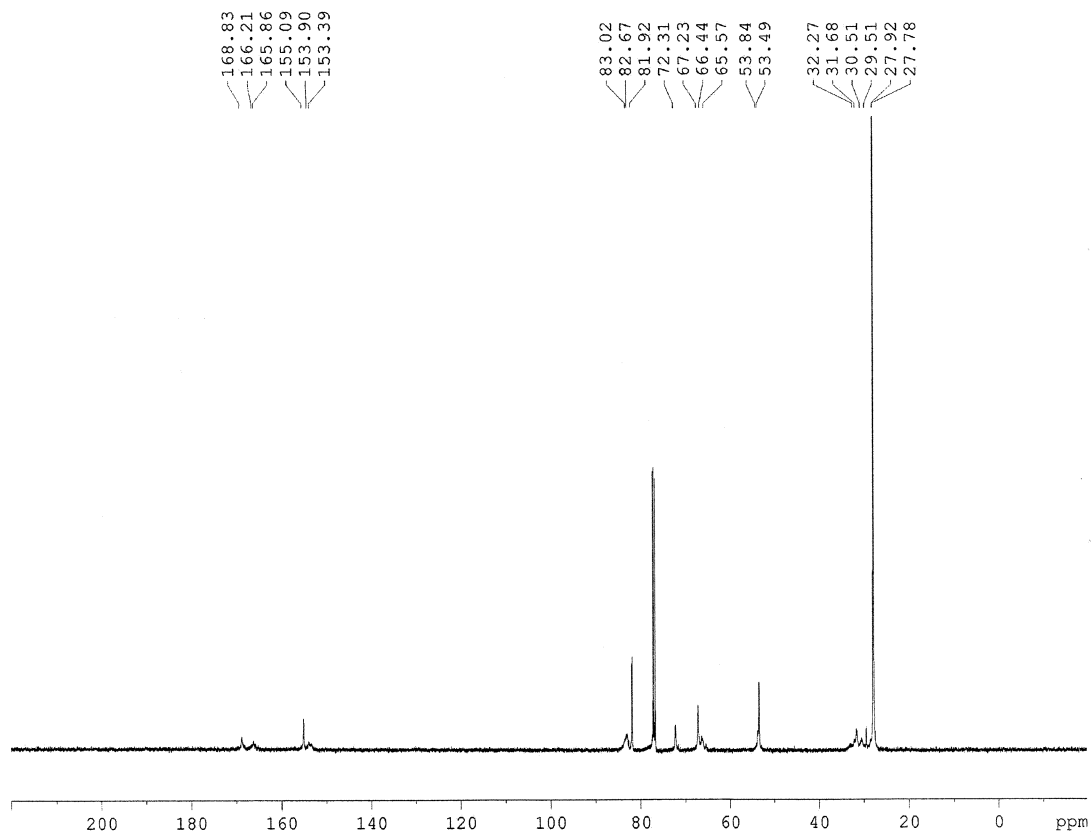
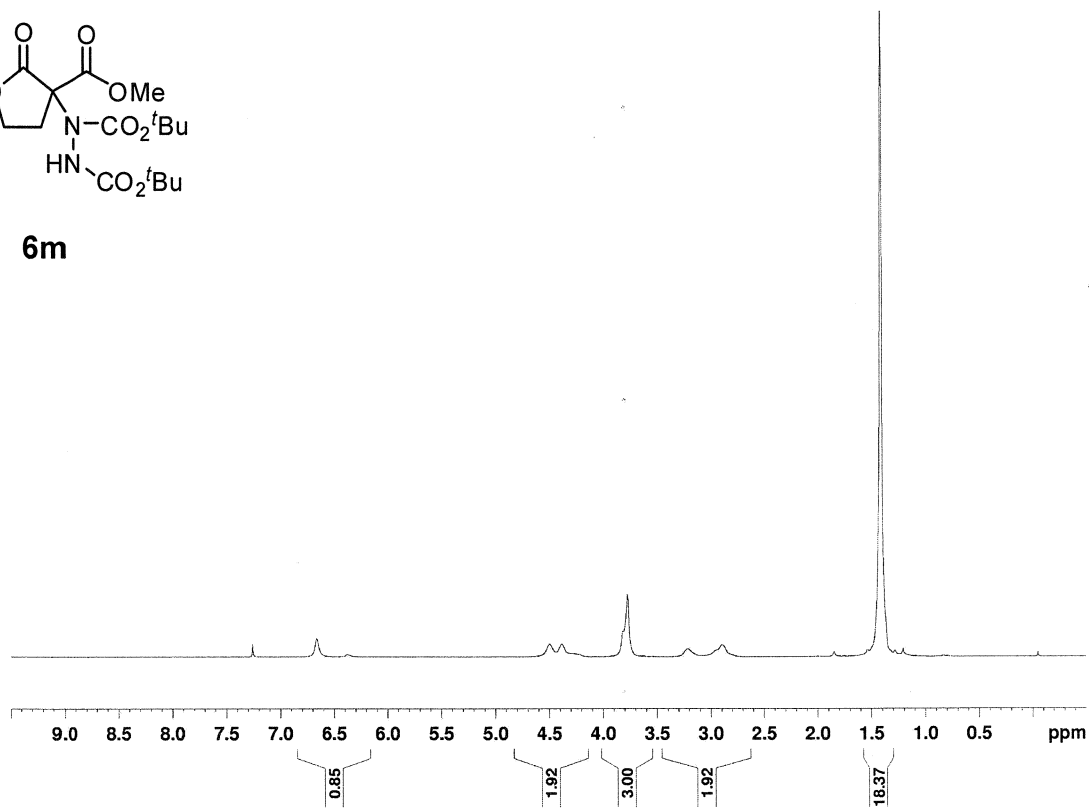


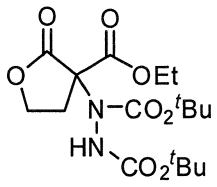
61



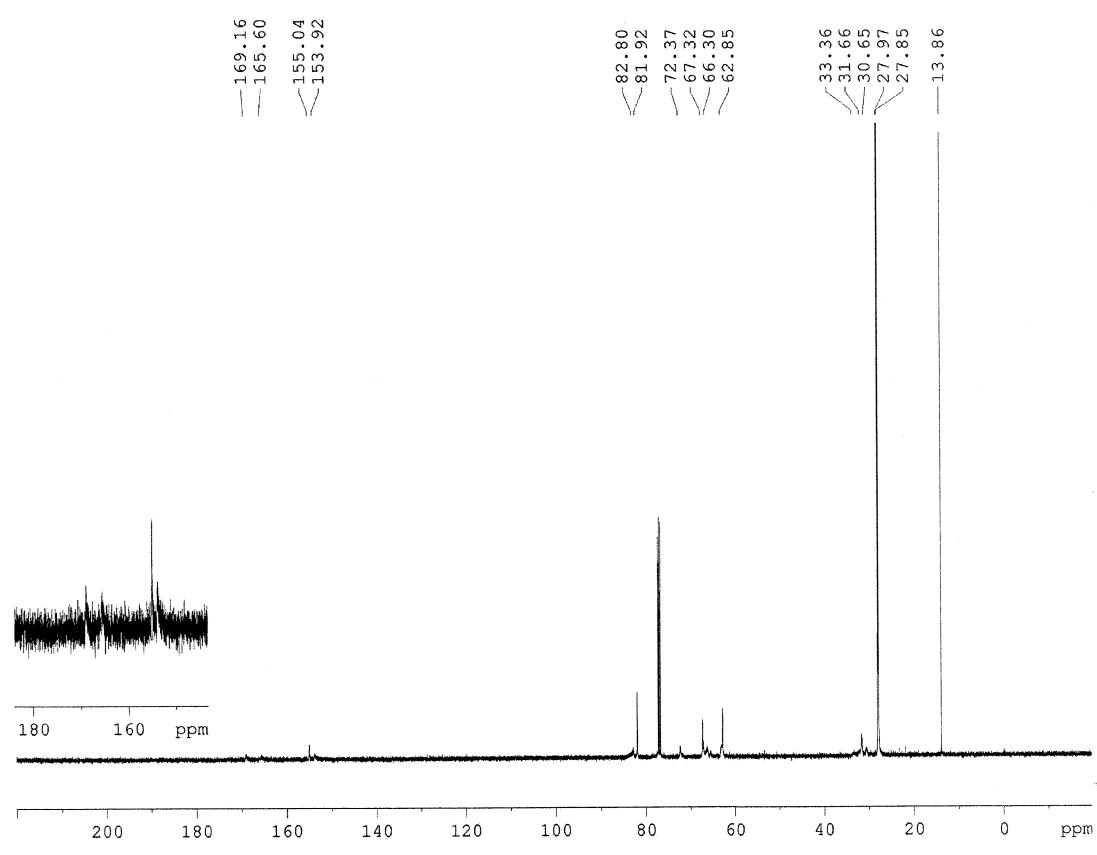
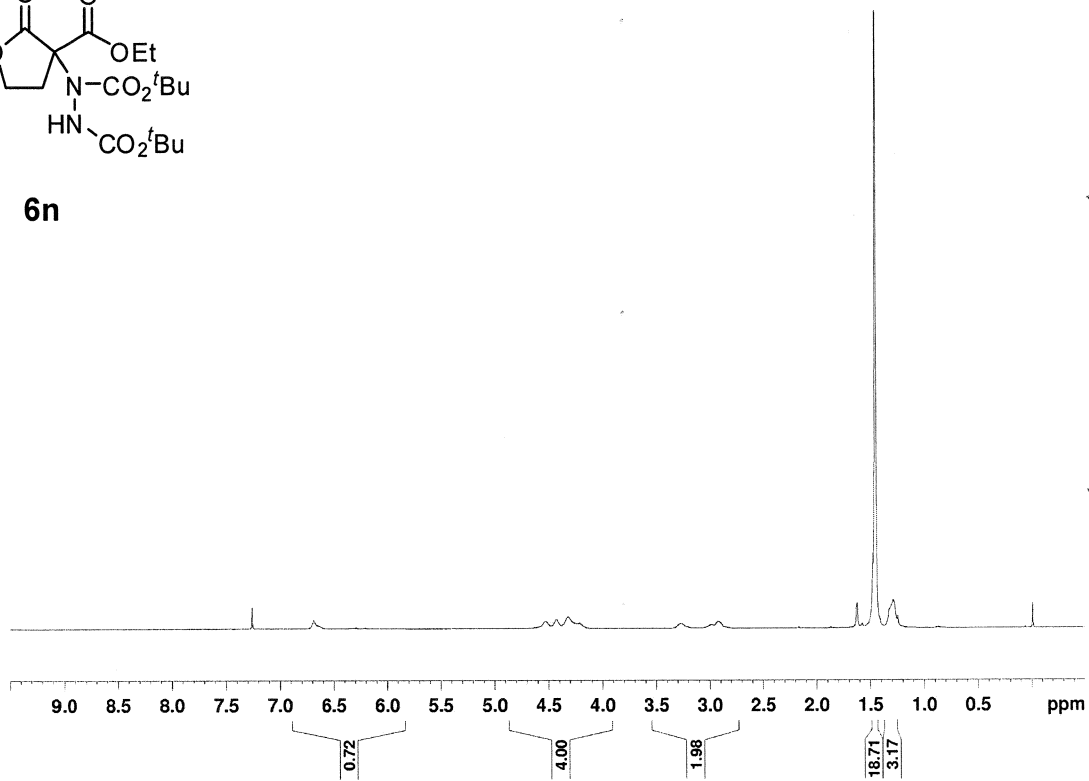


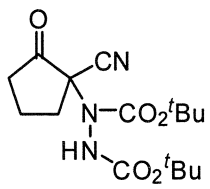
6m



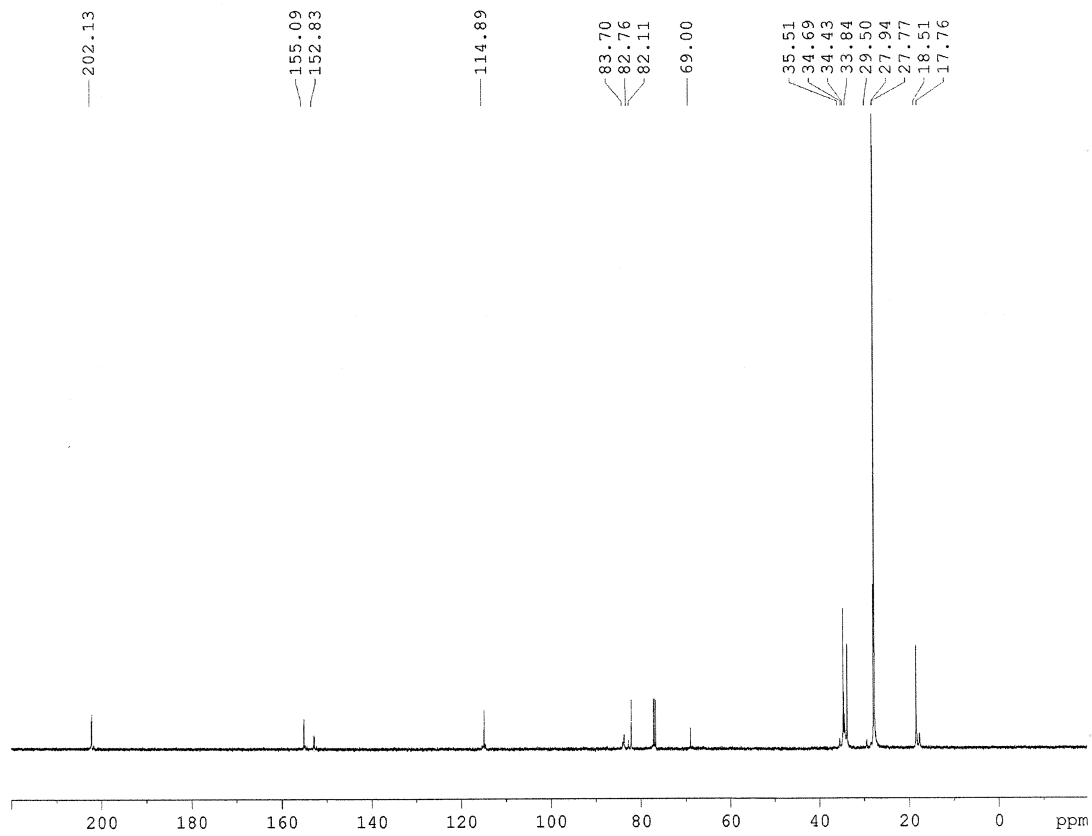
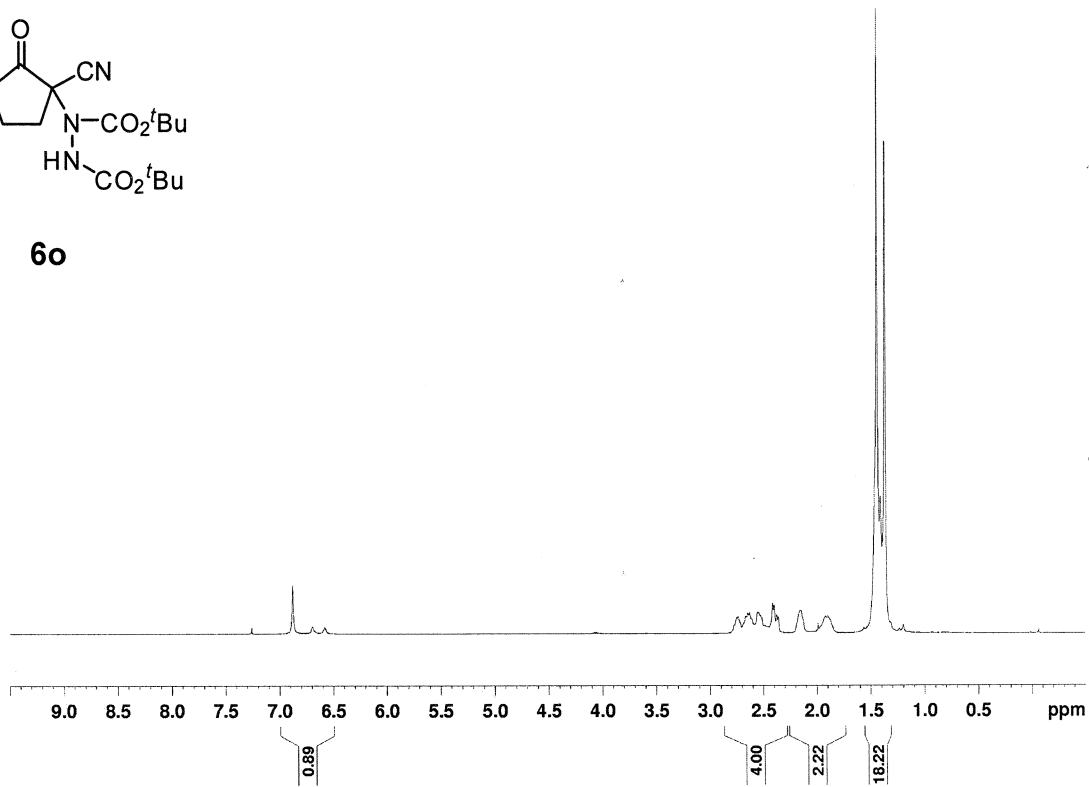


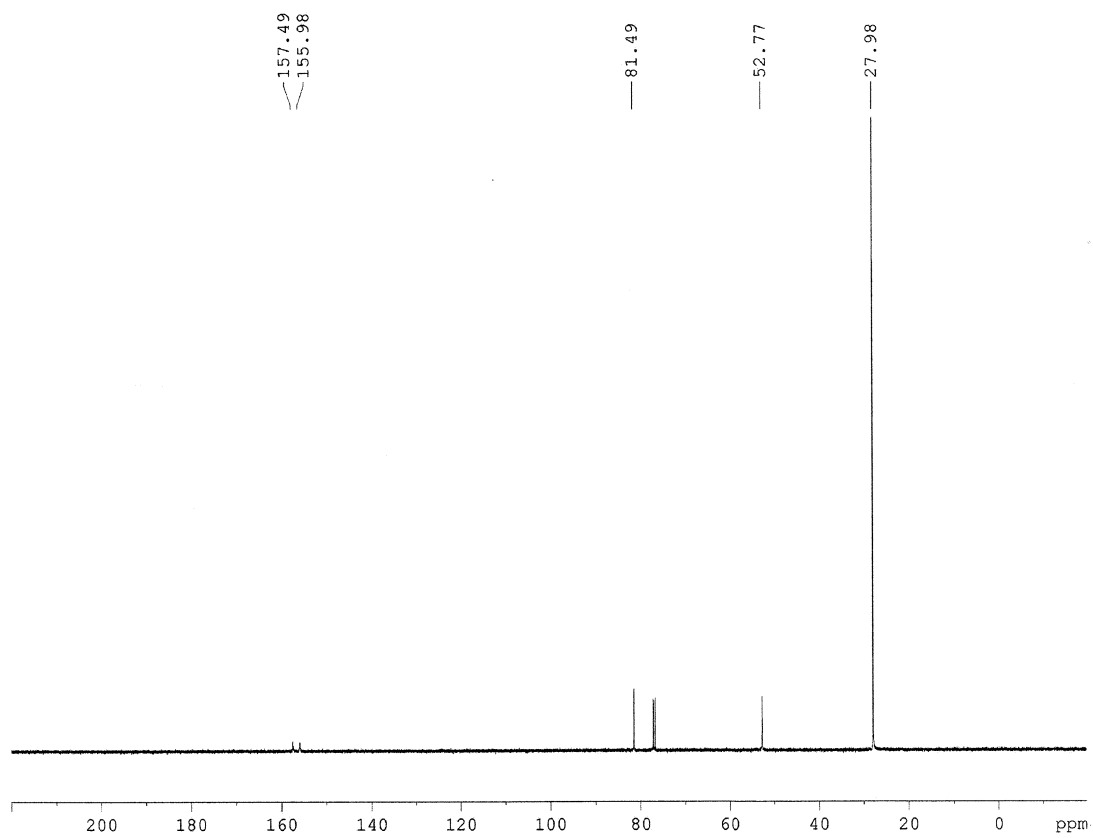
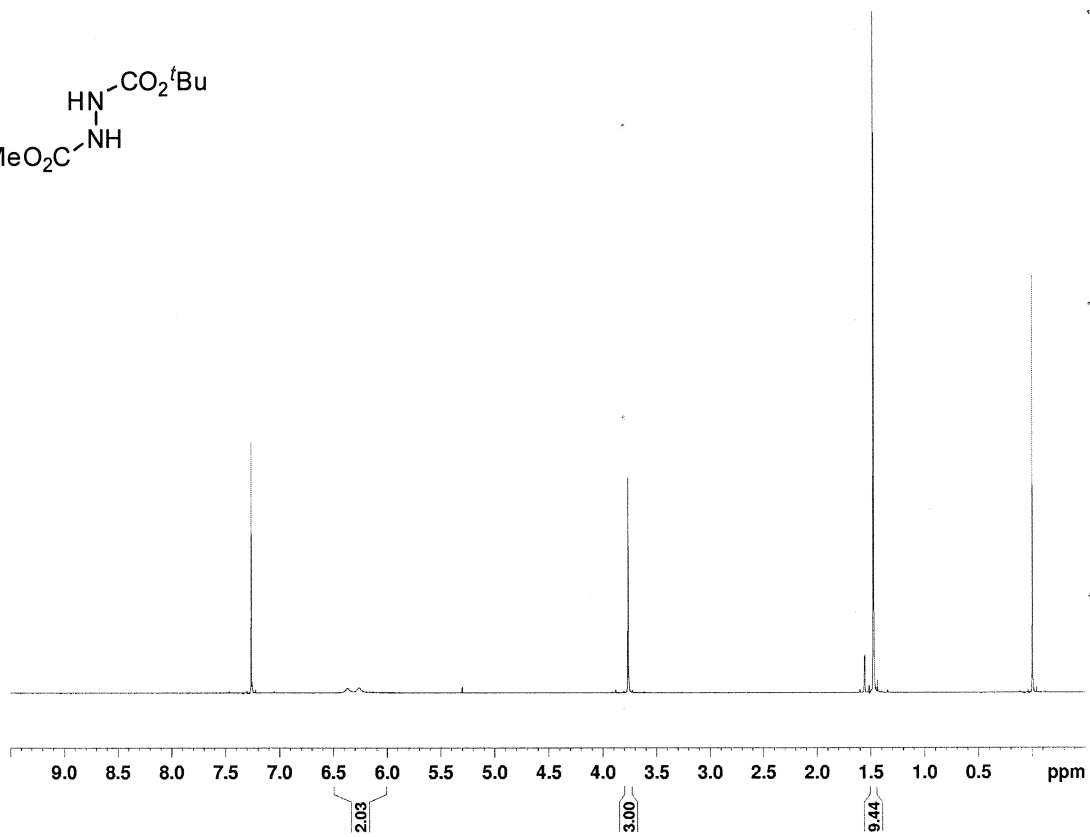
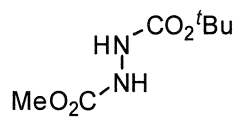
6n

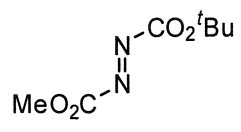




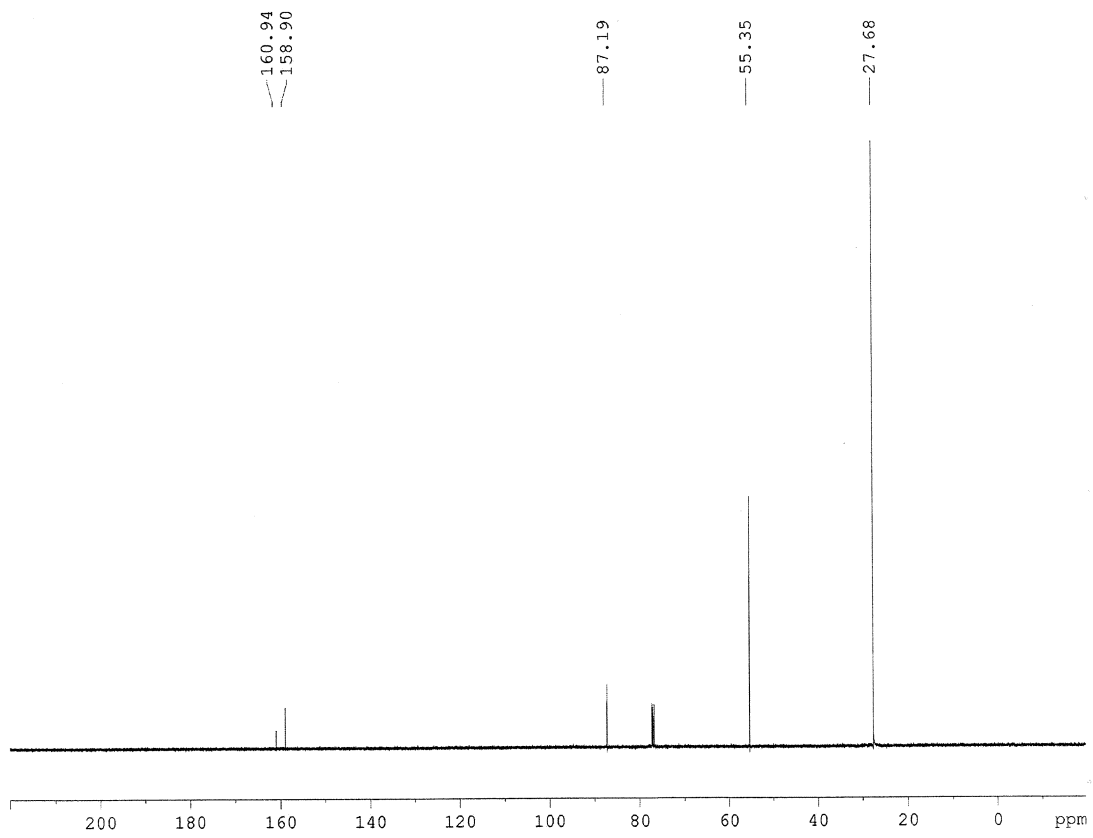
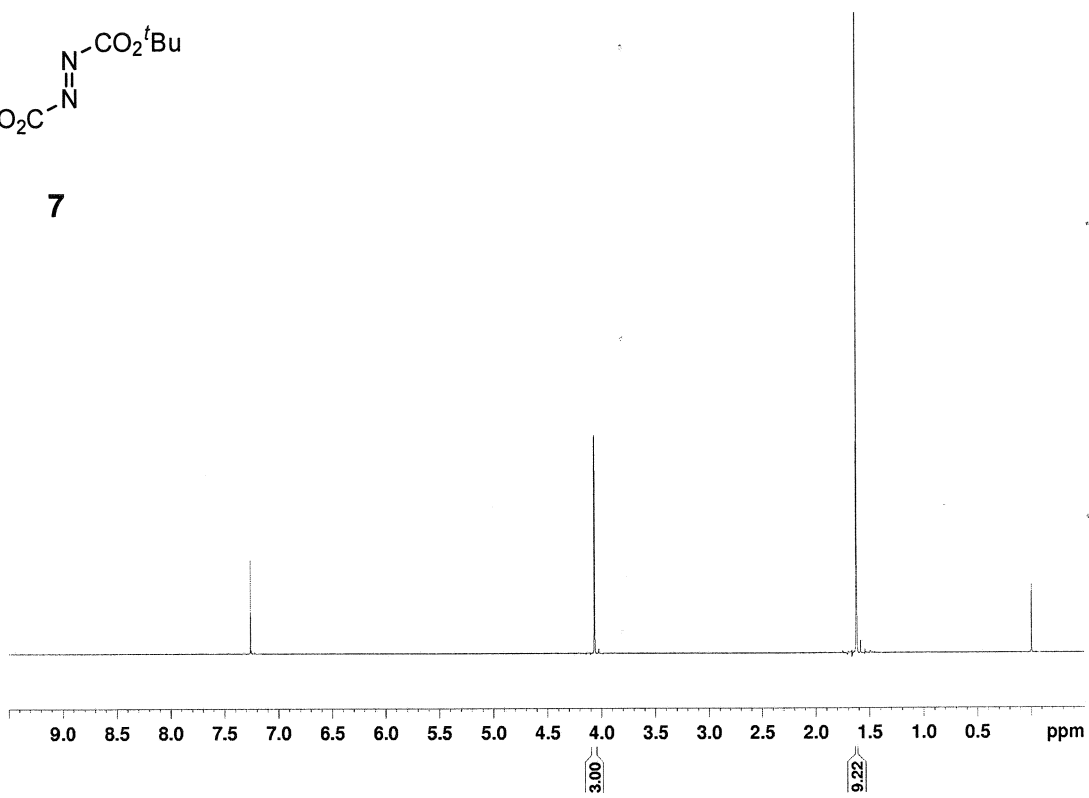
60

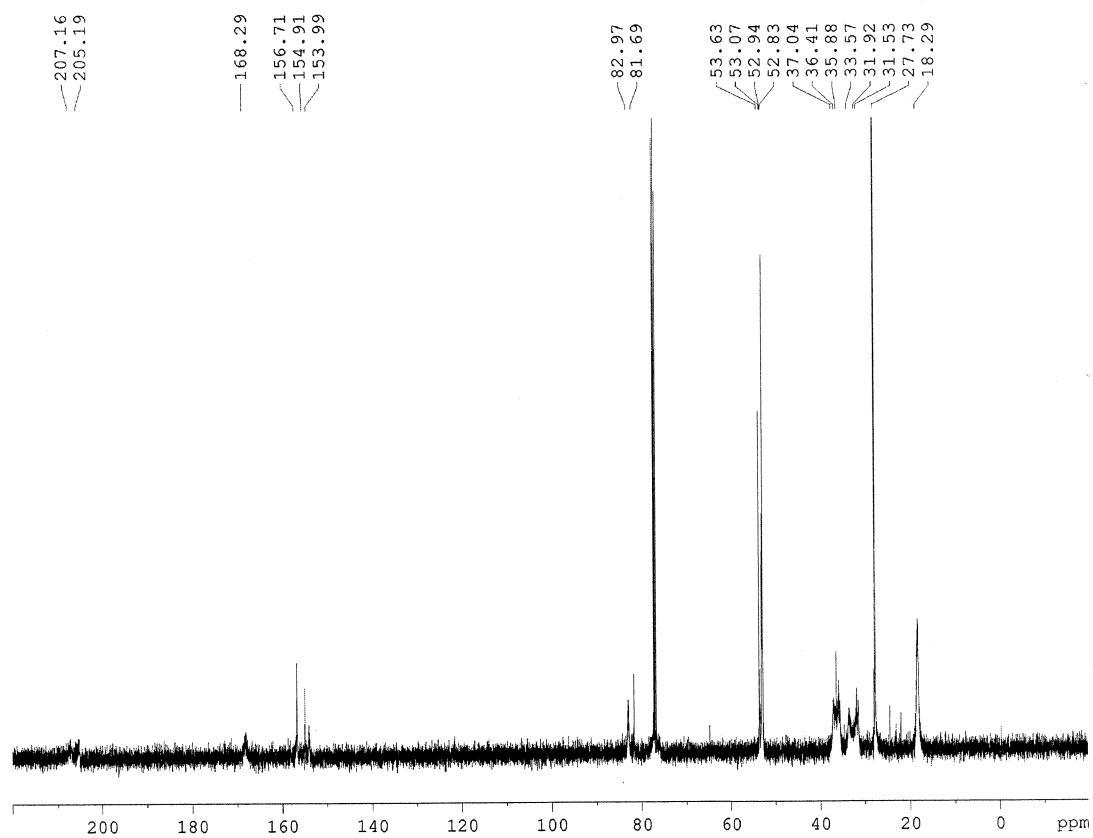
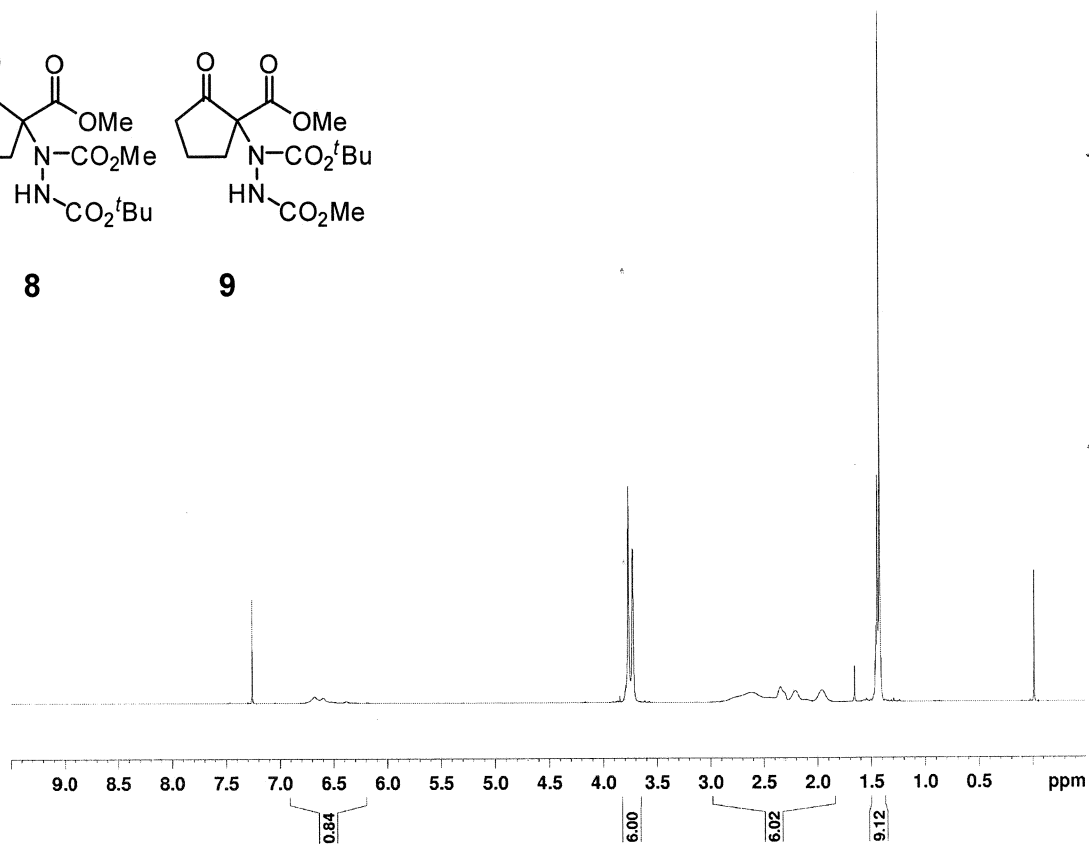
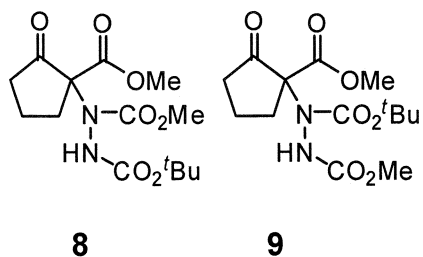


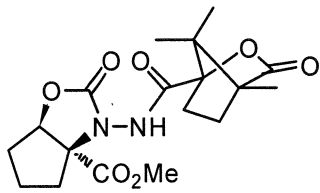




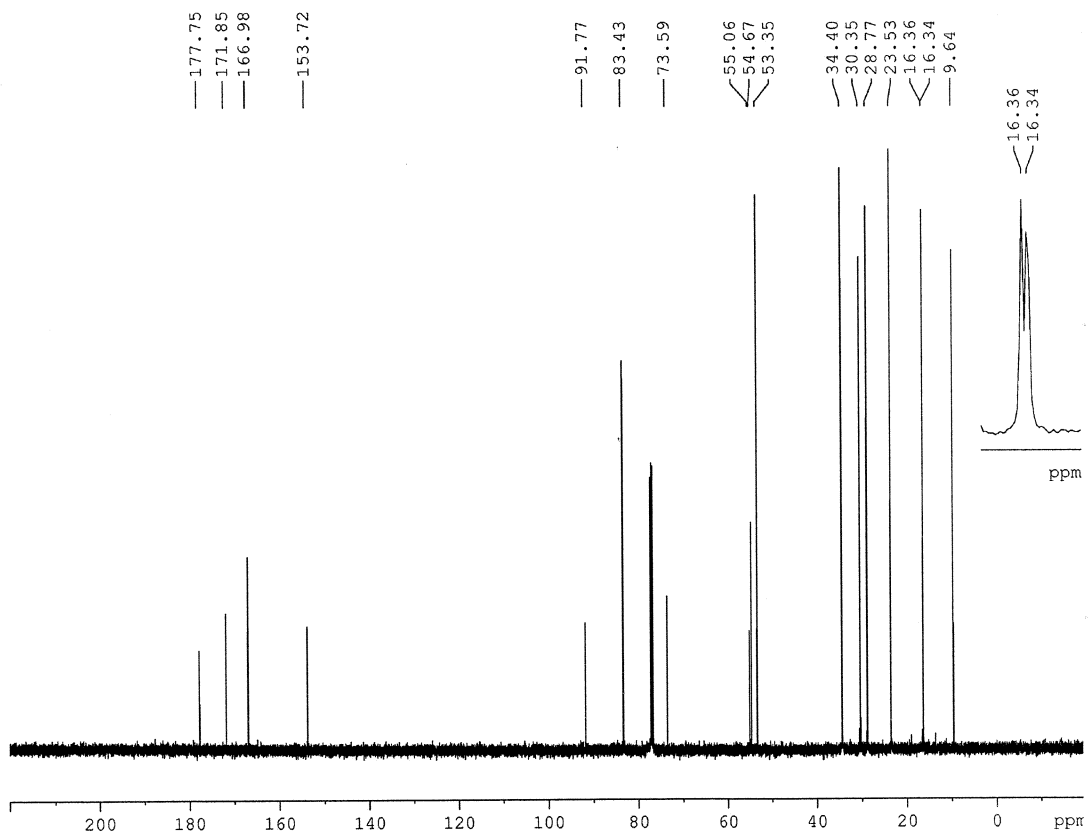
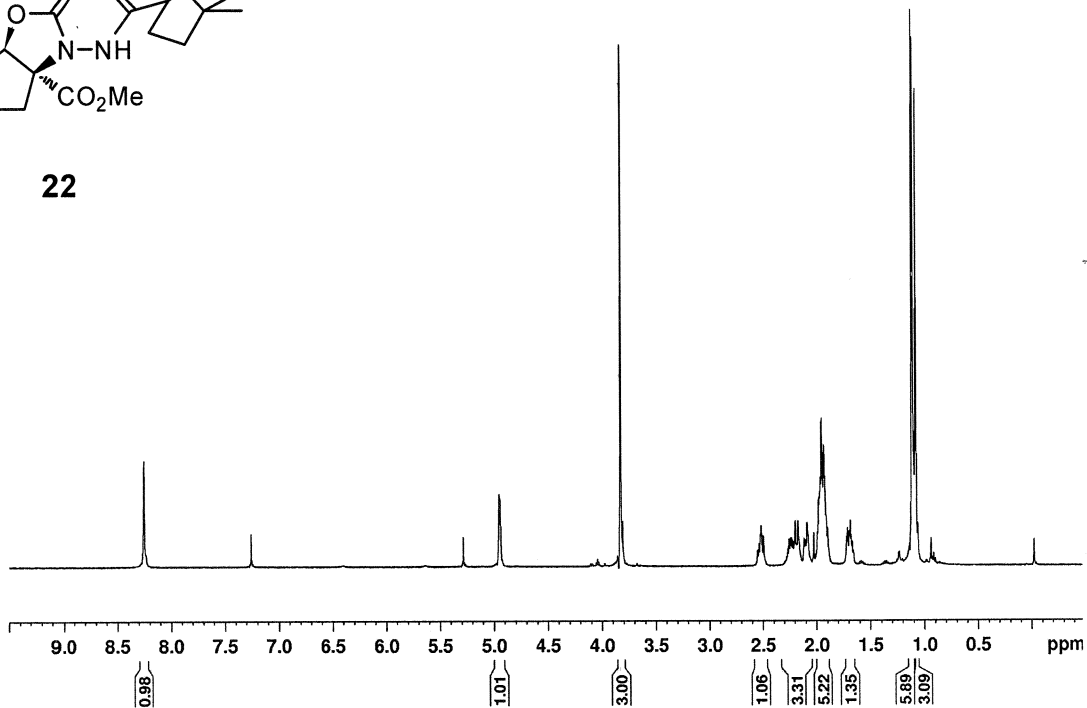
7

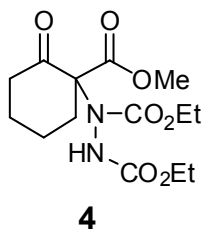




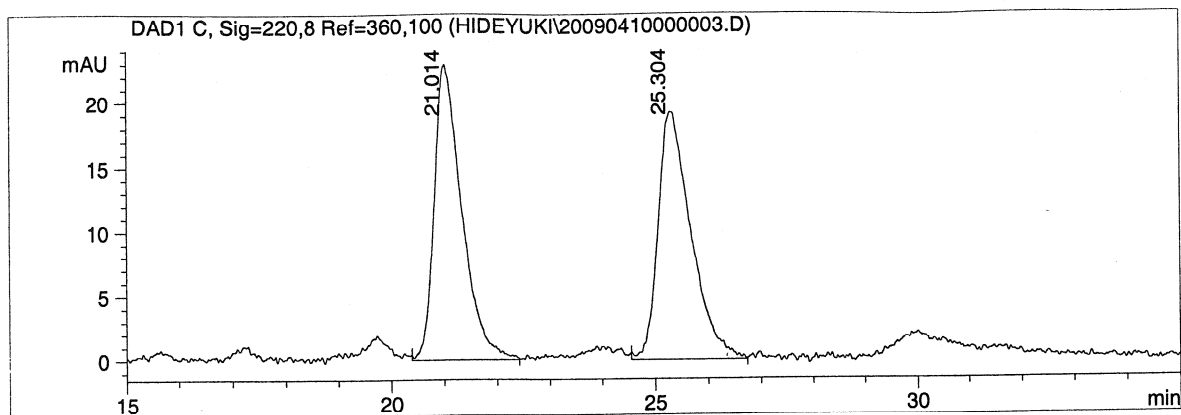


22

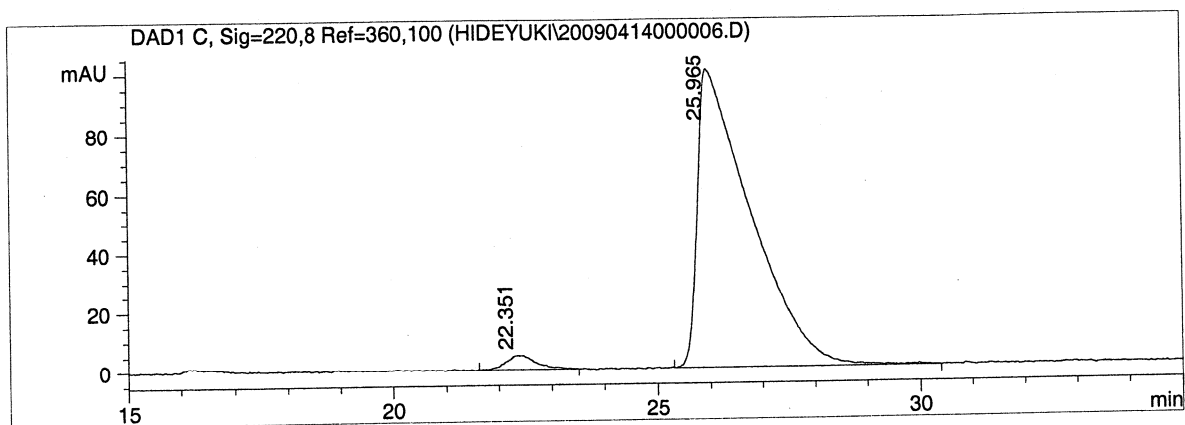




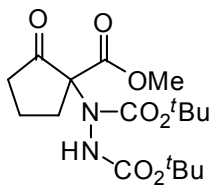
IA, hexanes/2-propanol = 95/5, flow rate 1.0 mL/min, 220 nm



#	RT (min)	Peak Area	Peak Area %
1	21.014	834.101	50.015
2	25.304	833.603	49.985

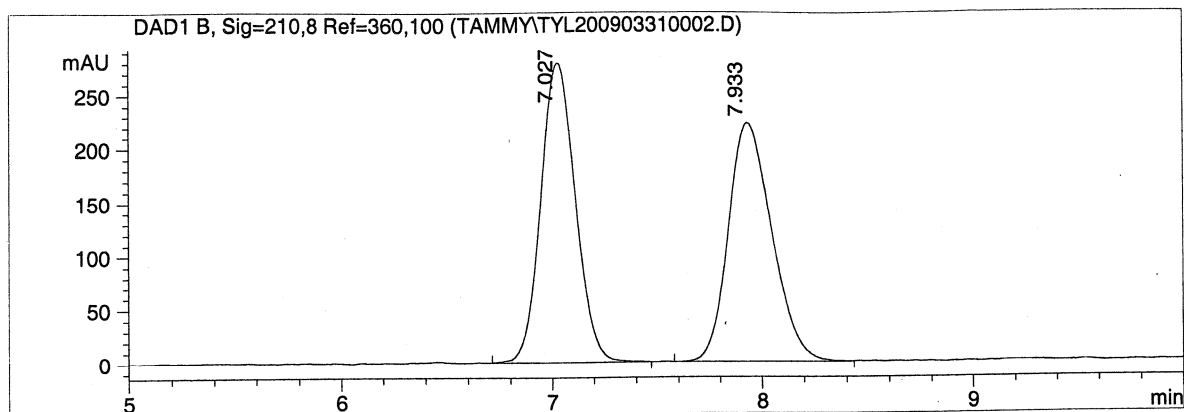


#	RT (min)	Peak Area	Peak Area %
1	22.351	188.483	2.584
2	25.965	7104.512	97.416

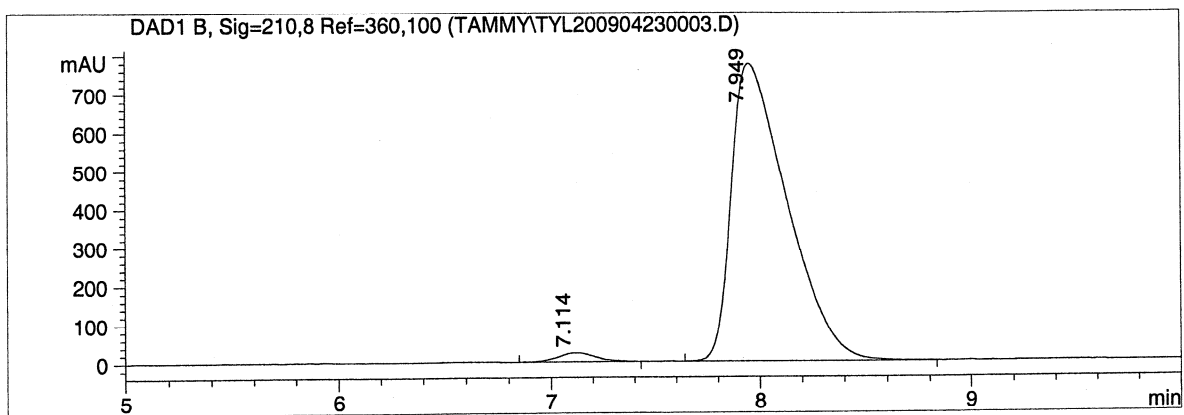


6b

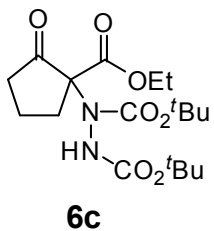
IA, hexanes/ethanol = 95/5, flow rate 1.0 mL/min, 210 nm



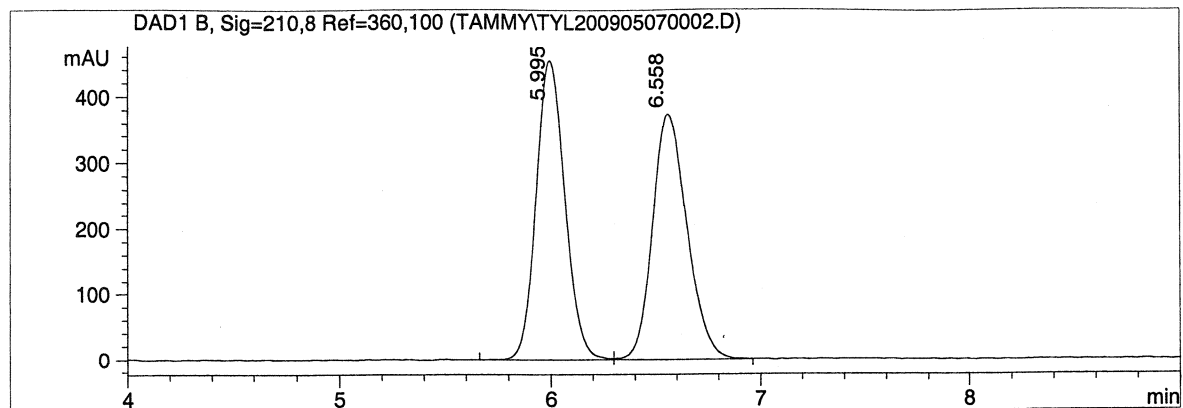
#	RT (min)	Peak Area	Peak Area %
1	7.027	3216.136	49.980
2	7.933	3218.664	50.020



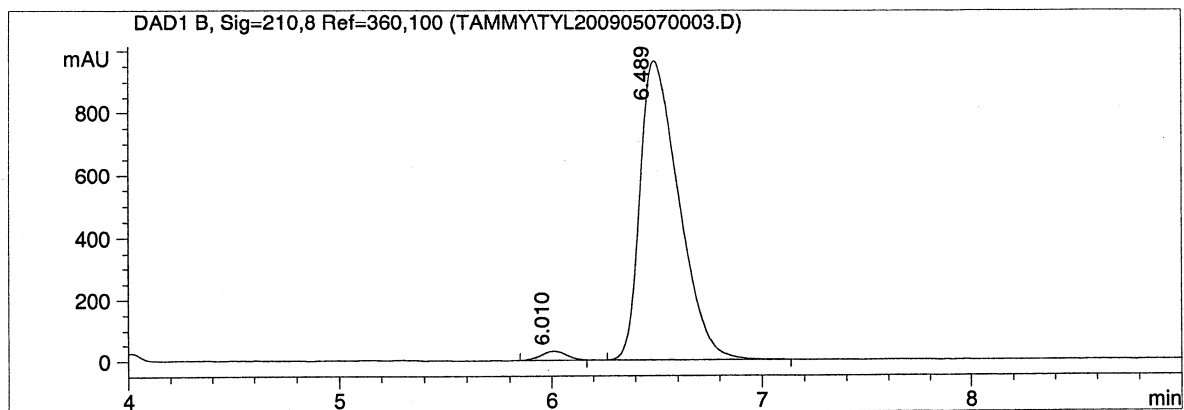
#	RT (min)	Peak Area	Peak Area %
1	7.114	299.066	2.049
2	7.949	14297.740	97.951



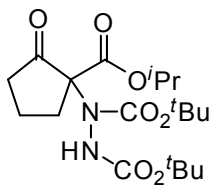
IA, hexanes/ethanol = 95/5, flow rate 1.0 mL/min, 210 nm



#	RT (min)	Peak Area	Peak Area %
1	5.995	4284.202	49.831
2	6.558	4313.176	50.169

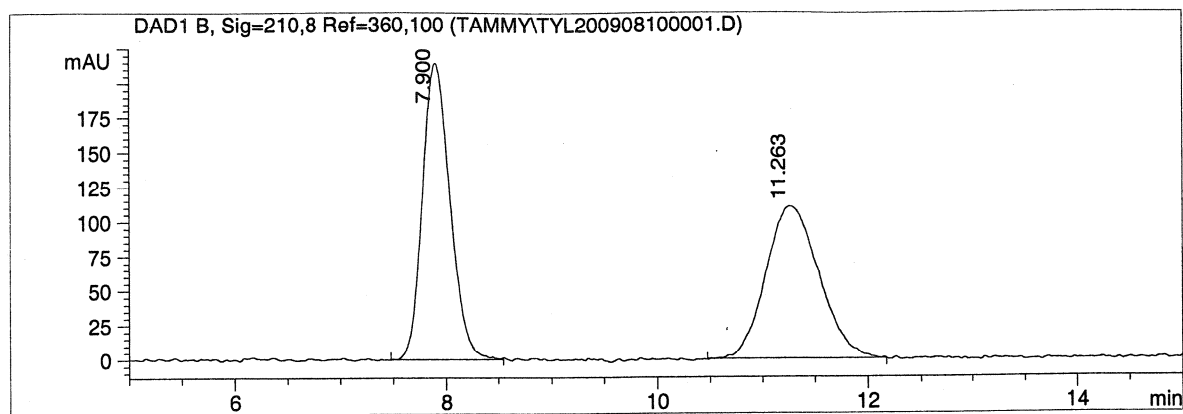


#	RT (min)	Peak Area	Peak Area %
1	6.010	264.794	2.094
2	6.489	12381.440	97.906

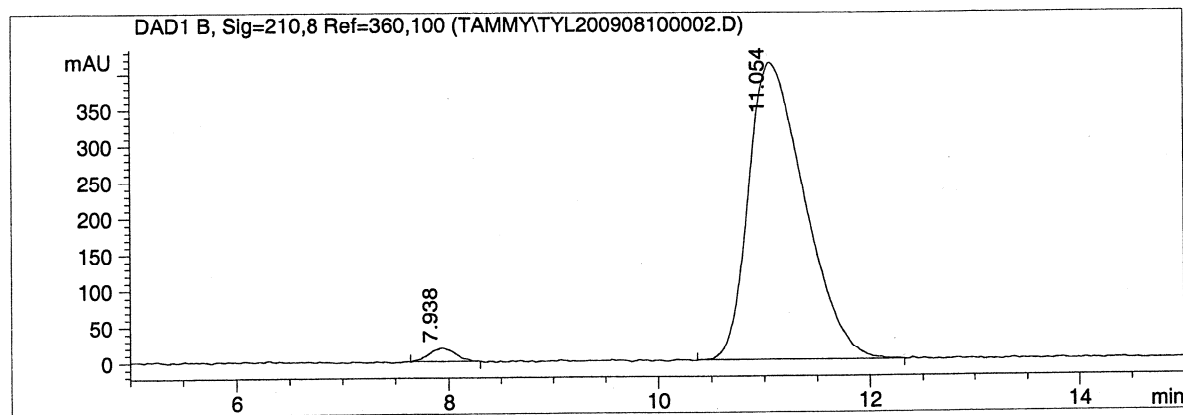


6d

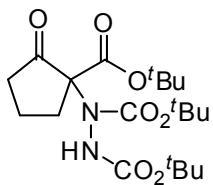
IA, hexanes/2-propanol = 95/5, flow rate 1.0 mL/min, 210 nm



#	RT (min)	Peak Area	Peak Area %
1	7.900	3911.406	50.101
2	11.263	3895.644	49.899

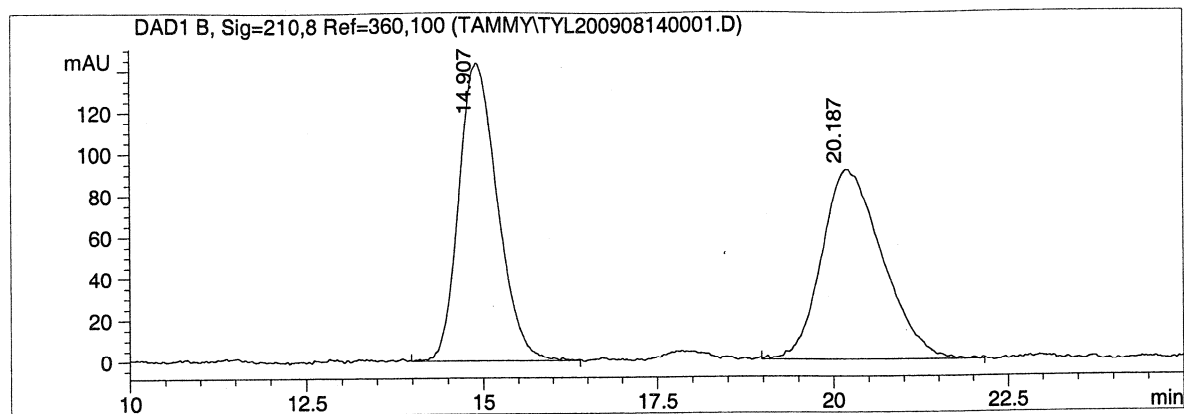


#	RT (min)	Peak Area	Peak Area %
1	7.938	329.818	2.119
2	11.054	15233.700	97.881

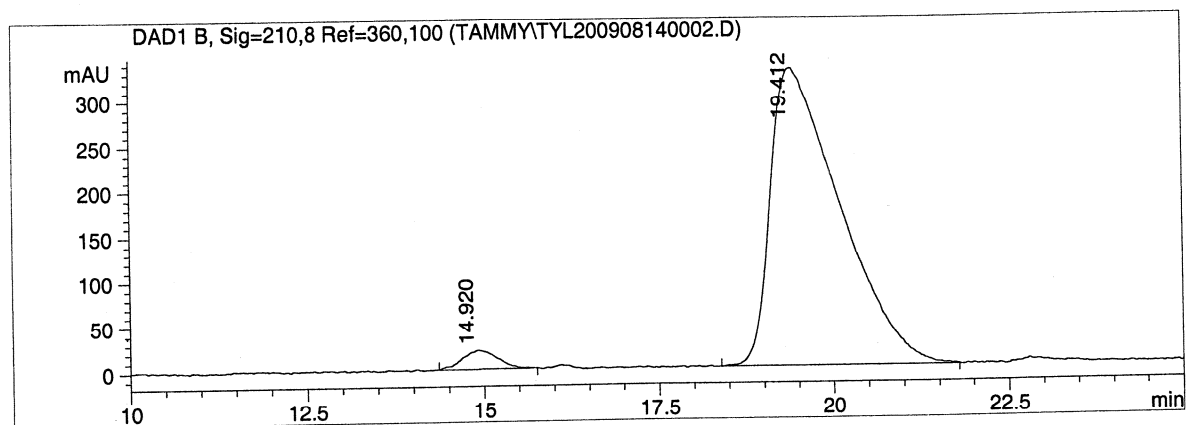


6e

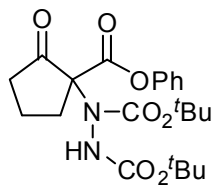
IA, hexanes/2-propanol = 98/2, flow rate 1.0 mL/min, 210 nm



#	RT (min)	Peak Area	Peak Area %
1	14.907	5497.500	49.743
2	20.187	5554.371	50.257

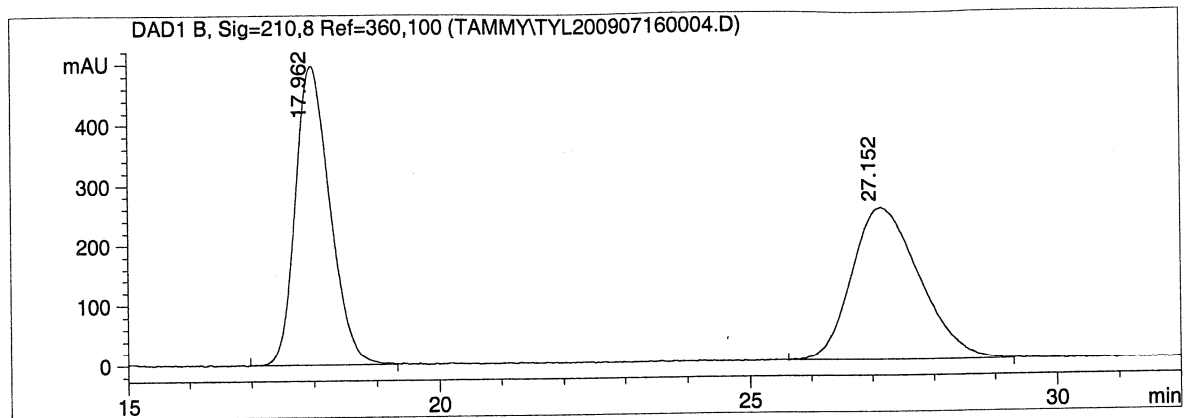


#	RT (min)	Peak Area	Peak Area %
1	14.920	718.585	3.044
2	19.412	22891.068	96.956

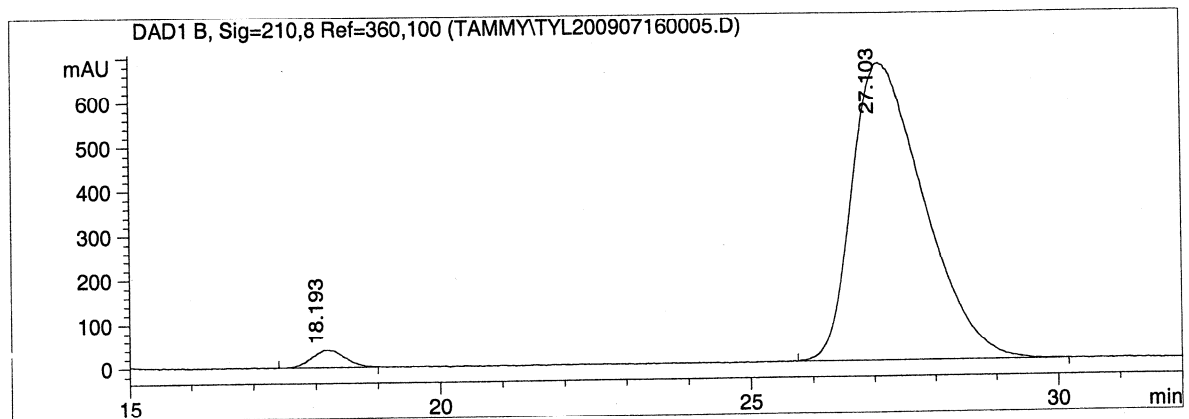


6f

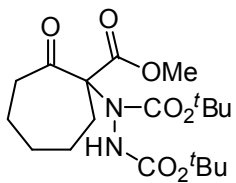
IA, hexanes/2-propanol = 97/3, flow rate 1.0 mL/min, 210 nm



#	RT (min)	Peak Area	Peak Area %
1	17.962	19084.936	49.556
2	27.152	19426.564	50.444

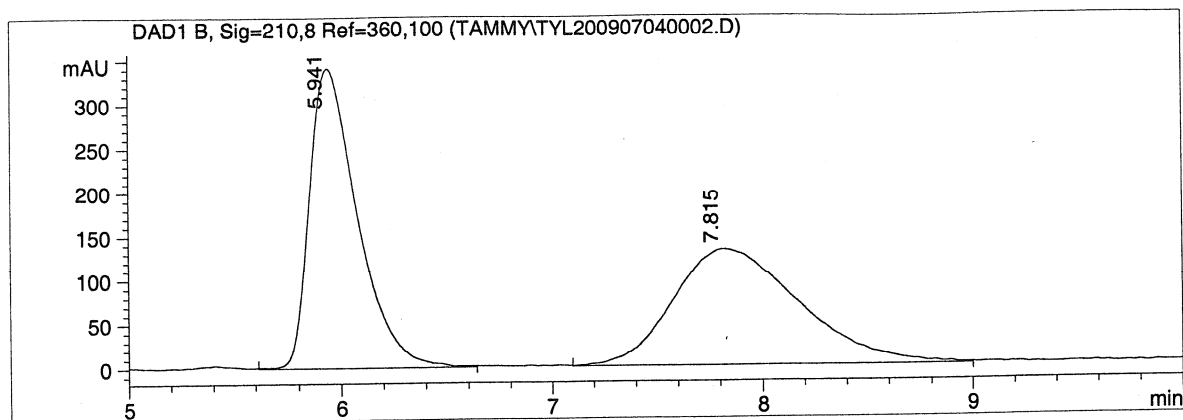


#	RT (min)	Peak Area	Peak Area %
1	18.193	1461.093	2.571
2	27.103	55360.926	97.429

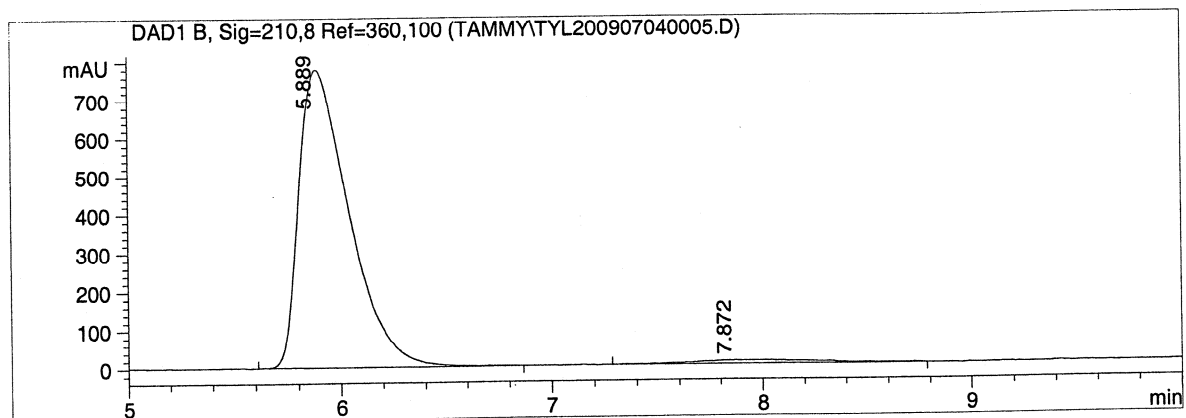


6g

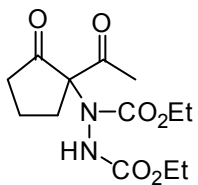
OD-H, hexanes/2-propanol = 97/3, flow rate 1.0 mL/min, 210 nm



#	RT (min)	Peak Area	Peak Area %
1	5.941	5414.586	49.612
2	7.815	5499.339	50.388

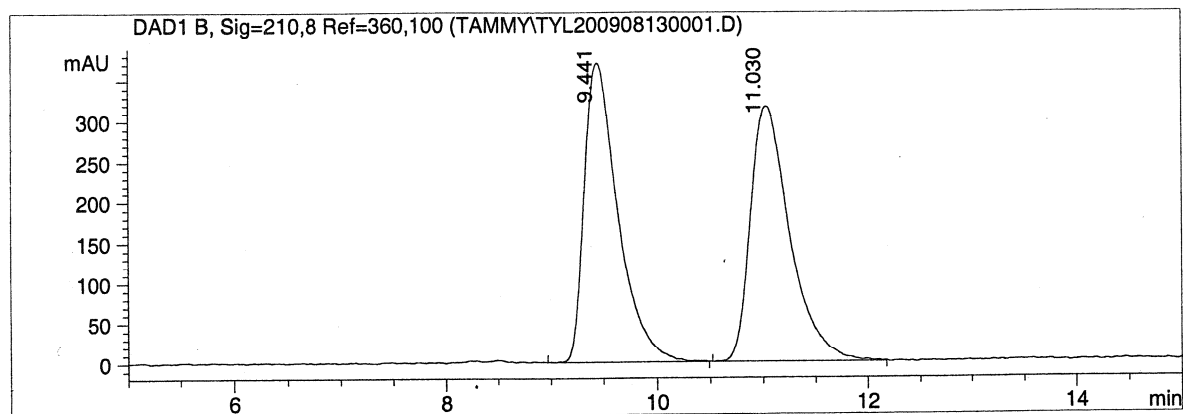


#	RT (min)	Peak Area	Peak Area %
1	5.889	12835.195	97.206
2	7.872	368.864	2.794

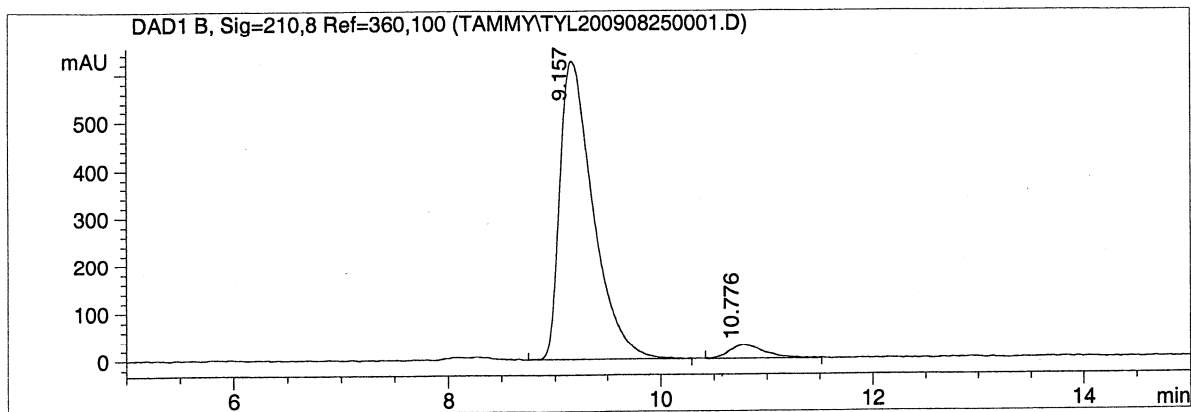


6h

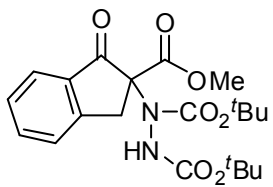
OD-H, hexanes/ethanol = 95/5, flow rate 1.0 mL/min, 210 nm



#	RT (min)	Peak Area	Peak Area %
1	9.441	8217.245	49.814
2	11.030	8278.474	50.186

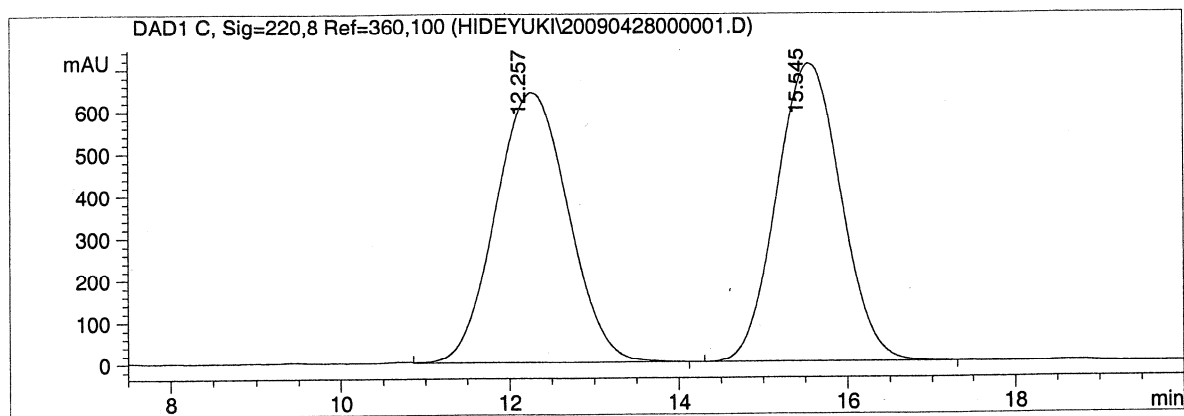


#	RT (min)	Peak Area	Peak Area %
1	9.157	13863.753	95.510
2	10.776	651.711	4.490

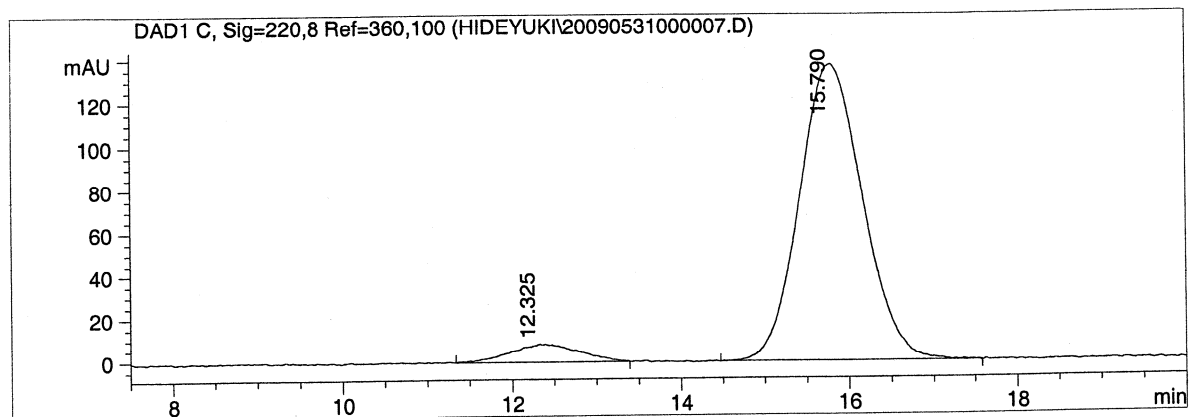


6i

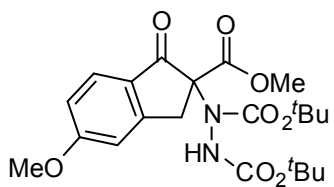
IA, hexanes/2-propanol = 90/10, flow rate 1.0 mL/min, 220 nm



#	RT (min)	Peak Area	Peak Area %
1	12.257	38427.844	50.415
2	15.545	37795.027	49.585

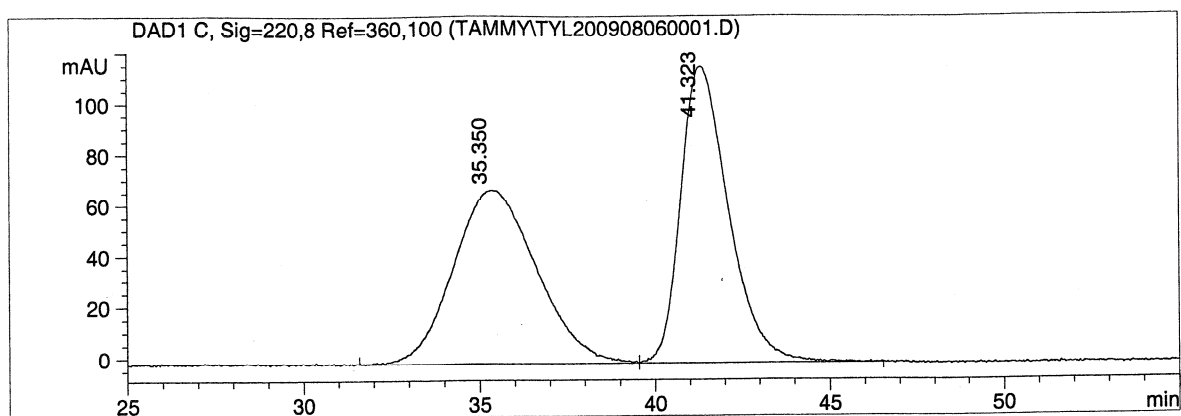


#	RT (min)	Peak Area	Peak Area %
1	12.325	473.780	6.145
2	15.790	7236.606	93.855

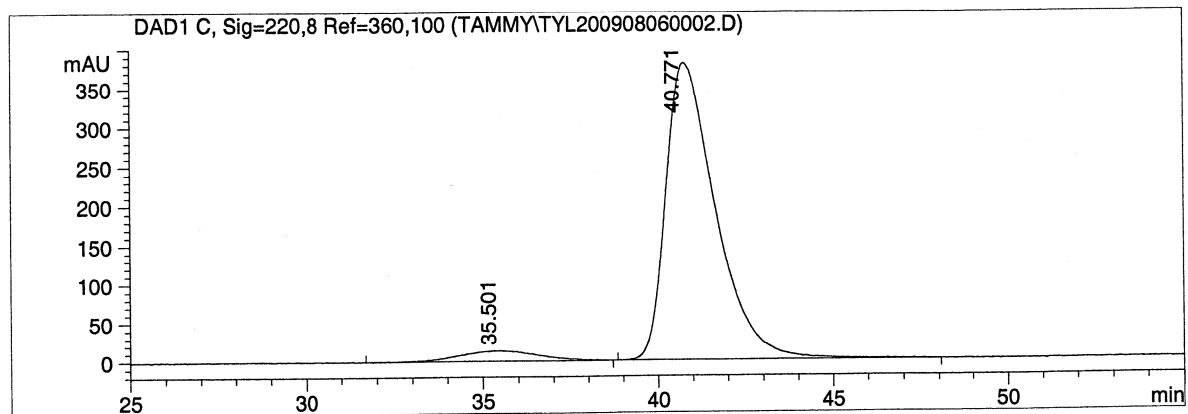


6j

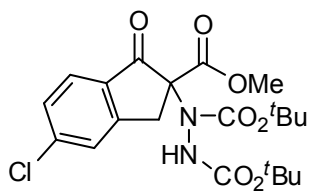
IA, hexanes/2-propanol = 90/10, flow rate 0.5 mL/min, 220 nm



#	RT (min)	Peak Area	Peak Area %
1	35.350	11187.977	50.048
2	41.323	11166.677	49.952

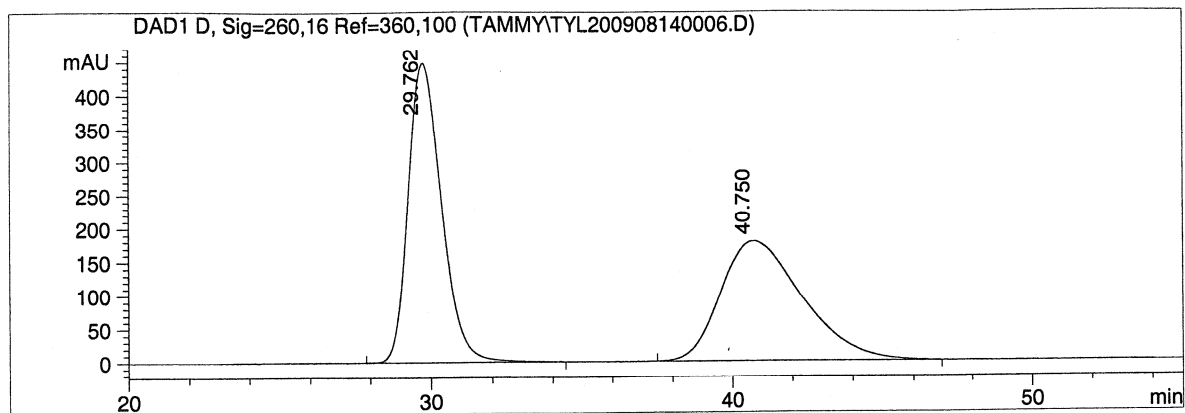


#	RT (min)	Peak Area	Peak Area %
1	35.501	2024.990	5.090
2	40.771	37755.855	94.910

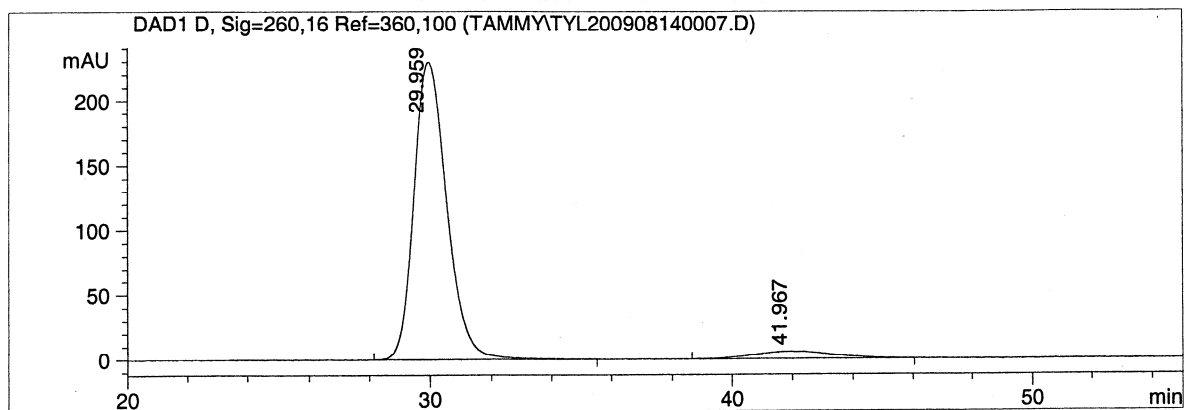


6k

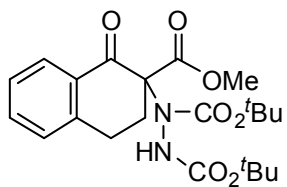
IA, hexanes/2-propanol = 97/3, flow rate 0.8 mL/min, 220 nm



#	RT (min)	Peak Area	Peak Area %
1	29.762	33991.820	49.918
2	40.750	34103.551	50.082

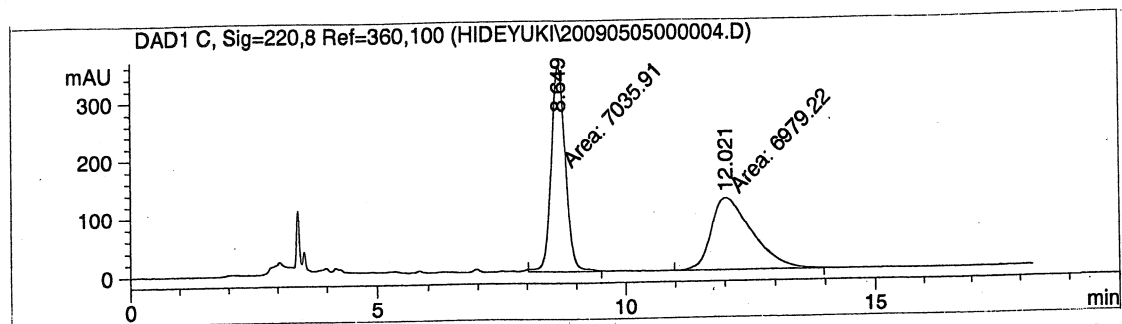


#	RT (min)	Peak Area	Peak Area %
1	29.959	17347.281	93.993
2	41.967	1108.562	6.007

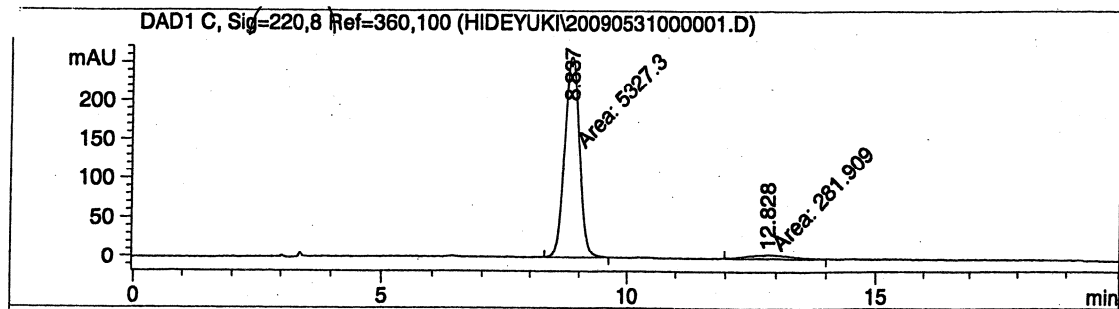


6I

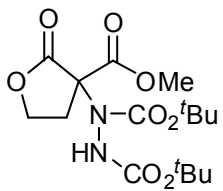
IA, hexanes/2-propanol = 80/20, flow rate 1.0 mL/min, 220 nm



Peak #	RetTime [min]	Type	Width [min]	Area [mAU*s]	Height [mAU]	Area %
1	8.649	MM	0.3331	7035.91455	351.99857	50.2023
2	12.021	MM	0.9407	6979.21875	123.65813	49.7977

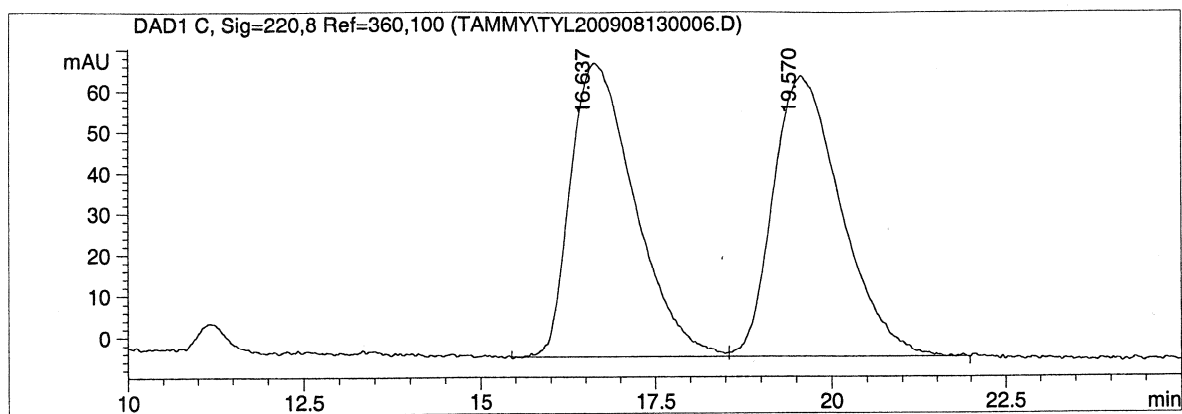


Peak #	RetTime [min]	Type	Width [min]	Area [mAU*s]	Height [mAU]	Area %
1	8.837	MM	0.3446	5327.29688	257.66333	94.9742
2	12.828	MM	0.9123	281.90860	5.15015	5.0258

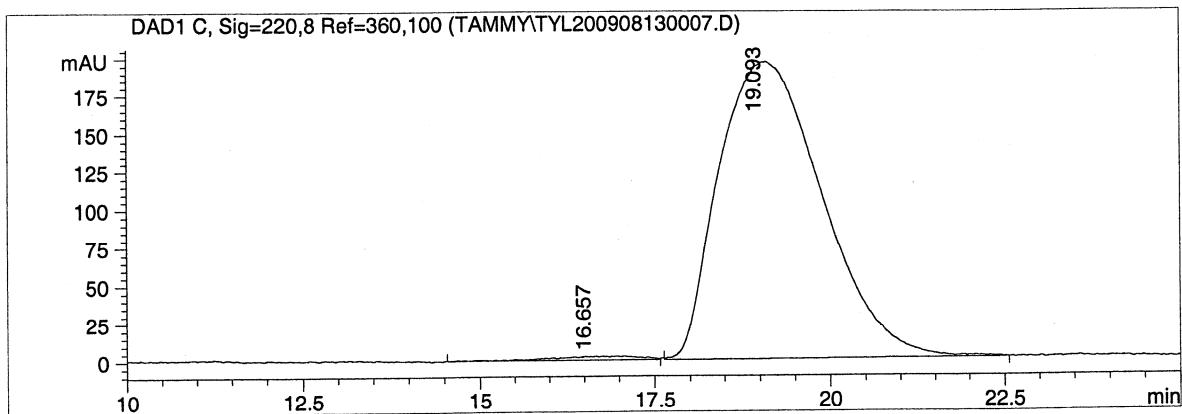


6m

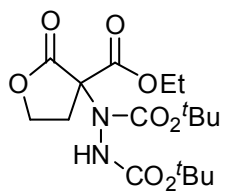
OD-H, hexanes/2-propanol = 97/3, flow rate 0.5 mL/min, 220 nm



#	RT (min)	Peak Area	Peak Area %
1	16.637	4593.434	50.073
2	19.570	4580.126	49.927

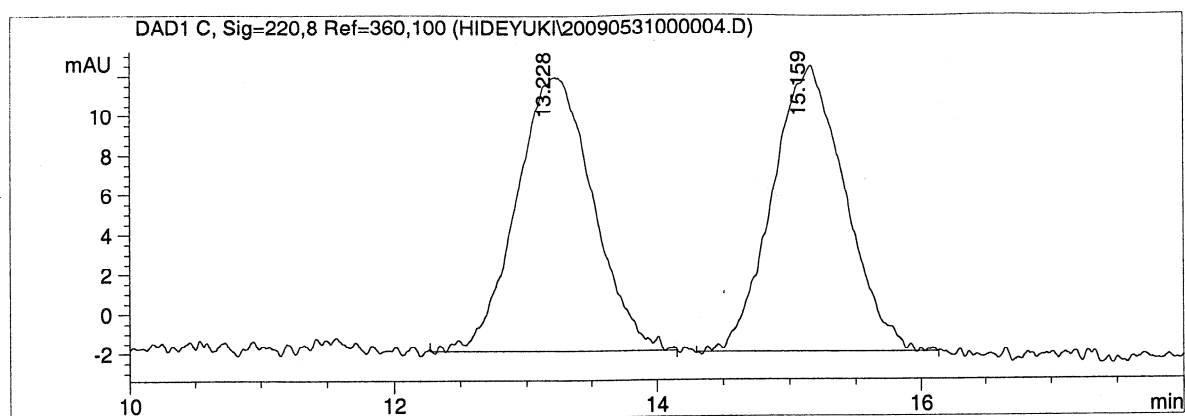


#	RT (min)	Peak Area	Peak Area %
1	16.657	220.668	1.091
2	19.093	20012.615	98.909

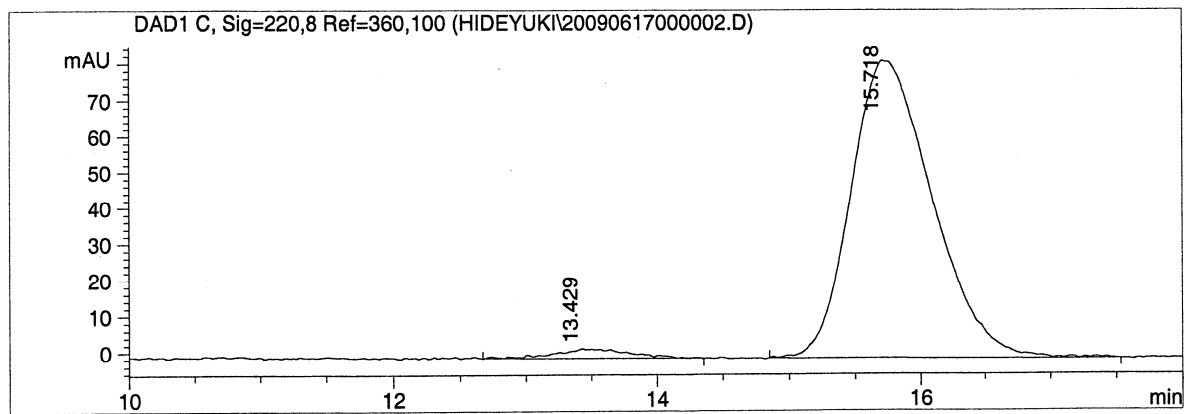


6n

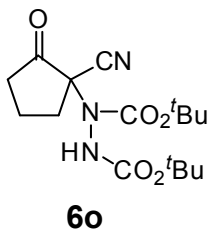
IA, hexanes/2-propanol = 97/3, flow rate 1.0 mL/min, 220 nm



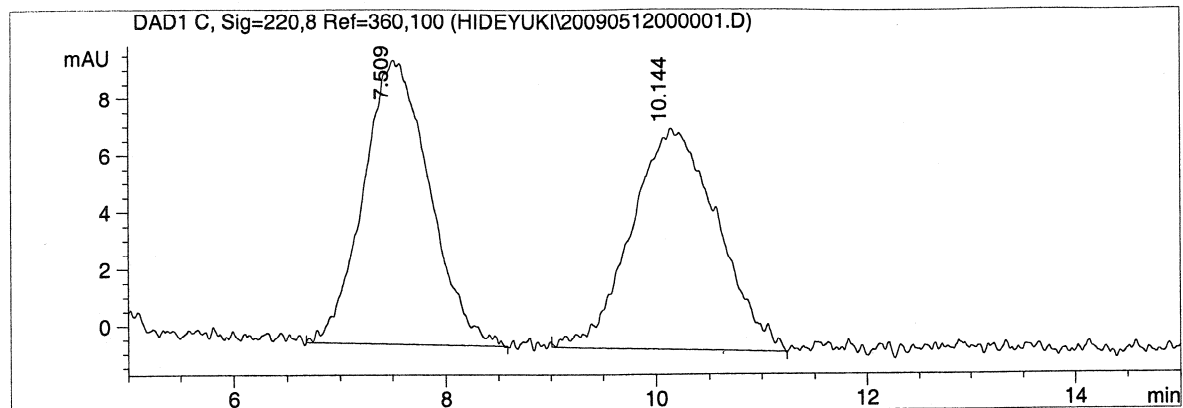
#	RT (min)	Peak Area	Peak Area %
1	13.228	568.257	50.665
2	15.159	553.341	49.335



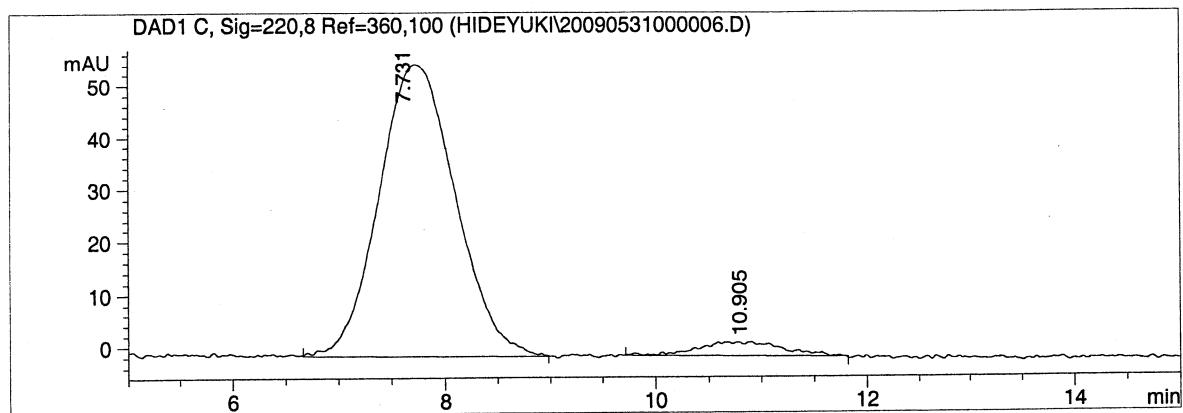
#	RT (min)	Peak Area	Peak Area %
1	13.429	99.612	2.724
2	15.718	3557.051	97.276



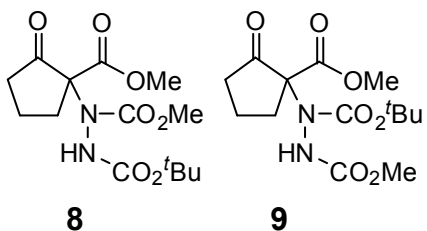
IA, hexanes/2-propanol = 90/10, flow rate 1.0 mL/min, 220 nm



#	RT (min)	Peak Area	Peak Area %
1	7.509	434.034	49.734
2	10.144	438.680	50.266

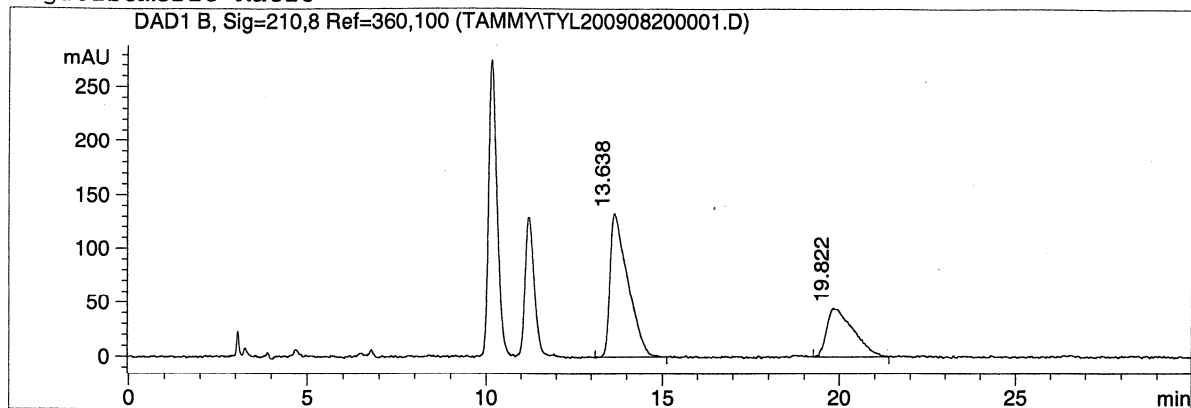


#	RT (min)	Peak Area	Peak Area %
1	7.731	2781.927	95.124
2	10.905	142.608	4.876



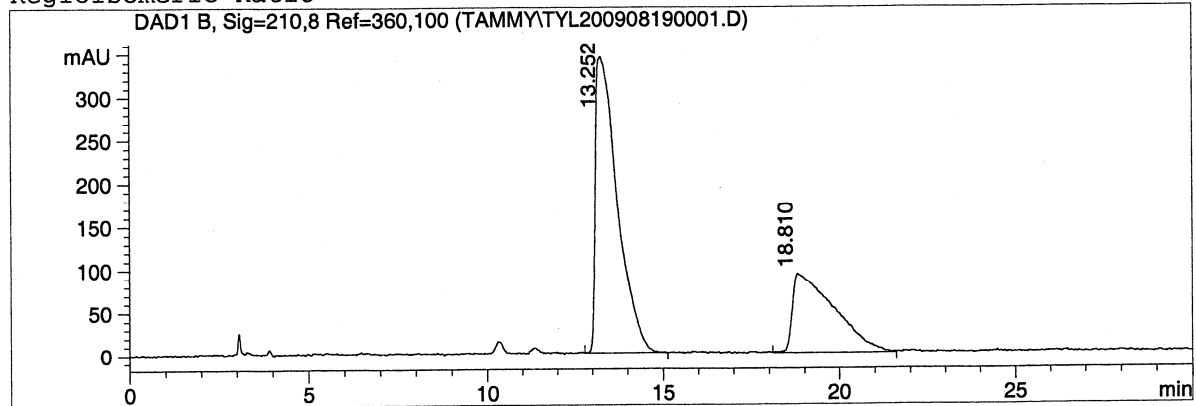
IA, hexanes/2-propanol = 90/10, flow rate 1.0 mL/min, 210 nm

Regioisomeric Ratio

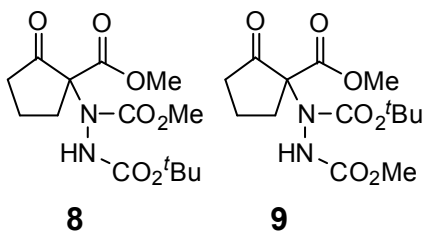


#	RT (min)	Peak Area	Peak Area %
1	13.638	4598.940	66.375
2	19.822	2329.814	33.625

Regioisomeric Ratio

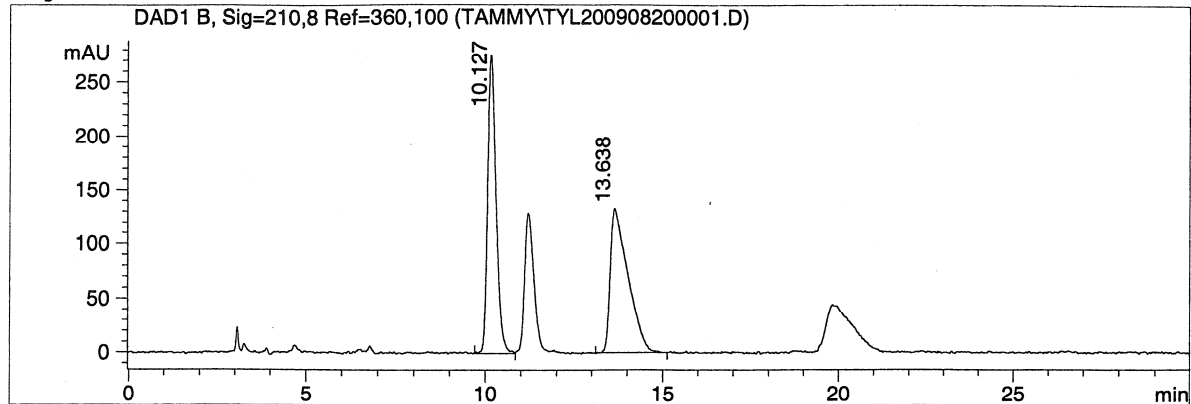


#	RT (min)	Peak Area	Peak Area %
1	13.252	14881.391	66.199
2	18.810	7598.236	33.801



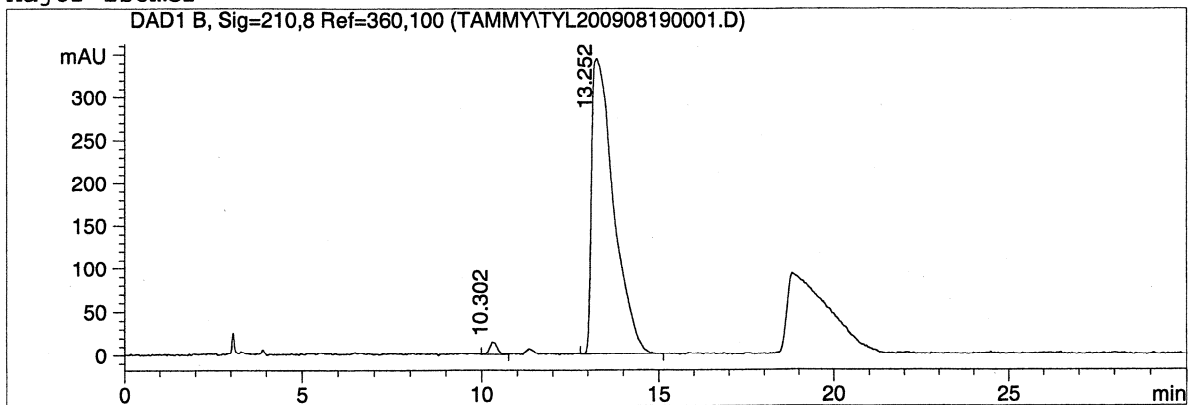
IA, hexanes/2-propanol = 90/10, flow rate 1.0 mL/min, 210 nm

Major Isomer

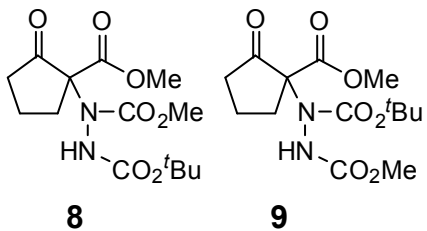


#	RT (min)	Peak Area	Peak Area %
1	10.127	4595.646	49.982
2	13.638	4598.940	50.018

Major Isomer

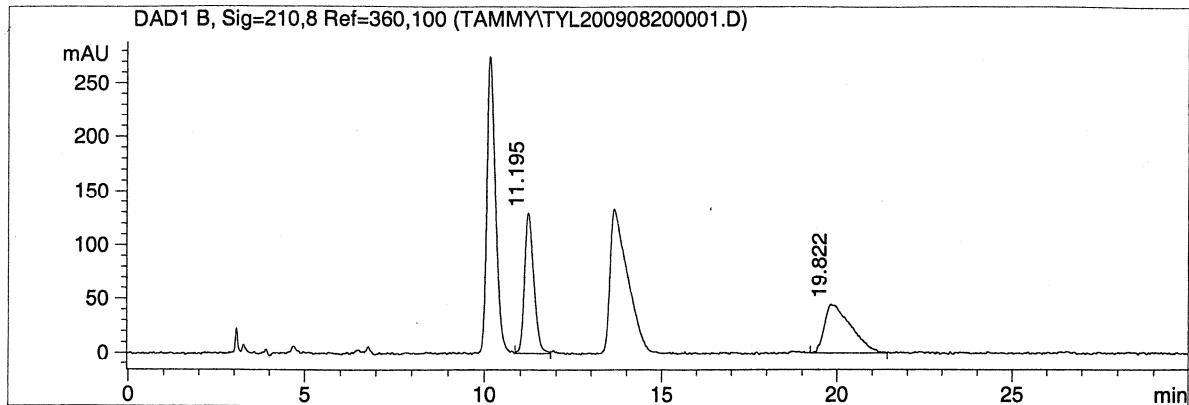


#	RT (min)	Peak Area	Peak Area %
1	10.302	232.164	1.536
2	13.252	14881.391	98.464



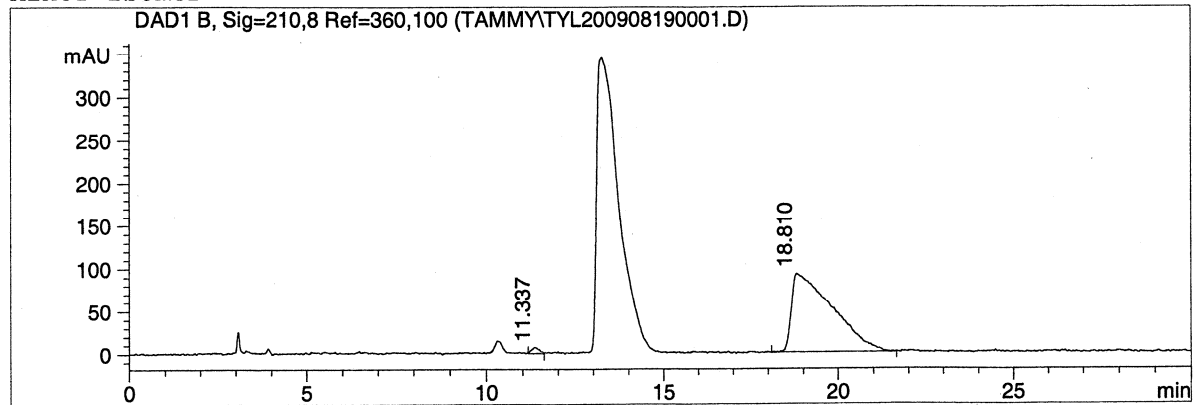
IA, hexanes/2-propanol = 90/10, flow rate 1.0 mL/min, 210 nm

Minor Isomer



#	RT (min)	Peak Area	Peak Area %
1	11.195	2356.082	50.271
2	19.822	2330.722	49.729

Minor Isomer



#	RT (min)	Peak Area	Peak Area %
1	11.337	108.247	1.429
2	18.810	7464.358	98.571

Table 1. Crystal and structure refinement for **22**.

Identification Code	Lam02	
Empirical formula	$C_{18}H_{24}N_2O_7$	
Formula weight	380.39	
Temperature	100 K	
Wavelength	0.71073 Å	
Crystal system	Monoclinic	
Space Group	$P2_1$	
Unit cell dimensions	$a = 8.8090(16)$ Å	$\alpha = 90.0^\circ$
	$b = 9.2002(17)$ Å	$\beta = 92.499(3)^\circ$
	$c = 11.103(2)$ Å	$\gamma = 90.0^\circ$
Volume	$899.0(3)$ Å ³	
Z	2	
Density (calculated)	1.405 Mg/m ³	
Absorption coefficient	0.109 mm ⁻¹	
F(000)	404	
Crystal size, color, habit	0.40 x 0.40 x 0.40mm, clear, irregular	
Theta range for data collection	1.84 – 28.29 °	
Index ranges	$-11 \leq h \leq 11, -12 \leq k \leq 11, -14 \leq l \leq 14$	
Reflections collected	10,783	
Independent reflections	3,966 ($R_{int} = 0.0238$)	
Reflections with $I > 4\sigma(F_o)$	4,237	
Flack parameter	indeterminate	
Absorption correction	SADABS based on redundant diffractions	
Max. and min. transmission	1.0, 0.749	
Refinement method	Full-matrix least squares on F^2	
Weighting scheme	$w = q [\sigma^2 (F_o^2) + (aP)^2 + bP]^{-1}$ where: $P = (F_o^2 + 2F_c^2)/3, a = 0.0655, b = 0.0, q = 1$	
Data / restraints / parameters	4237 / 0 / 248	
Goodness-of-fit on F^2	0.925	
Final R indices [$I > 2 \sigma(I)$]	$R1 = 0.0389, wR2 = 0.0934$	
R indices (all data)	$R1 = 0.0411, wR2 = 0.0947$	
Largest diff. peak and hole	0.308, -0.201 eÅ ⁻³	

Table 2. Atomic coordinates [$\times 10^4$] and equivalent isotropic displacement parameters [$\text{\AA}^2 \times 10^3$] for **22**. U(eq) is defined as one third of the trace of the orthogonalized U_{ij} tensor.

	x	y	z	U (eq)	SOF
C(1)	8008(2)	10379(2)	5910(2)	23(1)	
C(2)	5374(2)	10663(2)	6263(1)	15(1)	
C(3)	3753(2)	10185(2)	5874(1)	15(1)	
C(4)	3600(2)	9080(2)	4842(2)	18(1)	
C(5)	2097(2)	9472(2)	4164(2)	21(1)	
C(6)	2140(2)	11138(2)	4185(2)	22(1)	
C(7)	2731(2)	11511(2)	5459(1)	17(1)	
C(8)	1660(2)	10483(2)	7132(1)	17(1)	
C(9)	2476(2)	7309(2)	7383(1)	16(1)	
C(10)	2839(2)	6015(2)	8185(1)	15(1)	
C(11)	2762(2)	4531(2)	7563(2)	20(1)	
C(12)	2798(2)	3472(2)	8645(2)	20(1)	
C(13)	2860(2)	4511(2)	9756(1)	16(1)	
C(14)	4416(2)	5198(2)	9697(1)	17(1)	
C(15)	197(2)	5455(2)	8991(2)	20(1)	
C(16)	1862(2)	5821(2)	9309(1)	16(1)	
C(17)	1929(2)	7120(2)	10170(2)	19(1)	
C(18)	2553(2)	3813(2)	10956(2)	20(1)	
N(1)	2982(2)	9764(2)	6948(1)	16(1)	
N(2)	3363(2)	8513(1)	7576(1)	15(1)	
O(1)	6423(1)	10014(1)	5616(1)	21(1)	
O(2)	5636(1)	11525(1)	7056(1)	24(1)	
O(3)	1486(1)	11534(1)	6278(1)	19(1)	
O(4)	778(1)	10277(1)	7907(1)	22(1)	
O(5)	1446(1)	7254(1)	6618(1)	20(1)	
O(6)	4377(1)	6137(1)	8735(1)	17(1)	
O(7)	5561(1)	5011(1)	10303(1)	22(1)	

Table 3. Bond lengths [Å] and angles [°] for **22**.

C(1)-O(1)	1.4595(19)	C(9)-N(2)	1.367(2)
C(2)-O(2)	1.200(2)	C(9)-C(10)	1.512(2)
C(2)-O(1)	1.335(2)	C(10)-O(6)	1.4658(18)
C(2)-C(3)	1.538(2)	C(10)-C(11)	1.531(2)
C(3)-N(1)	1.451(2)	C(10)-C(16)	1.556(2)
C(3)-C(4)	1.533(2)	C(11)-C(12)	1.546(2)
C(3)-C(7)	1.573(2)	C(12)-C(13)	1.559(2)
C(4)-C(5)	1.537(2)	C(13)-C(14)	1.513(2)
C(5)-C(6)	1.534(3)	C(13)-C(18)	1.514(2)
C(6)-C(7)	1.525(2)	C(13)-C(16)	1.560(2)
C(7)-O(3)	1.454(2)	C(14)-O(7)	1.2003(18)
C(8)-O(4)	1.199(2)	C(14)-O(6)	1.373(2)
C(8)-O(3)	1.358(2)	C(15)-C(16)	1.532(2)
C(8)-N(1)	1.363(2)	C(16)-C(17)	1.530(2)
C(9)-O(5)	1.2172(19)	N(1)-N(2)	1.3789(19)
O(2)-C(2)-O(1)	125.09(14)	C(11)-C(10)-C(16)	104.12(13)
O(2)-C(2)-C(3)	122.76(15)	C(10)-C(11)-C(12)	102.28(13)
O(1)-C(2)-C(3)	112.15(13)	C(11)-C(12)-C(13)	103.11(13)
N(1)-C(3)-C(4)	114.10(13)	C(14)-C(13)-C(18)	114.37(14)
N(1)-C(3)-C(2)	107.90(12)	C(14)-C(13)-C(12)	102.86(13)
C(4)-C(3)-C(2)	116.71(13)	C(18)-C(13)-C(12)	115.74(14)
N(1)-C(3)-C(7)	99.52(12)	C(14)-C(13)-C(16)	99.35(13)
C(4)-C(3)-C(7)	105.38(12)	C(18)-C(13)-C(16)	119.17(14)
C(2)-C(3)-C(7)	111.92(13)	C(12)-C(13)-C(16)	102.84(12)
C(3)-C(4)-C(5)	104.84(13)	O(7)-C(14)-O(6)	121.24(14)
C(6)-C(4)-C(5)	101.94(14)	O(7)-C(14)-C(13)	131.01(15)
C(7)-C(4)-C(5)	104.24(14)	O(6)-C(14)-C(13)	107.72(13)
O(3)-C(7)-C(6)	110.33(13)	C(17)-C(16)-C(15)	109.04(13)
O(3)-C(7)-C(3)	105.42(12)	C(17)-C(16)-C(10)	113.78(13)
C(6)-C(7)-C(3)	105.34(13)	C(15)-C(16)-C(10)	113.43(13)
O(4)-C(8)-O(3)	123.81(15)	C(17)-C(16)-C(13)	113.54(13)
O(4)-C(8)-N(1)	127.96(16)	C(15)-C(16)-C(13)	115.12(13)
O(3)-C(8)-N(1)	108.22(14)	C(10)-C(16)-C(13)	91.17(12)
O(5)-C(9)-N(2)	123.18(15)	C(8)-N(1)-N(2)	121.38(14)
O(5)-C(9)-C(10)	120.65(14)	C(8)-N(1)-C(3)	115.25(13)
N(2)-C(9)-C(10)	116.17(13)	N(2)-N(1)-C(3)	121.74(13)
O(6)-C(10)-C(9)	110.65(12)	C(9)-N(2)-N(1)	118.18(13)
O(6)-C(10)-C(11)	106.13(13)	C(2)-O(1)-C(1)	117.03(13)
C(9)-C(10)-C(11)	115.62(12)	C(8)-O(3)-C(7)	111.15(12)
O(6)-C(10)-C(16)	102.01(11)	C(14)-O(6)-C(10)	105.52(12)
C(9)-C(10)-C(16)	116.93(13)		

Table 4. Anisotropic displacement parameters [$\text{\AA}^2 \times 10^3$] for **22**. The anisotropic displacement factor exponent takes the form:
 $-2\pi^2[h^2a^{*2}U_{11} + \dots + 2hka^*b^*U_{12}]$

	U_{11}	U_{22}	U_{33}	U_{23}	U_{13}	U_{12}
C(1)	11(1)	30(1)	26(1)	3(1)	0(1)	-1(1)
C(2)	15(1)	15(1)	14(1)	4(1)	0(1)	0(1)
C(3)	14(1)	15(1)	15(1)	1(1)	1(1)	0(1)
C(4)	18(1)	19(1)	16(1)	-2(1)	1(1)	0(1)
C(5)	18(1)	26(1)	18(1)	-3(1)	-2(1)	0(1)
C(6)	21(1)	26(1)	18(1)	3(1)	-3(1)	2(1)
C(7)	17(1)	16(1)	18(1)	3(1)	0(1)	1(1)
C(8)	16(1)	17(1)	17(1)	-4(1)	-3(1)	-1(1)
C(9)	15(1)	19(1)	14(1)	0(1)	4(1)	-2(1)
C(10)	15(1)	16(1)	15(1)	-1(1)	-1(1)	-1(1)
C(11)	24(1)	18(1)	18(1)	-3(1)	2(1)	0(1)
C(12)	24(1)	15(1)	20(1)	-1(1)	2(1)	0(1)
C(13)	17(1)	14(1)	17(1)	-2(1)	1(1)	0(1)
C(14)	19(1)	15(1)	16(1)	0(1)	2(1)	2(1)
C(15)	18(1)	21(1)	21(1)	2(1)	1(1)	-1(1)
C(16)	18(1)	14(1)	15(1)	1(1)	1(1)	0(1)
C(17)	24(1)	17(1)	18(1)	-2(1)	3(1)	2(1)
C(18)	23(1)	18(1)	18(1)	3(1)	1(1)	0(1)
N(1)	16(1)	15(1)	16(1)	2(1)	2(1)	0(1)
N(2)	16(1)	15(1)	15(1)	4(1)	-3(1)	-1(1)
O(1)	13(1)	26(1)	24(1)	-3(1)	0(1)	1(1)
O(2)	21(1)	26(1)	23(1)	-5(1)	0(1)	-4(1)
O(3)	16(1)	20(1)	22(1)	0(1)	1(1)	4(1)
O(4)	18(1)	28(1)	21(1)	-3(1)	5(1)	-2(1)
O(5)	20(1)	22(1)	17(1)	2(1)	-3(1)	-5(1)
O(6)	15(1)	20(1)	17(1)	3(1)	0(1)	-2(1)
O(7)	20(1)	24(1)	23(1)	4(1)	-3(1)	1(1)

Table 5. Hydrogen coordinates [$\times 10^4$] and isotropic displacement parameters [$\text{\AA}^2 \times 10^3$] for **22**.

	x	y	z	U(eq)
H(1A)	8423	10926	5242	34
H(1B)	8595	9484	6043	34
H(1C)	8071	10973	6643	34
H(4A)	3566	8076	5160	21
H(4B)	4463	9163	4304	21
H(5A)	2066	9094	3328	25
H(5B)	1213	9093	4586	25
H(6A)	2831	11517	3579	26
H(6B)	1113	11549	4021	26
H(7)	3314	12444	5483	21
H(11A)	3644	4378	7055	24
H(11B)	1812	4423	7060	24
H(12A)	3706	2838	8645	23
H(12B)	1874	2858	8634	23
H(15A)	-344	5301	9733	30
H(15B)	143	4568	8501	30
H(15C)	-275	6260	8535	30
H(17A)	1471	7970	9765	29
H(17B)	2991	7332	10406	29
H(17C)	1369	6890	10889	29
H(18A)	3181	2940	11064	30
H(18B)	1477	3546	10972	30
H(18C)	2801	4502	11608	30
H(2)	4156	8490	8086	18

Table 6. Torsion angles [$^{\circ}$] for **22**.

O(2)-C(2)-C(3)-N(1)	-50.3(2)	O(6)-C(10)-C(16)-C(15)	-172.07(13)
O(1)-C(2)-C(3)-N(1)	129.97(14)	C(9)-C(10)-C(16)-C(15)	67.09(18)
O(2)-C(2)-C(3)-C(4)	179.71(14)	C(11)-C(10)-C(16)-C(15)	-61.81(16)
O(1)-C(2)-C(3)-C(4)	-0.03(19)	O(6)-C(10)-C(16)-C(13)	-53.93(13)
O(2)-C(2)-C(3)-C(7)	58.2(2)	C(9)-C(10)-C(16)-C(13)	-174.77(13)
O(1)-C(2)-C(3)-C(7)	-121.53(14)	C(11)-C(10)-C(16)-C(13)	56.33(13)
N(1)-C(3)-C(4)-C(5)	85.92(15)	C(14)-C(13)-C(16)-C(17)	-65.56(16)
C(2)-C(3)-C(4)-C(5)	-147.08(14)	C(18)-C(13)-C(16)-C(17)	59.25(19)
C(7)-C(3)-C(4)-C(5)	-22.20(16)	C(12)-C(13)-C(16)-C(17)	-171.15(13)
C(3)-C(4)-C(5)-C(6)	39.63(16)	C(14)-C(13)-C(16)-C(15)	167.77(13)
C(4)-C(5)-C(6)-C(7)	-42.06(17)	C(18)-C(13)-C(16)-C(15)	-67.42(19)
C(5)-C(6)-C(7)-O(3)	-84.93(16)	C(12)-C(13)-C(16)-C(15)	62.18(17)
C(5)-C(6)-C(7)-C(3)	28.38(17)	C(14)-C(13)-C(16)-C(10)	51.11(13)
N(1)-C(3)-C(7)-O(3)	-5.47(15)	C(18)-C(13)-C(16)-C(10)	175.92(14)
C(4)-C(3)-C(7)-O(3)	112.93(13)	C(12)-C(13)-C(16)-C(10)	-54.49(13)
C(2)-C(3)-C(7)-O(3)	-119.25(13)	O(4)-C(8)-N(1)-N(2)	9.7(3)
N(1)-C(3)-C(7)-C(6)	-122.18(14)	O(3)-C(8)-N(1)-N(2)	-171.22(13)
C(4)-C(3)-C(7)-C(6)	-3.78(17)	O(4)-C(8)-N(1)-C(3)	175.36(16)
C(2)-C(3)-C(7)-C(6)	124.04(14)	O(3)-C(8)-N(1)-C(3)	-5.56(18)
O(5)-C(9)-C(10)-O(6)	161.13(14)	C(4)-C(3)-N(1)-C(8)	-104.85(16)
N(2)-C(9)-C(10)-O(6)	-18.97(19)	C(2)-C(3)-N(1)-C(8)	123.70(15)
O(5)-C(9)-C(10)-C(11)	40.5(2)	C(7)-C(3)-N(1)-C(8)	6.84(17)
N(2)-C(9)-C(10)-C(11)	-139.64(15)	C(4)-C(3)-N(1)-N(2)	60.75(18)
O(5)-C(9)-C(10)-C(16)	-82.71(19)	C(2)-C(3)-N(1)-N(2)	-70.69(18)
N(2)-C(9)-C(10)-C(16)	97.19(17)	C(7)-C(3)-N(1)-N(2)	172.44(13)
O(6)-C(10)-C(11)-C(12)	69.95(15)	O(5)-C(9)-N(2)-N(1)	6.1(2)
C(9)-C(10)-C(11)-C(12)	-166.97(13)	C(10)-C(9)-N(2)-N(1)	-173.78(13)
C(16)-C(10)-C(11)-C(12)	-37.27(15)	C(8)-N(1)-N(2)-C(9)	65.20(19)
C(10)-C(11)-C(12)-C(13)	1.05(16)	C(3)-N(1)-N(2)-C(9)	-99.52(17)
C(11)-C(12)-C(13)-C(14)	-67.75(15)	O(2)-C(2)-O(1)-C(1)	0.6(2)
C(11)-C(12)-C(13)-C(18)	166.80(14)	C(3)-C(2)-O(1)-C(1)	-179.70(13)
C(11)-C(12)-C(13)-C(16)	35.13(16)	O(4)-C(8)-O(3)-C(7)	-179.62(15)
C(18)-C(13)-C(14)-O(7)	19.8(3)	N(1)-C(8)-O(3)-C(7)	1.26(17)
C(12)-C(13)-C(14)-O(7)	-106.6(2)	C(6)-C(7)-O(3)-C(8)	116.16(15)
C(16)-C(13)-C(14)-O(7)	147.85(18)	C(3)-C(7)-O(3)-C(8)	2.91(16)
C(18)-C(13)-C(14)-O(6)	-162.25(13)	O(7)-C(14)-O(6)-C(10)	176.96(15)
C(12)-C(13)-C(14)-O(6)	71.42(15)	C(13)-C(14)-O(6)-C(10)	-1.26(16)
C(16)-C(13)-C(14)-O(6)	-34.16(15)	C(9)-C(10)-O(6)-C(14)	161.80(12)
O(6)-C(10)-C(16)-C(17)	62.52(16)	C(11)-C(10)-O(6)-C(14)	-72.04(15)
C(9)-C(10)-C(16)-C(17)	-58.31(17)	C(16)-C(10)-O(6)-C(14)	36.70(15)
C(11)-C(10)-C(16)-C(17)	172.78(13)		